

Instructional Scanning Tunneling Microscope™

Workbook

R. J. Dwayne Miller Ph.D.
Department of Chemistry & the Institute of Optics
University of Rochester
Rochester, NY 14627

H. A. Mizes Ph.D.
Webster Research Center
Xerox Corporation
Rochester, NY 14580

A. Samsavar Ph.D.
Burleigh Instruments Inc.
Fishers, NY 14453

ISTM is a trademark of Burleigh Instruments, Inc.

© Copyright 1992 Burleigh Instruments, Inc.
All Rights Reserved

burleigh

Burleigh Instruments, Inc.
Burleigh Park
P.O. Box E
Fishers, NY 14453-0755
Tel. (716) 924-9355
Fax. (716) 924-9072

TABLE OF CONTENTS

1. INTRODUCTION: The History of Microscopy	1-1
1.1. Optical Microscopy.....	1-1
1.2. Electron Microscopy.....	1-4
1.3. Acoustical Microscopy	1-8
1.4. Scanning Probe Microscopy	1-10
1.5. The First Important Discovery Using an STM	1-12
1.6. Atomic Force Microscopy.....	1-13
2. OPERATING PRINCIPLES OF THE STM.....	2-1
2.1. How the STM Works.....	2-1
2.2. Quantum Mechanical Tunneling	2-1
2.3. Quantifying the Tunneling Process.....	2-7
2.4. Angstrom Motion Using Piezoelectrics.....	2-14
2.4.1. What are Piezoelectrics?.....	2-14
2.4.2. Scanning with Piezoelectrics.....	2-15
2.5. Negative Feedback.....	2-17
2.6. Vibration Isolation	2-18
2.7. Electronic Data Collection.....	2-20
3. OPERATING INSTRUCTIONS.....	3-1
3.1. A General Overview of the Burleigh ISTM	3-1
3.2. The ISTM Head	3-3
3.2.1. Head Characteristics	3-3
3.2.2. Setting up the Head	3-6
3.2.2.1. Sample-Tip Set.....	3-8

3.2.2.2. Mounting Samples	3-9
3.2.2.3. Tip Preparation	3-9
3.2.2.4. Loading the Sample and Tip into the Head	3-13
3.3. ISTM Control Electronics	3-14
3.3.1. Tunneling Controls	3-15
3.3.2. Scan/Offset Controls	3-16
3.3.3. Tip Approach Controls.....	3-17
3.3.4. Monitor Outputs.....	3-18
3.4. True-Image™ Software Overview.....	3-19
3.4.1. Menu Structure.....	3-20
3.4.1.1. The File Menu.....	3-21
3.4.1.2. The Collect Menu.....	3-22
3.4.1.3. The Window Menu.....	3-24
3.4.1.4. The Display Menu.....	3-25
3.4.1.5. The Filter Menu.....	3-26
3.4.1.6. The Analysis Menu	3-30
3.4.2. Image-Processing with True-Image.....	3-31
3.5. Data Collection Modes.....	3-37
3.5.1. Constant Height Mode	3-37
3.5.2. Constant Current Mode.....	3-38
3.5.3. Basic Tunneling Instructions (Constant Height Mode).....	3-39
4. LABORATORY EXPERIMENTS	4-1
4.1. Gold Surfaces — An Example of a Metal	4-2
4.1.1. Experiment.....	4-9
4.1.1.1. Holographic Gold Grating: STM Magnification.....	4-9

Procedure:	4-9
Head Preparation	4-9
Software Preparation.....	4-10
Electronics Preparation.....	4-10
Tunneling.....	4-11
4.1.1.2 Questions	4-13
4.2. Graphite — Semimetals.....	4-15
4.2.1. Atomic Resolution Images of Graphite.....	4-20
4.2.1.1. Distortions in Images Caused by Multiple Atomic Tips	4-22
4.2.2. Experiment.....	4-24
4.2.2.1. Imaging Graphite	4-24
Procedure:	4-24
Head Preparation	4-24
Software Preparation.....	4-24
Electronics Preparation.....	4-24
Tunneling.....	4-25
4.2.2.2 Observation of a Chemical Reaction: Oxidation of Graphite...	4-26
Procedure:	4-27
4.2.2.3 Questions	4-28
4.3. Molybdenum Disulfide — Semiconductors	4-29
4.3.1. Experiment.....	4-35
4.3.1.1 Imaging MoS ₂	4-35
Procedure:	4-35
Head Preparation	4-35
Software Preparation.....	4-35

Electronics Preparation.....	4-35
Tunneling.....	4-36
4.3.1.2. Questions	4-37
4.4. Molecular Ordering on Graphite — Liquid Crystals and Long Chain Alkanes.....	4-38
4.4.1. Liquid Crystals.....	4-40
4.4.2. Alkanes Adsorbed on Graphite	4-43
4.4.3. Experiments	4-44
4.4.3.1. Imaging Surfaces Under Liquids.....	4-44
Procedure:	4-44
Head Preparation	4-44
Software Preparation.....	4-44
Electronics Preparation.....	4-45
Tunneling.....	4-45
4.4.3.2. Imaging Alkanes on Graphite	4-46
Procedure:	4-46
Head Preparation	4-46
Software Preparation.....	4-47
Electronics Preparation.....	4-47
Tunneling.....	4-47
4.4.3.3. Imaging Liquid Crystals	4-49
Procedure:	4-49
Head Preparation	4-49
Software Preparation.....	4-50
Electronics Preparation.....	4-50
Tunneling.....	4-51

4.4.2.4. Questions	4-53
4.5. Lattice Distortions	4-54
4.5.1. Periodic Lattice Distortions and Charge Density Waves	4-54
4.5.2. Two- and Three-Dimensional Systems.....	4-55

PREFACE

The Instructional Scanning Tunneling Microscope™ (ISTM) and Workbook represent the synthesis of efforts between the University of Rochester's Science and Technology Center, Xerox, Inc., and Burleigh Instruments, Inc. The scanning tunneling microscope (STM) was first used as a teaching instrument at the University of Rochester in 1988. At that time the response from students was overwhelming and the teaching value of the STM became apparent. Using the STM, difficult concepts involving quantum phenomena, such as electron tunneling and atomic structure, can be made dramatically clear to the student in a single afternoon. One should keep in mind that the development of the atomic theory and the various principles of quantum mechanics rest on innumerable experiments, ranging from high-resolution spectroscopy of atoms and molecules (optical, infrared, microwave, and Nuclear Magnetic Resonance) and critical measurements of the electron mass and charge to electron and X-ray diffraction. This has involved complicated experiments that have taken thousands of work-years to develop.

Students must take a tremendous amount of information on faith. In fact, it has been speculated that the demands of the scientific discipline do not necessarily select the minds of the highest I.Q. but those of the highest O.Q. (obedience quotient). The STM opens up the atomic world to the student with experiments that are understandable. In addition, it allows students to better understand quantum mechanical tunneling, a concept that is at the heart of quantum theory and that is extremely difficult to comprehend, even for receptive minds. Perhaps the single most important feature of the STM as a teaching tool is the highly visual impact of its experiments. People are exceptionally well-adapted to learning through visual experience and the STM provides the perfect medium for teaching difficult concepts of atomic structure.

In 1989, the University of Rochester received a seed grant from the DANA Foundation to develop an STM for teaching purposes. Further support was obtained through the National Science Foundation for Photoinduced Charge Transfer. This initiated a three way cooperative program between the University of Rochester's Science and Technology Center, Xerox and Burleigh Instruments. The goals of this program were to develop an STM that was specifically designed for students and could be used by a number of inexperienced users. The instrument, designed at Burleigh Instruments, was engineered to minimize student access to components that were prone to failure, if handled incorrectly, and to provide maximum ease of use. The instrument has an extensive library of image-processing filters that are some of the most advanced developed to date. We had one other objective: to make the device affordable so it could be brought into teaching and laboratory environments in practice, not just in concept.

The application of the STM as a teaching tool is still very new. The experiments we have included in this workbook cover material properties of metals, semimetals, semiconductors, and molecular ordering on surfaces. A direct connection is made between atomic structure and electronic structure. There are eight experiments in all, with each experiment described as a self contained unit. It is our hope that as the STM field develops, more and more experiments will be developed that can be brought into the classroom.

The experiments described in the manual were designed for a junior or senior advanced laboratory. It is assumed that the students have one or two laboratory periods of three to four hours to use the STM. The students can typically get gratifying results on two different surfaces in a single period. For more constrained laboratory scheduling, the students should be able to image graphite and gold within a single period. In terms of handling the logistics in implementing the STM into your course, we have found it possible to have four students per instrument. One group of two prepares tips for their measurements while the other group does an experiment. Depending on the size of the class continued rotation of student throughout a semester generally enables all the students to get hands on experience. In addition, the Instructional STM has full fledged research capabilities and should provide fertile ground for you and your students in more advanced projects.

ARIS is a registered trademark and Instructional STM and True-Image are trademarks of Burleigh Instruments, Inc. Microsoft and MS-DOS are registered trademarks and Windows is a trademark of Microsoft Corporation.

In commendation of γ^e Microscope

Of all the Inventions none there is Surpasses

the Noble Florentine's Dioptrick Glasses

For what a better, fitter guift Could bee

in this World's Aged Luciosity.

To help our Blindnesse so as to devize

a paire of new & Artificial eyes

By those augmenting power wee now see more

than all the world Has ever down Before.

HENRY POWERS 1664

This manual is dedicated to teachers and students everywhere with the philosophy

"I hear and I forget

I see and I remember

I do and I understand"

CHINESE PROVERB

1. INTRODUCTION: The History of Microscopy

The word microscope refers to an instrument capable of magnifying the dimensions of an object so that it can be seen by the human eye. The eye itself is an extraordinary device with a lens and a two-dimensional array for image capture provided by the retina. The resolution of the naked eye is approximately 100 microns. This resolution is determined by the density of rods and cones in the retina that detect the image. In general, the word microscope is confined to resolving structures of less than 100 microns.

1.1. Optical Microscopy

In the past, our ability to observe the tiniest fabric of life was limited by the magnifying power of the optical microscope. The optical microscope uses light in the visible part of the spectrum (380 - 680 nanometer) to magnify objects. The diffraction of light limits the resolution to approximately 0.1 - 0.2 microns, i.e. $\lambda/2n$, where λ is the wavelength of light and n is the index of refraction of the intervening medium. This limit defines a factor of 1000x magnification over the eye. This level of magnification is sufficient to observe microorganisms, bacteria, certain types of viruses, and single cells.

The exact time frame for the development of the first optical microscope is uncertain. References to simple magnifying lenses date back to the Romans. The first simple compound microscope has been attributed to Hans and Zacharia Jansen, who developed a low-power microscope in 1590 using two lenses mounted in sliding cylinders for focus adjustment.¹ The most famous early microscope was developed by Antony van Leeuwenhoek in the 1670s based on a hand-ground single spherical quartz lens.² These lenses are still landmarks in human patience. Some of these lenses are less than a millimeter in radius with magnifying power approaching that of the best compound lens made to date (magnifications close to 500x). This simple microscope had sufficient magnifying power to observe protozoa and other single-cell organisms swimming in rainwater — van Leeuwenhoek's "animalcules." Around the same time Hooke observed that living organisms were comprised of small building blocks he called "cells." This observation was made by studying cross sections of cork trees with a low-power compound microscope of the Jansen design. It was not for another hundred years that this observation would lend itself to the development of the cellular theory of organisms.

The optical microscope made it possible to observe that living things are made up of smaller units called cells and that each cell contains a full complement of genetic information for the whole organism encoded in DNA. We have since learned that cells of multicellular organisms vary in how they differentiate to attain highly specialized functions within an organism. The microscope also made possible a one-to-one connection of disease to bacterial and viral agents, which played a significant role in the development of germ theory. Cellular differentiation, cell aging, and the interconnection between structure and disease are tremendously active fields of research. One can see from these examples the important role an imaging device can play in the field of science and technology. An imaging device enables a tremendous correlation of events to be interpreted in a single experiment.

The utility of microscopy as a teaching tool has also been amply demonstrated in biology. Almost everyone has had the opportunity in high school to visualize a biological specimen with an optical microscope. The teaching value of the microscope, in this regard, follows the old adage that "seeing is believing." The scanning tunneling microscope (STM) should have the same impact on the teaching of chemistry and solid state physics that the optical microscope has had on the teaching of biology.

Figure 1.1 shows a photograph of one of the first microscopes developed by van Leeuwenhoek. It consists of a glass bead which was used as the focusing lens. The lensing action of the bead was controlled by two orthogonal screws that adjusted the position of the lens relative to the sample; the viewer's head had to be placed in the correct position to bring the lens into focus. The first microscopes were extremely crude relative to modern versions of the optical microscope, as can be seen by comparing Figures 1.1 and 1.2. Today's microscopes can be modified to image cells or make a number of spectroscopic measurements related to composition and activity of living cells. It is even possible to utilize lasers in combination with a microscope to focus the laser beam in the cell and use the intense electric fields at the laser focus to manipulate organelles within the cell through a form of "optical tweezers."³ It is interesting to compare Figure 1.1, which represents one of the first optical microscopes, with Figure 1.3, one of the first STMs in common use. The similarity is striking.

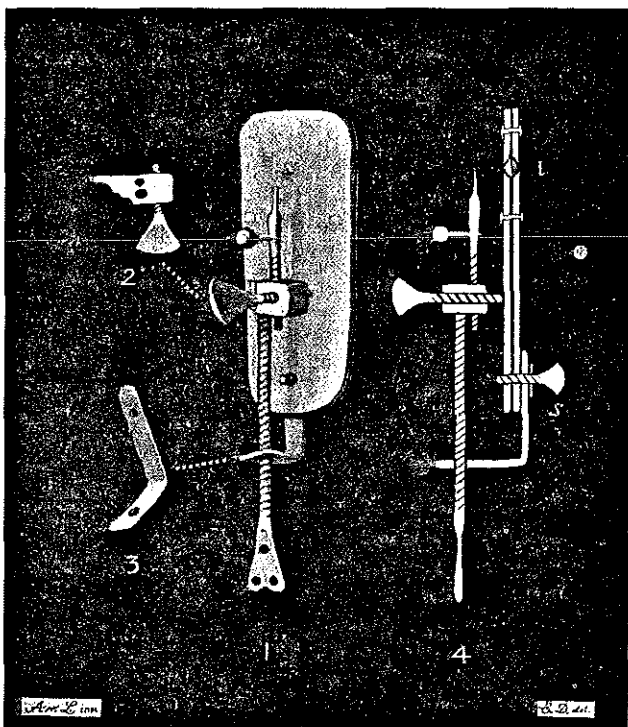


Figure 1.1. A. van Leeuwenhoek microscope, viewed from the back [1] and in diagrammatic section [4]. The specimen, on a movable pin, is examined through a minute biconvex lens [2], held between two metal plates. (Photo courtesy of Harcourt, Brace and Company.)

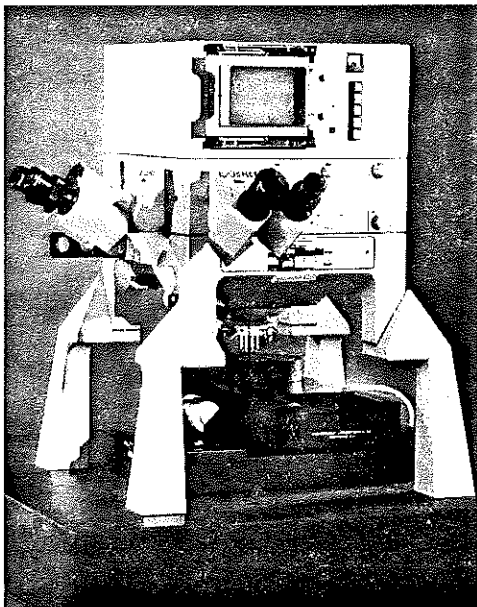


Figure 1.2. Photo of a Zeiss Axiomat NDC-Pol transmitted light microscope.

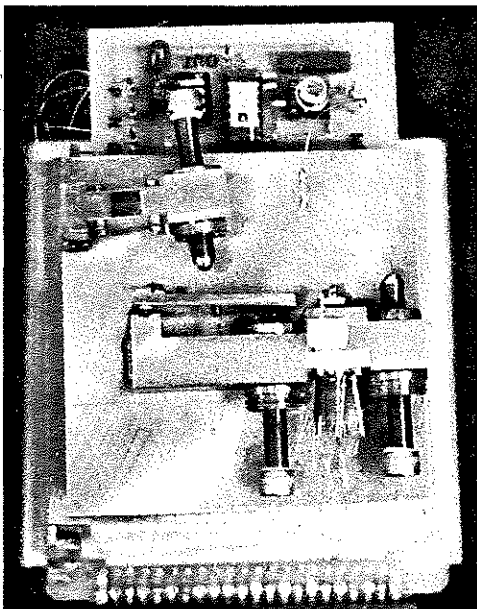


Figure 1.3. A reproduction of the microscope designed by D.P.E. Smith. It was one of the first STMs and was the first commercially sold STM. The design involves a coarse approach lever arm to bring the STM tip within 100 microns and a second lever, with a reduction of approximately 5x, that serves as the fine approach. The tip is brought into tunneling by hand. This very simple design gives high quality atomic resolution. Note the similarity to the screw approach mechanism of van Leeuwenhoek's microscope. A comparison of Figures 1.1, 1.2 and 1.3 gives some indication of what advances we can expect in STMs of the future.

1.2. Electron Microscopy

The resolution of light-based microscopes can be extended by using shorter wavelengths. There have also been some very promising recent developments in the area of X-ray based microscopes. The problem in using shorter wavelengths, however, is the need for suitable focusing elements and light sources. These light sources must have wavelength ranges with reasonable transparency so that light can penetrate the sample. In principle, an X-ray based microscope should be able to attain atomic resolution if these considerations can be addressed.

Following the discovery of the optical microscope, the next major advance awaited the hypothesis of de Broglie that both matter and light have wave properties, i.e.:

$$\lambda = \frac{h}{p} \quad (1.1)$$

where λ is the electron wavelength, h is Planck's constant, and p is the electron momentum ($m_e v$).⁴ The discovery by Davidson and Germer that electrons are diffracted by a regular lattice demonstrated that matter did indeed have wave properties.⁵ Davidson and Germer found that wavelengths of electrons could be tuned by simply changing the voltage over which an electron beam is accelerated. For potential drops on the order of 10,000 volts ($p = (2m_e V)^{1/2}$ in Equation 1.1), the electron wavelength can be made less than an angstrom (\AA).⁶

By analogy with the optical microscope, it is possible to use the wave properties of electrons for microscopy. With a diffraction-limited focusing system, electron waves have the potential of attaining subangstrom resolution. The possibility of using this very short wavelength in microscopy was not lost on many researchers. The transmission electron microscope (TEM) was developed in 1932 by E. Ruska using focusing elements constructed essentially from induction coils for magnetic field focusing.⁷ The first demonstration of electron microscopy achieved 17x magnification. It was not until 40 years later that the atomic resolution limit was achieved.

Modern transmission electron microscopes are especially well-adapted for the study of regular lattices. They have a very wide field of view in which specific features can be magnified to the atomic limit by focusing the electron beam to a specific area. There are some beautiful recent examples in which the lattice structure of individual quantum dots (colloidal semiconductors) of CdSe as small as 100 \AA have been resolved (see Figure 1.4).⁸ As with the optical microscope, the electrons bombarding the sample can also be used for spectroscopy that provides both spatial and elemental analysis capabilities. The TEM requires that the samples be housed in a high vacuum chamber to avoid electron scattering and adsorption by intervening gases. This prevents the instrument from being used for *in situ*, non-destructive evaluation of materials. Nevertheless, much of our understanding of the atomic structure of many materials comes from TEM studies. A cursory review of any text on microbiology indicates the enormous impact the TEM has had on our understanding of the cellular structure and biological function of macromolecules.

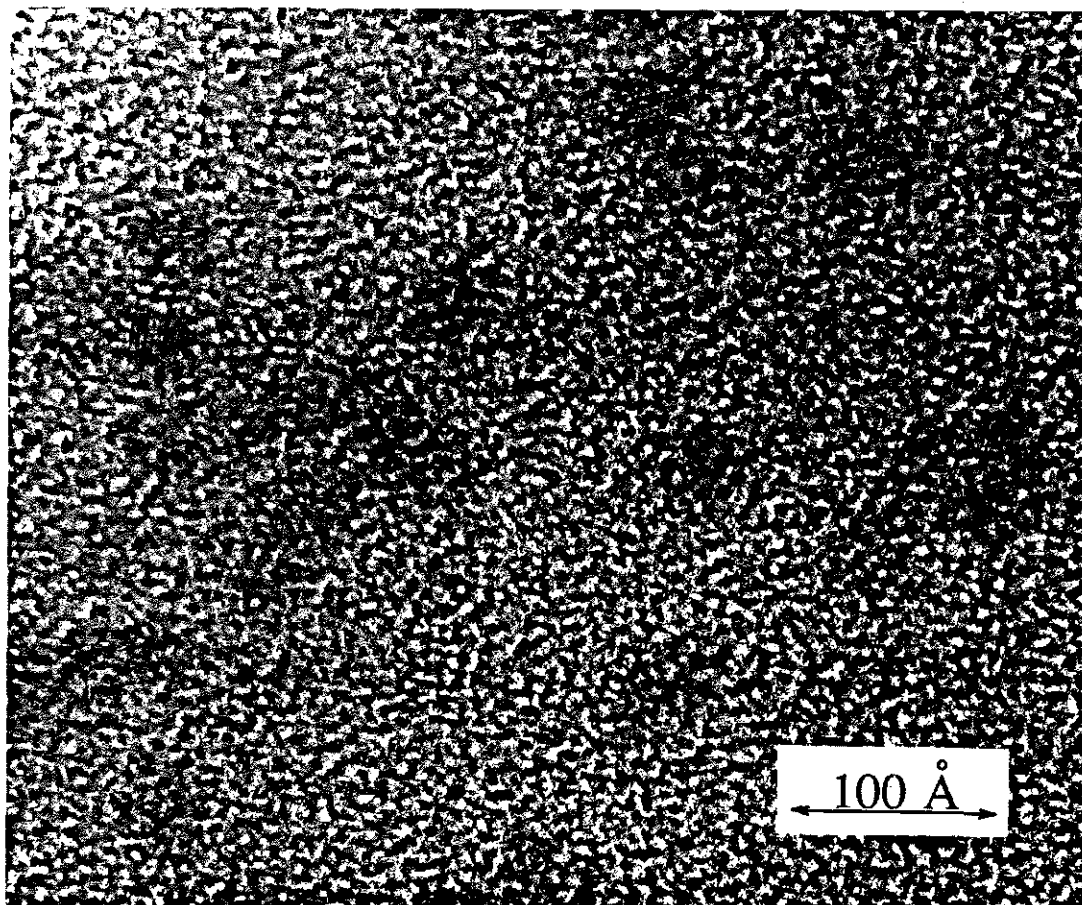


Figure 1.4. Bright field electron transmission micrograph of quantum dots of CdSe semiconductors. The size of the semiconductor cluster is approximately 60 Å. This work demonstrated that these small particles, which are between molecules and solid state crystals, obtain the bulk crystal structure. The individual lattice planes are observable. This was an important issue regarding the structural properties of these materials. The TEM was the ideal tool for this problem. (Photo courtesy of Lou Brus.)

The Scanning Electron Microscope (SEM) was developed in parallel with the TEM. This microscope images the surface of materials by analyzing the intensity of a reflected electron beam and any secondary electrons produced by an incident electron beam.⁹ Non-conductive samples must be coated by a thin film of gold to avoid charging effects. An electron beam is scanned across the surface in an X-Y fashion to obtain the surface topology in a point-by-point manner. Zworykin, Hillier, and Snyder obtained the first topographic images using this approach in 1942, obtaining approximately 1 micron resolution. With today's microscopes the resolution of the SEM is typically on the order of 100 Å but can approach 50 Å. SEM resolution is limited to 50 Å, primarily by the focus of the electron beam. However, the evaporated gold layer consists of grains that are also on the order of 50 Å which tends to distort any features less than the grain size. The analysis of both reflected and secondary electrons provides a stronger contrast mechanism relative to electron transmission of the TEM; SEM images are also easier to interpret (see Figure 1.5). The uses of the SEM include the study of biological materials, crystal growth, and optical components and numerous other applications in semiconductor nanotechnology. As with the TEM, the sample must be housed in a high vacuum chamber. This necessity and the metallic coating procedure make SEM microscopy unamenable to *in situ* studies.

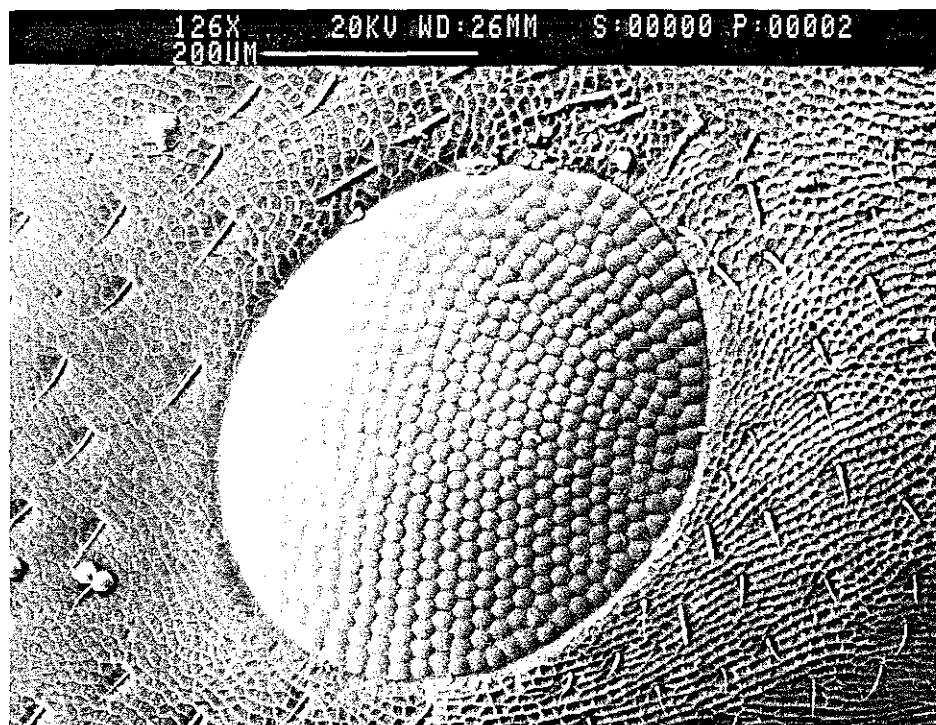


Figure 1.5. An SEM micrograph of an ant's eye. (Photograph courtesy of Brian McIntyre.)

One other type of electron microscopy should be mentioned here. Field Emission Microscopy (FEM) and Field Ion Microscopy (FIM) were both developed by E. W. Muller, in 1936 and 1950 respectively.¹⁰ This form of microscopy analyzes emitted electrons (FEM) or emitted ions (FIM) from a very sharp tip in the presence of a strong accelerating field. As with other electron microscopes, the resolution is limited by the radius of the tip and the particle wave diffraction. This form of microscopy is schematically drawn in Figure 1.6. The different atoms from the tip are accelerated off the tip at different angles and show up as individual spots on a phosphor screen. Individual atomic features were resolved with this method in the 1960s. This particular microscopy has been particularly important in the understanding of surface states, surface reactions, and atom diffusion on surfaces. Although it is fairly limited in its applications, this microscopy played a key role in our understanding of the atomic resolving power of the STM; the tips used for the STM are essentially identical to FEM and FIM point probes.

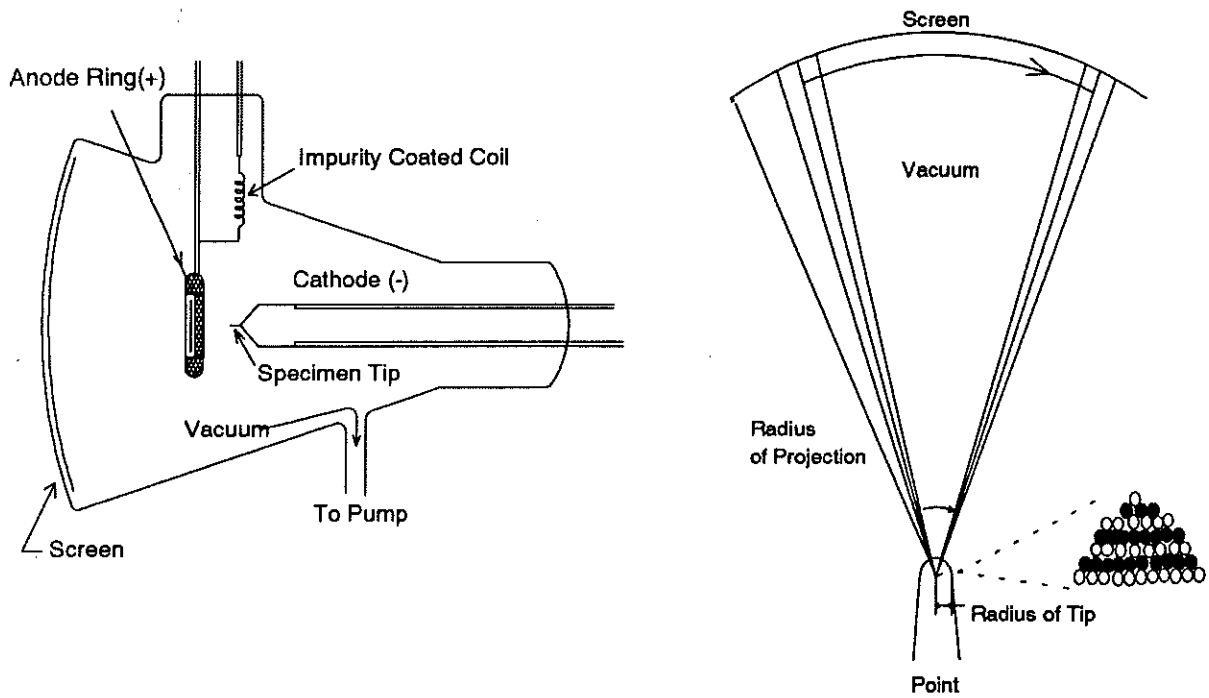


Figure 1.6. Field Emission Microscopy. This figure shows schematically how a very sharp tip can be brought near a ring electrode to image atomic ions or electrons that are emitted from the tip and accelerated to a phosphor screen for detection. This is a very elegant approach to attaining atomic resolution without any focusing elements. As long as the tip is sharp enough and the geometrical distance to the phosphor is far enough, individual atomic features can be observed. This was the first microscope to give atomic information. This microscopy also clearly revealed the atomic structure of tips, making it possible to achieve atomic resolution in STM studies. (Adopted from reference 8.)

1.3. Acoustical Microscopy

The other wave source that has been used for imaging is based on acoustics.¹¹ The distinct advantage of sound waves as a probe is that they can penetrate optically opaque materials and reveal hidden structures. One of the most important uses of ultrasonics, although not strictly microscopy, has been in biomedical applications for examining internal organs and fetal examinations. The problem in developing an acoustic microscope was primarily the lack of a two-dimensional method of capturing spatial variations in acoustic intensity. In the case of the optical microscope, the human eye serves this purpose; and, for electron microscopes, phosphor screens convert the electron density to a visual format; but there are no simple analogies for acoustics that have sufficient sensitivity. The acoustic microscope required the development of an acoustic lens and methods of rastering a focused acoustic spot across a sample, similar to the SEM. Either the sample or the acoustic lens is rastered and the acoustic intensity measured as a function of the position of the focused spot. The engineering solutions used to move the lens and collect the image in a point-by-point fashion helped set the stage for the development of the STM.

The resolution of the acoustic microscope follows the same criteria as that of the optical microscope, i.e. wave diffraction limits the resolution to $\lambda/2n$. However, there is one additional limitation in acoustic microscopy: a coupling fluid is needed to transmit the sound wave to the object under study. For a fixed speed of sound in the coupling fluid, the only way to improve the resolution is to go to higher frequencies to achieve shorter wavelengths. The problem, however, is that acoustic attenuation in the coupling fluid generally scales quadratically with frequency. Thus, higher frequencies are completely absorbed and no sound energy is reflected to produce an image. If water is used as the coupling fluid, the maximum resolution of an acoustic microscope is on the order of 0.2 microns. If super-fluid liquid helium at extremely low temperatures is used, the acoustic attenuation problems can be overcome and, in theory, acoustic wavelengths short enough to image individual molecules can be attained. This remains a fascinating field of endeavor.

One real advantage of acoustic microscopy is that the magnified image is constructed through a different contrast mechanism than that of optical microscopy. This point is demonstrated in Figure 1.7, which shows a comparison of the images obtained with an optical microscope and an acoustic microscope. The optical microscope picks up features that absorb visible light differently and the acoustic microscope differentiates structures through variations in acoustic attenuation. In cases where the mechanical properties of a material are of interest at a microscopic level, acoustic microscopy is a more important probe than optical microscopy: some examples include thermal conductivity, elasticity, stress fractures, and phase-transition phenomena. The comparison of the image constructed by a scanning acoustic microscope and an optical microscope highlights the need for several different types of microscopy. Each form of microscopy obtains a magnified image by different contrast mechanisms and thus provides more information about a structure.

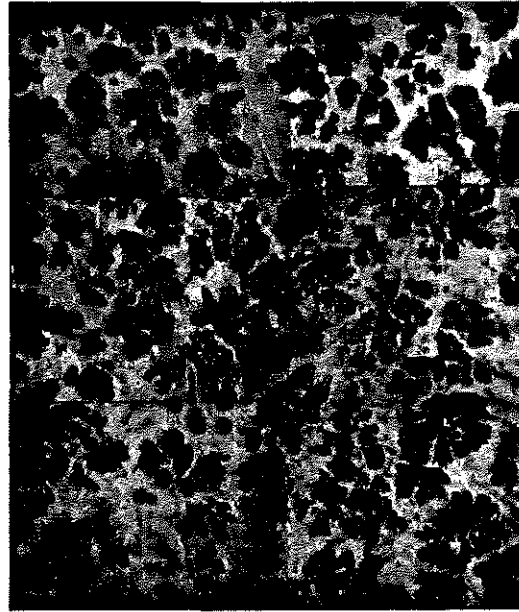
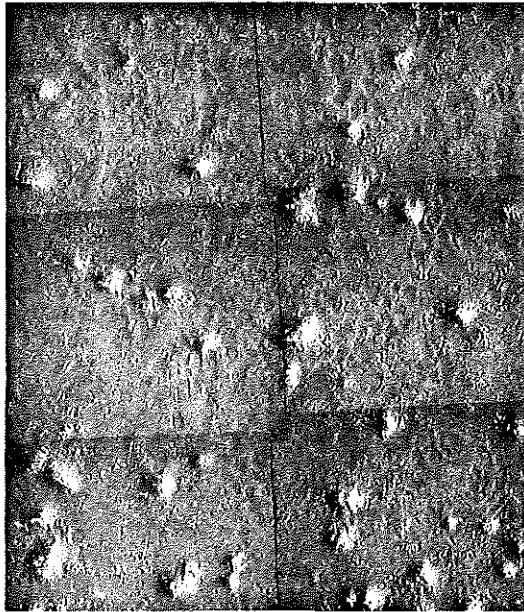


Figure 1.7. A comparison of images obtained from acoustic microscopy and optical microscopy for Co-Ti alloy: a) optical, b) acoustical (1100 MHz) image. Notice that the acoustic microscopy clearly brings out the different phases of the Co-Ti alloy. This comparison demonstrates the importance of different contrast mechanisms providing different information, (100 μm = 1 cm). (Photo courtesy of Calvin Quate.)

1.4. Scanning Probe Microscopy

The above are all examples of microscopy which rely on the interaction of a wave source with an object that affects either the index of refraction (wave speed) or the absorption. One can also obtain magnified images by using a scanning probe to obtain information on an object, much like a blind person's cane being swept across an object. This particular form of information gathering depends on a localized interaction with a point source rather than a wave source. In this form of microscopy only the surface topology is being sampled. The probe does not sample features below the surface, as would be possible for a wave-source microscope. The tip of the probe surveys the topology through a number of possible surface-tip interactions. These interactions can vary from attractive to repulsive atom-atom interactions to magnetic forces, electrostatics, or the exchange of charge (ions or electrons). All these different types of tip interactions with a surface form the foundations of different kinds of microscopy, here referred to collectively as scanning probe microscopy (SPM). The resolution of these different forms of microscopy depends on the distance-dependence of the surface-tip interaction and the radius of the tip. In the case of the STM, the image contrast depends on electron tunneling to produce a current which falls off exponentially with distance ($1/e^2$ per Å, as explained below). This distance sensitivity is the same as the atomic dimensions and is ultimately responsible for the atomic resolution of the STM.

The first scanning probe microscope was the scanning profilometer.¹² This instrument can be thought of as a sophisticated record player. A stylus probe is brought into contact with a surface and mechanically scanned across it. The image is constructed as variations in the deflection of the stylus. The resolution originally obtained with this instrument was limited by the sharpness of the stylus probe and its deflection sensitivity. (In the blind person's cane analogy, this resolution limit would be equivalent to the cane point and the sensitivity of the person's touch.) This instrument had all the essential features of today's SPMs. Related research by Young and co-workers at the National Institute of Standards and Technology, based on field emission current measurements, led to the development of the "surface topographiner,"¹³ which was very similar in concept to the STM. The main difference between the topographiner and the STM is that the topographiner's contrast is based on high voltage field emission, rather than tunneling. Again, the resolution is limited by the sharpness of the tip to approximately 1000 Å.

The key breakthrough in achieving atomic resolution in scanning probe microscopy was the pioneering work of Gerd Binnig and Heinrich Rohrer.¹⁴ They realized that if a metallic tip could be maintained 10 Å from a surface, tunneling currents in the nanoamp range could be easily detected. They also realized that the main technical obstacle was the mechanical problem of keeping a tip that close to a surface, especially since noise sources from thermal drift and mechanical vibrations would limit the resolution. Normal acoustics in mechanical components typically have amplitudes well in excess of 10 Å, which would average out the height variations as the tip was scanned. The first STM was constructed in 1981 using superconducting magnetic levitation to mechanically isolate the STM. This first STM showed remarkable promise, achieving a resolution approaching 10 Å, an order of magnitude better than anticipated.

In the continued evolution of the STM, Binnig and Rohrer found that different tip fabrication procedures produced strong spatial variations in the tip surface which would lead, in certain cases, to one atom being closer to the sample than all the others. Since the tunneling current is highly distance-dependent, the single atom provides an image contrast mechanism that has the right dimensions to give atomic resolution. Essentially Binnig and Rohrer discovered that a mechanical probe could be made atomically sharp. This discovery, and all the wonderful technical achievements that went with it, laid the foundation for the field of scanning probe microscopy.

During the initial development phase of the STM, Binnig and Rohrer experimented with several different designs. Each design had features to minimize acoustics, including one constructed from a glass infrastructure, which was huge by comparison to current versions. During the course of these studies Binnig and Rohrer realized that the STM should be made as small and rigid as possible to move the acoustic resonances outside of the scanning frequency and minimize vibrational noise on the image. The various STMs developed by Binnig and Rohrer between 1981 and 1986 are shown in Figure 1.8. As the underlying mechanism for the atomic resolution and the effects of vibrations on the operation of the STM became better understood, more and more simple designs evolved. One can see from this figure how, in just a few years, the STM has become a very elegant and compact instrument.

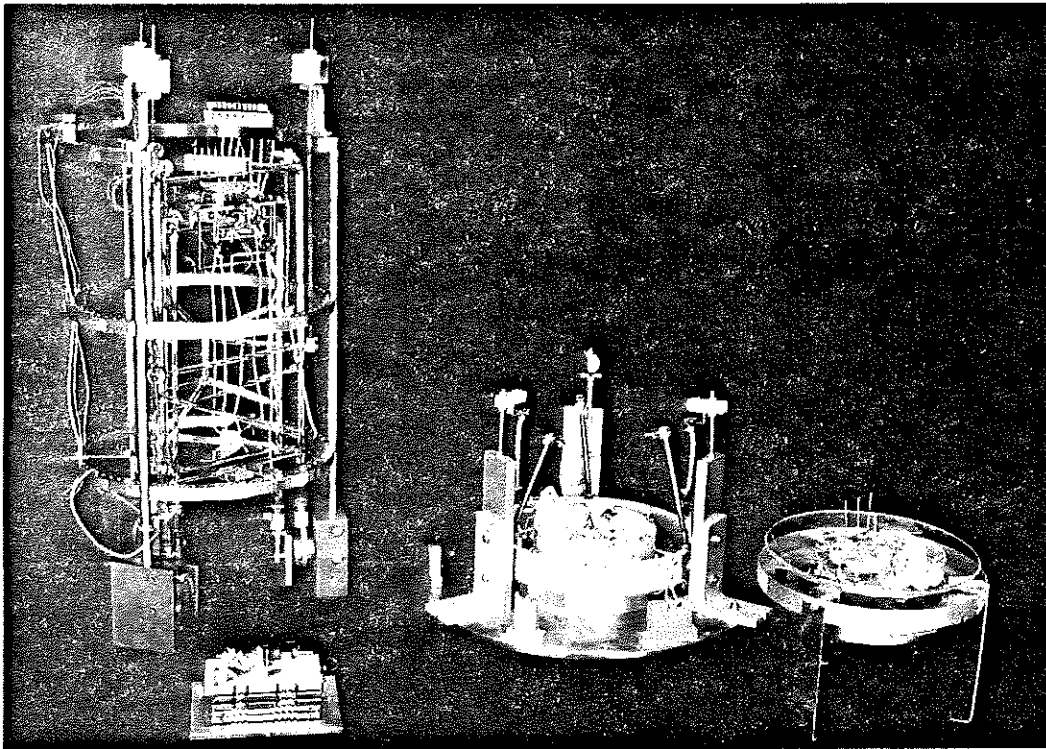


Figure 1.8. The evolution of the STM. The far right instrument was the first STM to resolve atomic steps. The second from the right is the first ultra high vacuum (UHV) STM, which solved the important Si(111) 7x7 surface structure. The larger STM featured in the upper left-hand corner was the next generation UHV STM, the first one to resolve atomic features of metals and single atom adsorbates. The lower left-hand corner shows the "Zurich Pocket STM," one of the most common STMs in use today. (Photo courtesy of G. Binnig.)

1.5. The First Important Discovery Using an STM

The first images that revealed atomic details were those of gold surfaces, Au(110), in 1983. However, the most important problem solved by the use of the STM was the so-called 7x7 reconstructed surface of silicon.¹⁵ The observation of a very unusual 7x7 Low Energy Electron Diffraction (LEED) pattern on clean surfaces of silicon was a long-standing mystery. This problem was especially important since silicon is still primarily the only semiconductor that has the right surface properties for solid state devices. The STM solved this problem within minutes of obtaining the first atomic resolution image of a silicon surface. The 7x7 structure arises from the relaxation of the silicon surface atoms to a new unit cell on the surface with hexagonal symmetry. This unit cell consists of 12 atoms on its top layer; it is 7x7 times larger than a bulk-terminated unreconstructed surface of silicon cut along (111) orientation. A representative STM image of silicon is shown in Figure 1.9 to illustrate this point. Solving this problem demonstrated the enormous potential of the STM in understanding structure and electronic properties at the atomic level. The first demonstration that the STM could be used for *in situ* studies under normal room conditions was demonstrated in 1985 with the atomic resolution of graphite surfaces. The rest, as we say, is history.

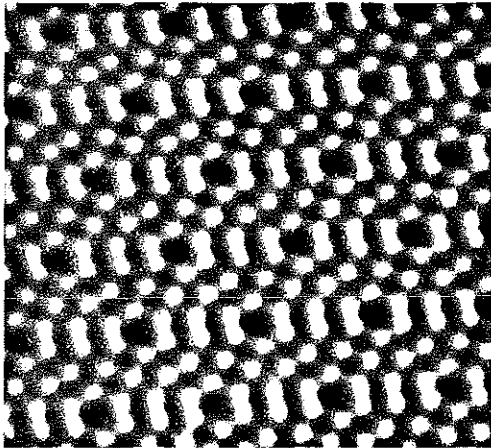


Figure 1.9. Si(111) surface showing clearly the symmetry of the 7x7 reconstructed surface. This image was taken under UHV using a Burleigh ARIS®-6100 STM.

1.6. Atomic Force Microscopy

Following the introduction of the STM, a number of new scanning probe microscopes have been developed that use key components of the STM. The most important is the atomic force microscope (AFM), a collaborative effort between Binnig, Quate, and Gerber.¹⁶ In atomic force microscopy a tip or cantilever is brought within interatomic separations of a surface, such that the atoms of the tip and surface are at the repulsive part of the interatomic potentials. In this microscopy the tip literally acts as the blind person's cane described above. As the tip is rastered along the surface, it bounces up and down with the contours of the surface. By measuring the displacement of the tip, one can map out a surface topology with atomic resolution. The deflection of the cantilever can be detected either through a piggy-backed STM or through optical methods (laser beam bounce or interference methods). This microscope is essentially identical in concept to the scanning profilometer, except that the deflection-sensitivity and resolution are improved by orders of magnitude. The most important achievement of the AFM is that it has opened up the atomic window to non-conducting materials. There are a large number of applications for the AFM, including biological systems, polymers, and a host of insulator and semiconductor materials. A number of very exciting applications have recently been reviewed.¹⁷

This historical perspective is intended to place the STM in the proper context with other microscopes. The optical microscope opened our eyes to the world of microorganisms and the cellular composition of larger life forms. With the advent of electron microscopes, we obtained our first glimpses of the details of structure at the atomic level. The real power of the STM is the wide variety of materials that can be readily studied at the atomic level, with the distinct advantage that the atomic positions are well-defined in the lab frame. With the combination of AFM and STM microscopes, one can now obtain information on structure and even manipulate structure at the atomic level.

2. OPERATING PRINCIPLES OF THE STM

2.1. How the STM Works

There are five scientific and technical processes or ideas that the STM integrates to make atomic resolution images of a surface possible. Each of these processes was used in other areas of science before the invention of the STM.

- The principle of quantum mechanical tunneling.
- Achievement of controlled motion over small distances using piezoelectrics.
- The principle of negative feedback.
- Vibration isolation.
- Electronic data collection.

This Chapter discusses each of these five concepts. The most detail is provided on the process of quantum mechanical tunneling, since this is the fundamental concept that allows the microscope to work. At the end of the discussion of all these concepts, one can see how they integrate to make an STM.

2.2. Quantum Mechanical Tunneling

Quantum mechanical tunneling is not some obscure process that only occurs under extreme conditions in a crowded basement laboratory of a research university. Quantum mechanical tunneling explains some of the most basic phenomena we observe in nature. One example is the radioactive decay of plutonium. If quantum mechanical tunneling did not occur, plutonium would remain plutonium instead of changing into elements lower on the periodic chart. Plutonium converts to other elements when 2 neutrons and 2 protons are ejected from the nucleus because of tunneling. Even the fundamental force that binds atoms into molecules can be thought of as a manifestation of quantum mechanical tunneling. In this lab, we will look at how tunneling manifests itself in another way. We will attempt to understand how a single electron starts out in one metal and then reappears in another metal, even though they are not touching.

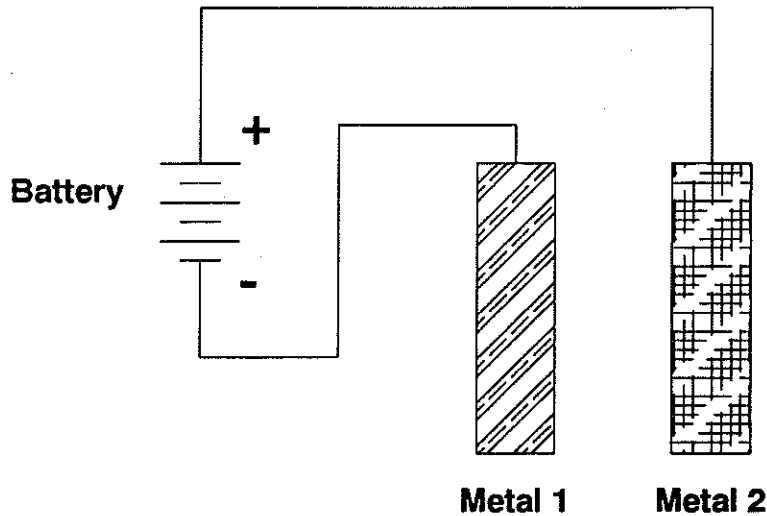


Figure 2.1. Two pieces of metal, each connected to a battery terminal. While the metals are well separated no current flows through the battery.

To begin, let's examine what electron tunneling means in the real world. Consider two pieces of metal. Metals are good conductors of electricity, i.e. electrons can move very easily and quickly from one end of the metal to the other. Imagine connecting one of the pieces of metal to the negative terminal of a battery and the other piece of metal to the positive terminal, as shown in Figure 2.1. If the metals are not touching, no current will flow through the battery. The electrons are free to move around the metal but cannot leave it. The electrons are analogous to water in a reservoir that is blocked by a dam. They can move about the reservoir but have no access to the river below. If the metals are brought together so that they touch, current will flow freely through the contacting area. The electrons have a free path from the negative terminal to the positive terminal of the battery. This current flow is analogous to opening up the gates of the dam and allowing the water to flow down the river into the ocean.

The unusual experimental feature of tunneling is this: when the metals are brought together, but are not quite touching, a small electric current can be measured. The current gets larger the closer the metals are brought together, until it reaches its maximum value when the metals are touching. The concept is analogous to making the dam thinner and thinner by removing cement and noticing that more and more water is leaking through the walls. However, there is a difference between the two analogies. The water physically moves through the pores between the cement, while the *electrons do not move in the space between the metals: they just suddenly appear in the other side*. The metals must be only 10 angstroms apart to produce detectable tunneling current. Figure 2.2 shows current as a function of the separation between metals [a]. Also plotted in this graph is the measured tunneling current if quantum mechanical tunneling did *not* occur [b]. The distances involved are so small that special tools are needed to adjust the distances or the small electric currents will not be detected. We will describe these tools in the section on piezoelectrics (see Section 2.4).

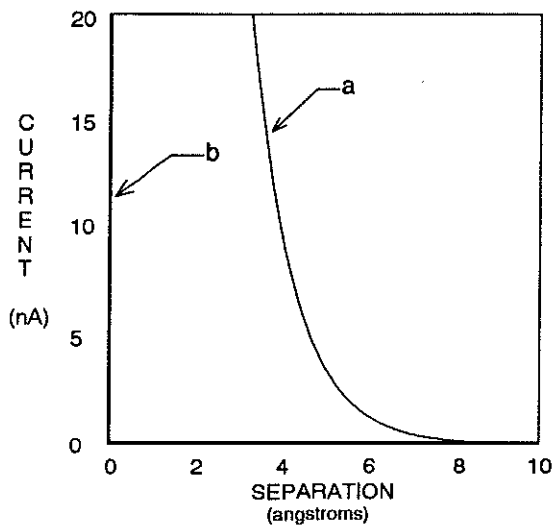


Figure 2.2. This graph shows a plot of current flowing through the battery as a function of the separation of the metals. [a] shows an exponential increase in current as the metals get closer; [b] in the absence of quantum mechanical tunneling, no current flows until the metals touch.

To understand why these small currents occur, the energies involved as the electron moves between the metals must be considered. An electron's energy can be split into two contributions: kinetic energy and potential energy. Kinetic energy (the energy of motion) is large for electrons moving fast and small for electrons moving slowly. Potential energy is the energy available for an electron to convert to kinetic energy if it moves along an electric field. Figure 2.3 plots the potential energy of the electron as it travels from one metal to the other metal. The potential energy shown neglects the complicated aspects of metals, including extra charges from atoms and other electrons on the metals, but does include the general concepts. The potential energy is lower in Metal 2 because this side is connected to the positive terminal of the battery (the terminal to which the electrons are attracted). There is also a large potential energy between the two metals. This is what tends to keep electrons inside their respective metal.

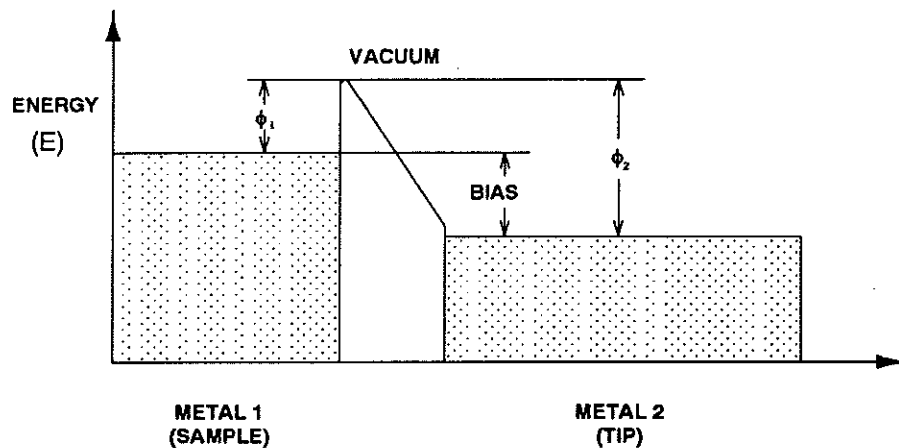


Figure 2.3. The potential energy that the electrons encounter as they travel from one metal to the other. ϕ_1 and ϕ_2 indicate the minimum amount of energy required to remove an electron from the metals (the work function). Note that Metal 2 is attached to the positive terminal, so its electrons have lower potential energy.

This picture shows that electrons are free to move around in their respective metals but cannot leave them. No electron in a metal has sufficient kinetic energy to go over the barrier.

One of the basic tenets of quantum mechanics is that electrons have both a particle and a wave nature. So we should picture the electron not as a hard ball impinging on the barrier, but as a cloud. The size of the cloud is related to the wavelength of the electron (a few angstroms). When the cloud collides with the barrier, part of the cloud may penetrate it. For thick barriers, however, the cloud will be reflected like a hard particle (see Figure 2.4). For thin barriers, however, part of the cloud may penetrate the barriers and appear on the other side. This process is called tunneling because the electron does not have enough kinetic energy to travel over the barrier, but is able to exist on the other side (see Figure 2.5). It is as if the electron found a way to dig a tunnel *through* the barrier.

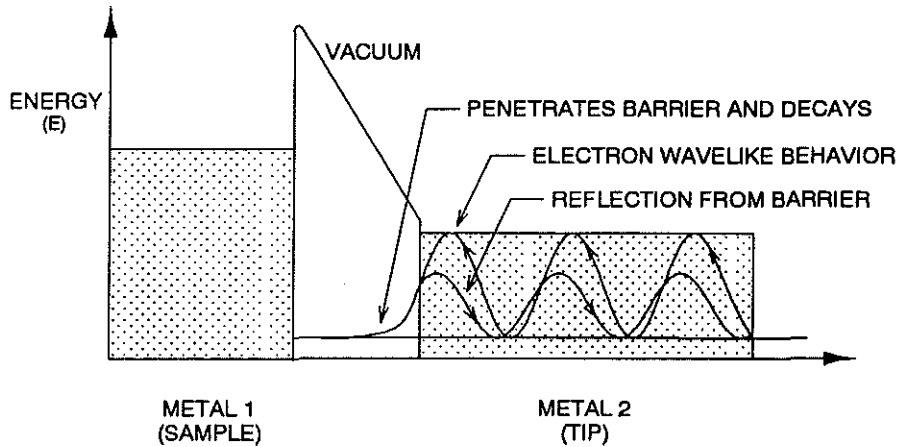


Figure 2.4. Electrons have a wave and particle nature. Upon impinging on the barrier they will be reflected from and penetrate the barrier. If the barrier is too "thick," the electron cloud will decay and no electron will tunnel to the other side of the barrier.

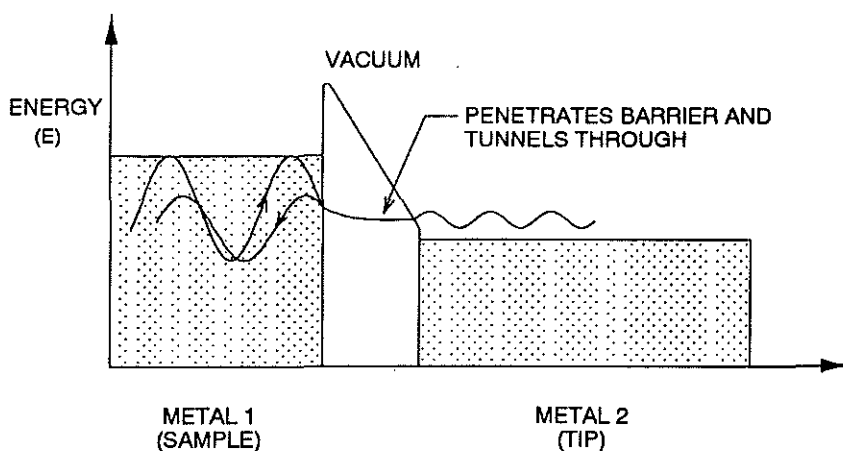


Figure 2.5. If the barrier is "thin," the electrons might tunnel and transmit through the barrier, thus creating an electrical current that can be measured.

In the scanning tunneling microscope, one of the metals is the sample being imaged (sample) and the other metal is the probe (tip). The sample is usually flatter than the probe, as shown in Figure 2.6. If the probe is sharpened into a tip it will most likely have one atom at the end. All of the tunneling electrons will pass through this atom. As we will discuss later, this feature leads to the atomic resolution capabilities of the microscope.

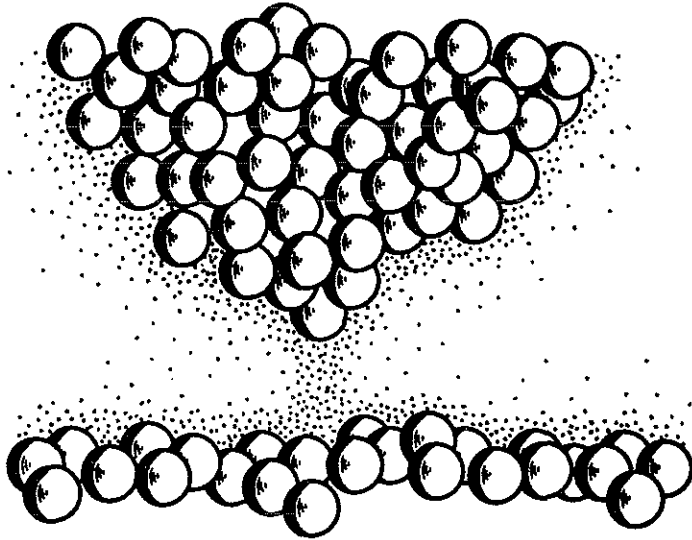


Figure 2.6. The tip consists of clusters of atoms in which one atom usually sticks out more than the others. This atom is primarily responsible for tunneling between the tip and sample.

2.3. Quantifying the Tunneling Process

Using Schrödinger's equation of quantum mechanics, we can actually predict how tunneling current increases as separation between two metals decreases. However, the final results of your tunneling experiments can be understood without knowing quantum mechanics. This more complete description is not necessary for understanding how the STM works; it therefore may be thought of as supplemental.

The Drude model of a metal states that the potential energy of a metal is given by the solid line in Figure 2.3. The energy of all the electrons in the metal is lower than the height of the wall. The difference in energy between the most energetic electron and the vacuum energy is called the workfunction and is denoted by the symbol ϕ .

The wave nature of an electron, illustrated in Figures 2.4 and 2.5, is critical to explaining tunneling. The movement and shape of the electron wave is governed by Schrödinger's equation, which might be thought of as the quantum mechanical analog of Newton's equation of motion, $F = ma$.¹

In the STM, tunneling takes place between the tip and the sample. A complete description of the tunneling process requires a solution of the three-dimensional form of Schrödinger's equation, which has the general form:

$$[H]\psi = E\psi \quad (2.1)$$

where $[H]$ is the Hamiltonian operator and E is the total energy eigenvalue. The time dependent Schrödinger's equation can be expressed as:

$$\frac{-\hbar^2}{2m} \nabla^2 \psi(r,t) + U\psi(r,t) = i\hbar \frac{\partial \psi(r,t)}{\partial t} \quad (2.2)$$

In this equation:

\hbar is Plank's constant, a fundamental quantity in quantum mechanics, divided by 2π

m is the mass of the electron

$\psi(r,t)$ is the wave representation of an electron

U is the potential barrier function form

∇^2 is the Laplacian operator

$\frac{\partial}{\partial t}$ is the partial time derivative

i is $\sqrt{-1}$

For our purpose it is sufficient to use a one-dimensional analysis, which the Schrödinger equation above is given by:

$$\frac{-\hbar^2}{2m} \frac{\partial^2 \psi(x,t)}{\partial x^2} + U(x)\psi(x,t) = i\hbar \frac{\partial \psi(x,t)}{\partial t} \quad (2.3)$$

where the equation:

$$\psi(x,t) = A e^{i(-kx-\omega t)} + B e^{i(kx-\omega t)} \quad (2.4)$$

is the plane wave representation for an electron wavefunction of wavenumber $k = 2\pi/\lambda$ and angular frequency ω .

In addition, we assume a steady-state (time-independent) situation in which electrons of energy $E(x, t) = E$ encountering a uniform potential barrier of height $U(x, t) = U(x)$ are continuously flowing from one metal to the other. It is then necessary to solve only the one-dimensional steady-state Schrödinger equation, given by:

$$\frac{-\hbar^2}{2m} \frac{\partial^2 \psi(x)}{\partial x^2} + U(x)\psi(x) = E\psi(x) \quad (2.5)$$

where E is the kinetic energy of the electron. Note that $U(x)$ is the potential energy of the electron as a function of position, as shown in Figure 2.3. $U(x)$ is smaller than the electron energy in the metals and larger than the electron energy in the barrier. For simplicity we can assume $U(x) = U_0$ a constant in the barrier.

In the metal, the general solution to the above equation is given by:

$$\psi(x) = Ae^{-ikx} + Be^{+ikx}, \quad k = \sqrt{\frac{2m(E - U_0)}{\hbar^2}} \quad (\text{Metal 1}) \quad (2.6)$$

$$\psi(x) = Ee^{-ikx} + Fe^{+ikx} \quad (\text{Metal 2}) \quad (2.7)$$

and in the barrier (the classically forbidden region) the solution is:

$$\psi(x) = Ce^{-\mu x} + De^{+\mu x}, \quad \mu = \sqrt{\frac{2m(U_0 - E)}{\hbar^2}} \quad (\text{barrier}) \quad (2.8)$$

Equations 2.6 and 2.7 show that the phase of the electron wavefunction varies uniformly in the metals. The wavelength is $\lambda = 2\pi/k$. Higher energy electrons have a smaller wavelength. When a high energy electron wave encounters the boundary of the metal, it "leaks out" a small amount, as discussed in the previous section. The "intensity" of the electron wave decays as a function of distance from the boundary. Mathematically, the argument of the exponential function becomes real and the electron wavefunction decays. (For imaginary arguments, the wave function would have oscillatory behavior.)

To gain a quantitative insight into the electron tunneling phenomena, it is necessary to derive an expression for the transmission coefficient, i.e. the transmitted flux from the sample to the tip through the barrier of width L . The barrier is considered wide but finite, such that the electron wavefunction exponential decay in the barrier is significant. Furthermore, the electron wavefunction and its first derivative must be continuous (join smoothly) at the sample-barrier and tip-barrier boundaries to conserve energy and mass. If we set up a coordinate system in which the surface of the sample (Metal 1) is at $x = 0$ and the tip (Metal 2) is at $x = L$, and apply the boundary conditions for continuity:

$$A + B \approx C$$

$$ik(A - B) \approx -\mu C \quad (2.9)$$

(at the sample surface, $x = 0$) where D , the amplitude of the reflected wavefunction at the sample-barrier boundary, is neglected, since $D \ll A, B, C$. However, D is *not* insignificant at the tip-barrier boundary. At the tip-barrier boundary, $x = L$, continuity would require:

$$Ce^{-\mu L} + De^{\mu L} = Fe^{ikL}$$

$$-\mu Ce^{-\mu L} + \mu De^{\mu L} = ikFe^{ikL} \quad (2.10)$$

Solving for B/A at $x = 0$, by solving for C and substituting for it, we get:

$$\frac{B}{A} \approx \frac{-(1 + ik\delta)}{1 - ik\delta} \quad (2.11)$$

where δ is $1/\mu$, A is the amplitude of the electron wavefunction in the sample surface incident on the barrier, and B represents the amplitude of the reflected wavefunction. The reflection coefficient (R) for the wavefunction is then defined as:

$$R \approx \left| \frac{B}{A} \right|^2 \quad (2.12)$$

where $| \quad |^2$ represents the product of a complex number and its conjugate. In this case, it represents the relative intensities of the incident and reflected wavefunctions.

An electron incident at the barrier will either be reflected or transmitted through the barrier. In terms of probability or frequency of occurrence, $R+T = 1$, where R and T are the reflection and transmission coefficients. Thus:

$$R \approx \left| \frac{B}{A} \right|^2 = \frac{-(1+ik\delta)}{1-ik\delta} \cdot \frac{-(1-ik\delta)}{1+ik\delta} \approx 1 \quad (2.13)$$

and, therefore:

$$T = 1 - R \approx 0 \quad (2.14)$$

which indicates that, for an infinitely wide barrier, no electrons would be found in the barrier region. Nevertheless, dividing the first of the sample vacuum-barrier boundary conditions by A results in:

$$1 + \frac{B}{A} \approx \frac{C}{A} \quad (2.15)$$

The probability of finding an electron in the barrier region at $x = 0$, due to quantum tunneling, is given by:

$$\left| \frac{C}{A} \right|^2 \approx \frac{4(k\delta)^2}{1+(k\delta)^2} \quad (2.16)$$

To find the effective tunneling transmission coefficient, $\left|\frac{F}{A}\right|^2$ i.e. the relative probability or frequency of occurrence of an electron tunneling out of the sample surface, across the sample-tip-barrier region, and into the tip, combine the tip-barrier boundary equations (at $x = L$) and Equation 2.16 to get:

$$\frac{F}{A} \approx \frac{-4ik\delta}{(1-ik\delta)^2} e^{-L(\mu+ik)} \quad (2.17)$$

which produces the desired quantitative result:

$$T(E) \approx \left|\frac{F}{A}\right|^2 \approx \left(\frac{4k\delta}{(1+(k\delta)^2)}\right)^2 e^{\frac{2L}{\delta}} \propto e^{-L\sqrt{2m\phi/\hbar^2}} \quad (2.18)$$

where:

$$k^2 = \frac{2mE}{\hbar^2}$$

$$(k\delta)^2 = \frac{E}{(U_0 - E)} = \frac{E}{\phi} \quad (2.19)$$

Substituting typical numbers of $\phi = 5 \times 10^{-19}$ joules, $m = 9 \times 10^{-31}$ kilograms, and $\hbar = 1.05 \times 10^{-34}$ joules-seconds, results in:

$$T(E) = e^{-2L}, \quad L \text{ in angstroms} \quad (2.20)$$

This formula shows that for each angstrom change in separation, the probability that an electron tunnels decreases by an order of magnitude. This demonstrates mathematically that tunneling current is indeed a sensitive measure of the distance between the tip and sample.

In the STM, one of the metals is the sample being looked at and the other metal is the probe. The sample is usually flatter than the probe, as shown in Figure 2.6. Because the probe is formed of atoms, if it is sharpened into a tip, it will most likely have one atom at the end of the tip. The spacing between atoms is about 3 angstroms. Therefore, any tunneling through atoms that are one atom back from the closest atom is a fraction $[e^{-2}(3) = 0.002]$ of tunneling through the atom at the tip, as shown in Figure 2.6. Virtually all of the tunneling electrons will pass through the single atom closest to the surface. This feature produces the atomic resolution capabilities of the microscope. The transmission probability of electrons integrated over time manifests as nanoamp currents for the sample and tip separation of few angstroms, as indicated in Figure 2.2.

2.4. Angstrom Motion Using Piezoelectrics

2.4.1. What are Piezoelectrics?

In the last section, we claimed that electron tunneling occurs only when the sample and tip are separated by 10 angstroms. How can two pieces of material be moved together with this precision? To image a surface with atomic resolution, the surface must be moved with the precision of less than that of an atom's length. This motion is accomplished using piezoelectric ceramics (in general called PZT).²

If an electric field E is applied across a piezoelectric ceramic, it will expand in one direction and contract in the other. This process is illustrated in Figure 2.7. Piezoelectricity is quite common in nature. Quartz, for example, exhibits this effect. Materials which exhibit the piezoelectric effect are all electrets. An electret is analogous to a magnet, but instead of having a permanent magnetic field that causes it to attract iron bits and other magnets, an electret has a permanent electric field. The reason an electret has a permanent electric field is that it is composed of at least two different kinds of atoms, one that is positively charged and another that is negatively charged. Certain arrangements of these charged atoms can lead to a permanent electric field in the crystal, as illustrated in Figure 2.8. When another electric field is applied across the crystal, the negatively charged atoms will move up and the positively charged atoms will move down, leading to a net expansion of the crystal. In general, PZT ceramics consist of such crystalline grains which align in response to external electric fields and cause the dimensions of the PZT to change.

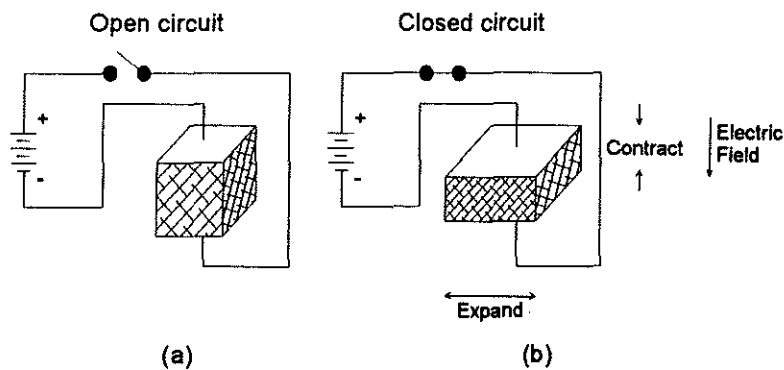


Figure 2.7. PZT in response to applied electric fields changes dimensions.

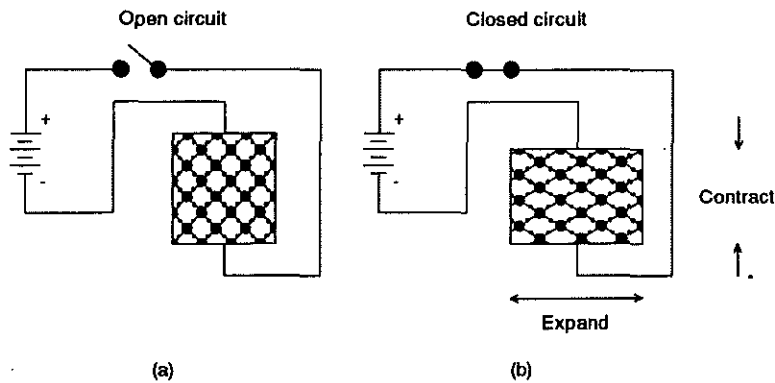


Figure 2.8. Large and small circles represent two different kinds of atoms. These atoms are arranged to have a permanent electric field (an electret). When an electric field is applied, the atoms realign in response to the field. This can cause a physical change in the crystal's dimensions.

The sensitivity of piezoelectric ceramic depends on the particular arrangement of the atoms in the crystal and its thickness. The sensitivity of the piezoelectric materials used in the STM is about 150 angstroms/volt. Because the computer running the microscope can control voltages with millivolt accuracy, it can control the motion of a PZT material to less than an angstrom sensitivity.

2.4.2. Scanning with Piezoelectrics

Three-dimensional motion is achieved by shaping a piezoelectric ceramic into a hollow cylinder. This piezoelectric device is illustrated in Figure 2.9. The tip is attached to the bottom of the cylinder, while the top of the piezoelectric and the sample are fixed. Four electrodes are formed on the outside of the cylinder, as shown in the figure, and one electrode is formed on the inside of the cylinder. By independently controlling the voltages applied across these electrodes, the piezoelectric cylinder can bend in any direction and be extended and retracted. We show two examples of this in Figure 2.10.

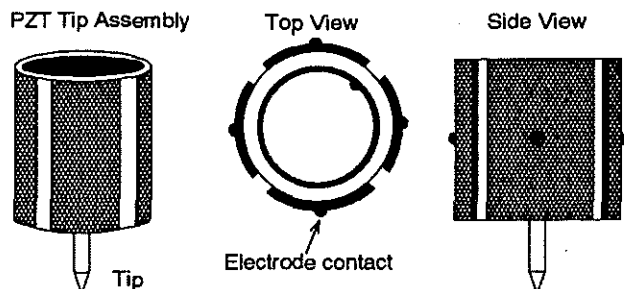


Figure 2.9. A PZT ceramic made into a hollow cylinder with quadrants is for "fine" motion control of the tip.

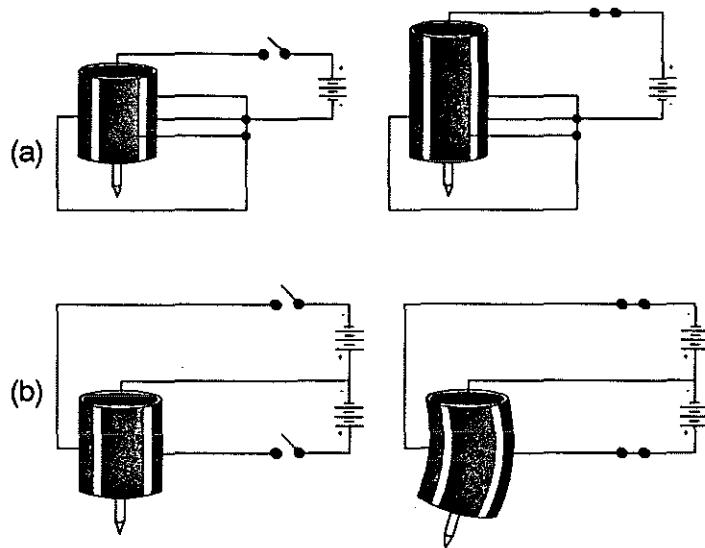


Figure 2.10. Applying a potential between the inner electrode of the PZT cylinder and its outer electrodes [a] will cause the PZT to become thinner and to elongate. Applying a potential between opposite outer electrodes of the PZT cylinder with respect to the inner electrode [b] will bend the PZT.

In Figure 2.10[a] a negative voltage is applied to the outside electrodes and a positive voltage is applied to the inside electrode. The electric field, therefore, points from the inside to the outside of the cylinder. This is opposite the poled direction of the tube. The cylinder will shrink between the electrodes (i.e. the wall will become slightly thinner) and, to keep the volume constant, the tube will become longer. If an opposite polarity is applied to the electrodes, the reverse will happen and the tube will shrink. Applying voltages in this way gives control of the motion parallel to the tube's centerline.

In Figure 2.10[b] a positive voltage is applied to the left electrode, a negative voltage to the right electrode, and the other electrodes are held at ground. In this example, the left side of the tube will shrink and the right side of the tube will lengthen, with the front and back of the tube staying the same length. The tube can accomplish this shrinking and growing by bending to the left. If an opposite polarity is put on the left and right electrodes, the tube will bend to the right. For small amounts of bending, the fact that the tip also moves down a little, as well as to the right and the left, can be neglected. If voltages are applied in the same way across the front and back electrodes, the tip bends to the front and to the back. The voltages to the left and right electrodes and to the front and back electrodes can be applied simultaneously to move the tip at any angle; a voltage applied to the inside electrode will cause up and down motion along with this bending. By applying voltages in this way, the end of the piezoelectric cylinder can be positioned anywhere within a three-dimensional region with subangstrom precision.

2.5. Negative Feedback

Measuring tunneling current provides a way to sense the location of the sample relative to the tip. If there is no tunneling current, the tip is too far from the sample. If there is a small tunneling current, the tip is near the sample. Negative feedback turns this position sensor into a microscope.

The device that measures the tunneling current is connected to electronic feedback circuitry that obeys the following rule: *if it senses a decrease in the current, it moves the tip closer to the sample, and if it senses an increase in the current, it moves the tip away from the sample.*

Now imagine a surface with some bumps on it. This surface is illustrated in Figure 2.11. The microscope is operated by positioning the tip somewhere over the left-hand side of the sample and lowering it toward the sample until a tunneling current is detected. The tip is then moved to the right. When the tip approaches a bump, the tunneling current increases. The feedback loop senses this increase and raises the tip to maintain a constant tunneling current. The tip will continue to rise until it is over the top of the bump. As the tip moves farther to the right, the current decreases and the tip must be lowered to maintain a constant tunneling current. By the time the tip has reached the far right, it has traced out a cross section of the topography of the sample, as illustrated in Figure 2.11.

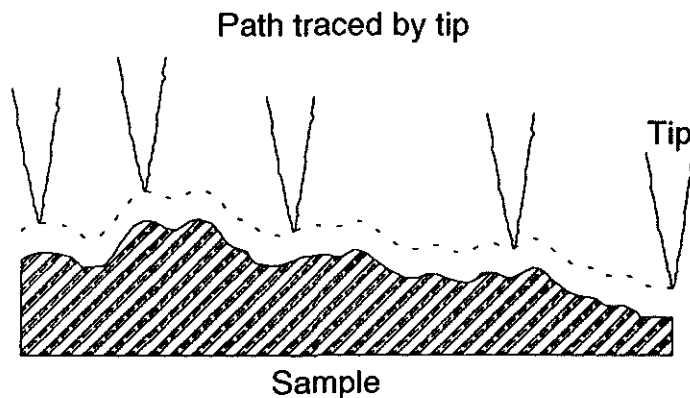


Figure 2.11. The tip traces the sample topography from left to right. When the tip gets close to a bump, tunneling current increases. The feedback loop, in response to an increase in the current above a preset reference tunneling current, moves the tip up. Conversely, if the feedback loop senses a decrease in current, it moves the tip in to compensate. Thus the tip traces the surface topography as it scans the sample, as shown by the dashed line.

2.6. Vibration Isolation

One of the problems that delayed the development of the STM was the intuitive feeling that it would be impossible to hold two objects only 10 \AA apart without having them crash into each other. Even though it cannot be seen by the eye, objects are always in motion relative to each other. Walking around a room causes desks and chairs to vibrate with an amplitude of about one micron, or 10,000 angstroms! To have the feedback loop operate as described above, these vibrations must be eliminated.

At first it may seem to be an impossible task to stop materials from vibrating on the angstrom-length scale of the STM sensitivity. However, it turns out to be quite easy to isolate the STM from these vibrations. Three methods of vibration isolation are illustrated in Figure 2.12.

Historically, the first method of vibration isolation used was superconducting levitation. Superconducting levitation is the phenomenon that if a magnet is placed above a superconductor, the superconductor will repel the magnet and not allow it to sit on its surface. If the STM is placed inside this magnet, it will essentially float and thus remain isolated from noise in the room.

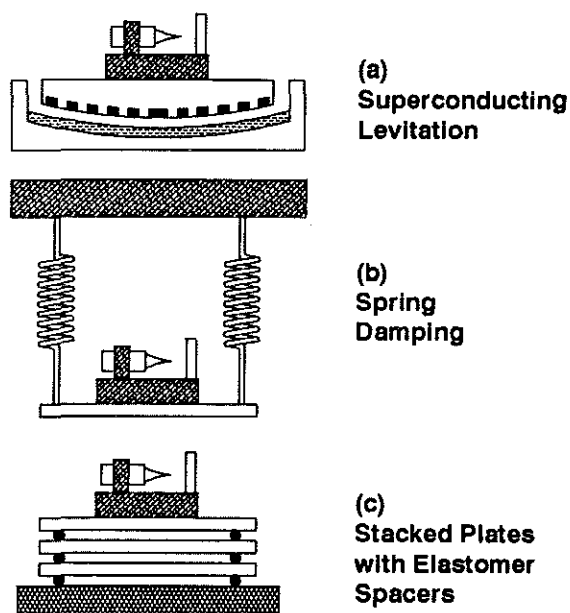


Figure 2.12. Three methods of vibration isolation. In [a] the microscope floats on top of a container filled with liquid nitrogen. In [b] springs, in conjunction with magnets for Eddie Current damping, provide an effective means of vibration isolation. Stacked plates with elastomer spacers [c] has become the standard configuration to isolate vibrations in most compact microscopes.

Another way to isolate the microscope from vibrations is to hang it by springs from a fixed surface. If the fixed surface vibrates, the springs will stretch to accommodate this vibration and the plate on which the tunneling microscope is placed will remain fixed.

A third way to isolate the microscope from vibrations is to place it on top of a series of metal plates. The plates are separated by elastomer spacers ("O" rings). The spacers act as springs and dampers. If a lower plate vibrates, the plate above it will vibrate less because the elastomer will compress and expand. The more plates that are stacked up, the smaller the vibrations will be by the time they get to the top plate. Assume that each plate will vibrate with $1/5$ less amplitude than the plate below it because of the spacers. If four plates are stacked, as illustrated in Figure 2.12, the top plate will vibrate with $1/125$ the amplitude of the bottom plate. Actual microscopes using these three different techniques are shown in Figure 1.8.

2.7. Electronic Data Collection

The final result of running the STM must be a picture. So how do we get from the concept of negative feedback and quantum mechanical tunneling to a picture? With an optical microscope the magnified image, due to reflected light, is something you can look at directly. With a scanning tunneling microscope, the image is a collection of voltages. The tunneling microscope must be interfaced to a computer with graphic capabilities to look at the image. This interface is shown in Figure 2.13.

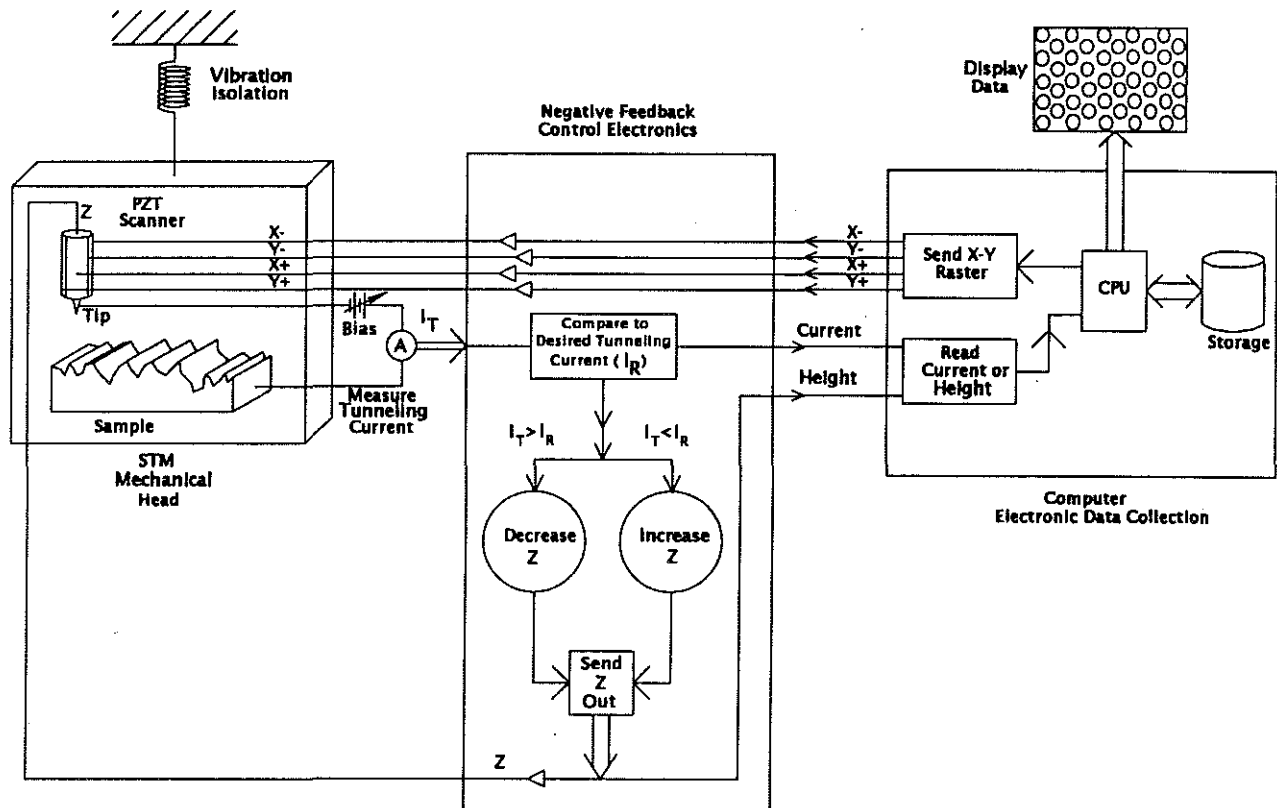


Figure 2.13. A block diagram of the STM system: the STM Mechanical Head, consisting of vibration-isolation mechanism, PZT, sample, and tip; Negative Feedback/Control Electronics, consisting of the feedback loop and X, Y, and Z power supplies; and Computer Electronic Data Collection, consisting of a computer, data acquisition card, and graphics display.

An STM image is built up one point at a time. A bias voltage is applied to produce a tunneling current between the sample and tip. (The direction of current flow depends on the sign of the bias voltage.) The tip is made to move across a surface from left to right (in the X direction), moving up a little bit each time (in the Y direction) as shown in Figure 2.14. The computer generates the voltages that move the tip in the X-Y pattern ("X-Y rastering") and sends this information to the control electronics, which subsequently amplifies the voltage to a large enough value to move the PZT scanner. The control electronics uses negative feedback to apply a voltage to the PZT scanner to move it away from and toward the surface (in the Z direction), so that the tip traces a contour of the surface. The control electronics simultaneously sends the Z axis voltage required to maintain a constant tunneling current back to the computer.

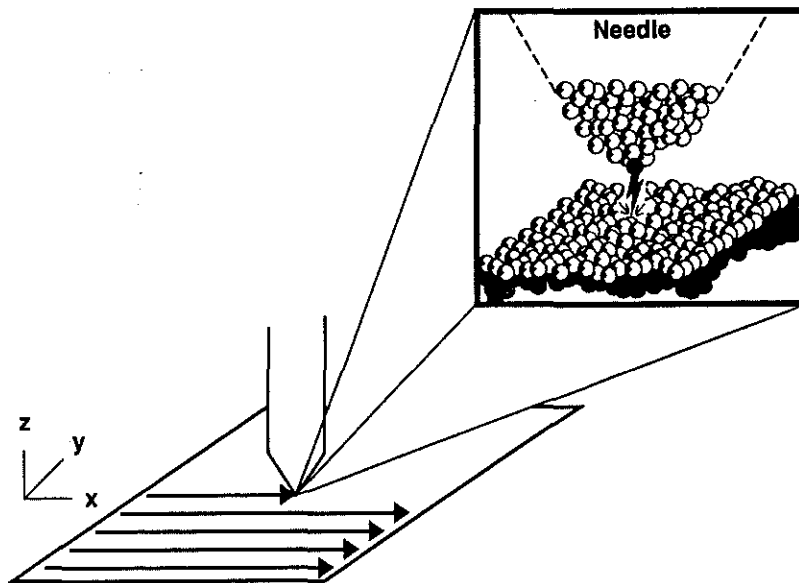


Figure 2.14. "X-Y raster": the tip moves across the surface from left to right (X) and up a little (Y) at the end of each X-raster.

From the computer's point of view, it sends out a voltage in the X and Y directions and retrieves a voltage in the Z direction. The X and Y voltages correspond to the lateral position along the sample and the Z voltage corresponds to the height of the sample. Thus, after the computer scans, it knows the height of the sample as a function of lateral position. This information can be plotted on the computer's display. The X and the Y position are the Cartesian coordinates of a point on the display, and the gray level is proportional to the Z value that the computer received. Plotted on the computer using this gray scale, high areas of the sample will appear white and low areas of the sample will appear dark.

3. OPERATING INSTRUCTIONS

We assume that the Instructional Scanning Tunneling Microscope (ISTM) is already unpacked and installed. If not, please refer to the *Instructional Scanning Tunneling Microscope Operating Manual and Quick-Start Procedures* for detailed instructions on how to unpack and install the system.

This section will give you an overview of the operation of the ISTM and basic setup procedures to start your exploration of the exciting world of scanning tunneling microscopy. It will also give you the necessary knowledge and skills for setting up the experiments which follow in Chapter 4.

3.1. A General Overview of the Burleigh ISTM

The ISTM is comprised of three subsystems: the electromechanical tunneling assembly, the control system and power supplies, and the display device. These parts will be referred to throughout the manual as: the head, the control electronics, and the computer. These parts are shown in Figure 3.1. In addition to the microscope itself, the system includes a set of samples and tips, described in Section 3.2.

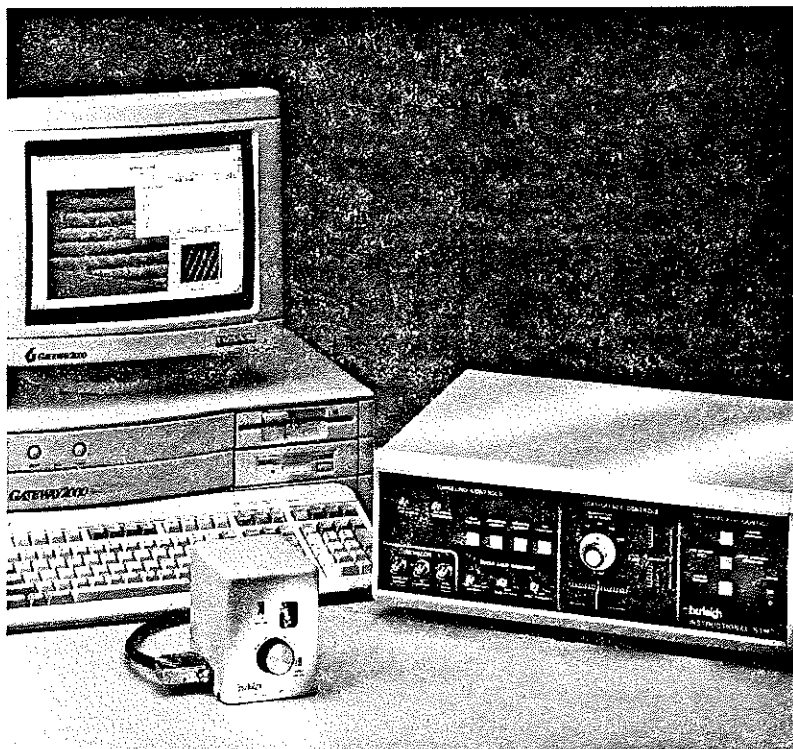


Figure 3.1. The Burleigh Instructional STM System.

The head houses the sample and tip, both of which are easy to install and remove. The tip is attached to a tubular PZT for X and Y rastering over the sample surface and "fine" Z movement perpendicular to the surface. These components are mounted on a vibration-isolation mechanism, also housed inside the ISTM Head. The head also contains an amplifier circuit that converts the small tunneling current to a voltage and then amplifies it to a usable level before sending it to the control electronics.

The control electronics uses the concept of "negative feedback" to keep the sample and tip within tunneling distance as the tip is rastered over the sample. The control electronics accomplishes this by increasing the voltage to the Z element of the PZT if the tunneling current falls below the desired value or decreasing the voltage if the tunneling current rises above the desired value.

As the control electronics applies corrections to keep tunneling current constant, an error signal is generated. This error signal and the amplified tunneling current are sent to the computer. In real time the computer reads this data, sends X and Y raster signals to the control electronics, and, synchronous with the raster, displays the data on its monitor, forming the image.

3.2. The ISTM Head

3.2.1. Head Characteristics

Figure 3.2 shows the ISTM Head. Though rugged and compact, the ISTM Head is a sensitive precision instrument and should be handled with care. The head has a unique design, allowing you to exchange samples and tips in seconds. Both the tip and sample are held in place magnetically and can be accessed through the small window on the front of the head. Figure 3.3 shows the sample holder and its carriage.

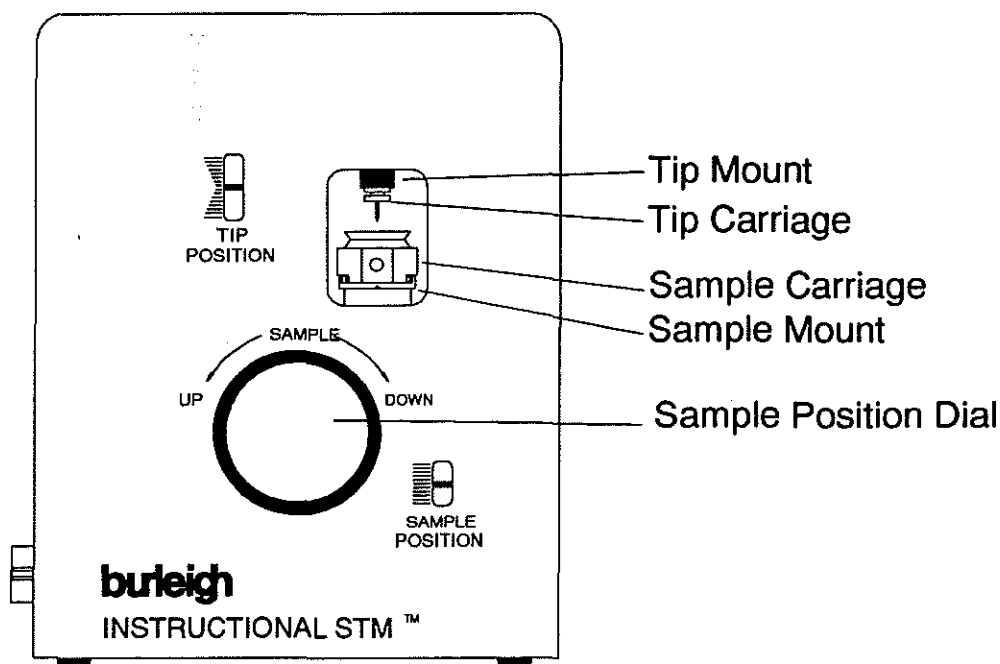


Figure 3.2. The ISTM Head and its components: the tip, fixed in a tip carriage, which is magnetically held in place by the tip mount; the SEM sample holder, which is plugged into the sample carriage and held magnetically in place on the sample mount; and the sample dial, which moves the sample up or down with respect to the tip.

The sample holder is a standard 1 cm aluminum SEM plug that has been incorporated into the design of the sample carriage. The sample holder inserts into the carriage (Figure 3.3) and is fixed by a small set screw (for detailed instructions see Section 3.2). Samples are changed by simply removing the SEM plug and replacing it with another. Figure 3.2 shows the ISTM Head loaded with a sample and a tip. The tip is also mounted in a removable holder as shown in Figure 3.4, and is held magnetically.

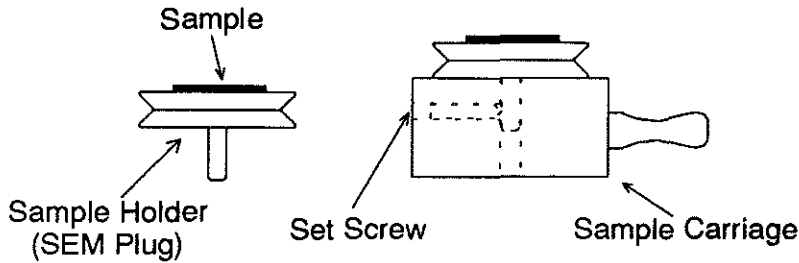


Figure 3.3. The sample is glued onto the Sample Holder (SEM Plug) and is inserted into the Sample Carriage. A #2 Set Screw holds the Sample Holder in place.

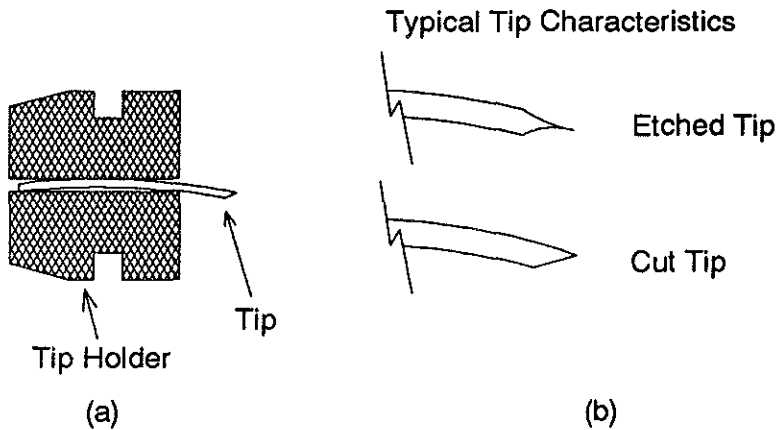


Figure 3.4. The tip is inserted into the Tip Holder [a]. Note that the tip is slightly bent to keep it more secure. Typically etched tips [b] look visually sharper than mechanically cut tips.

The tip can automatically be brought to within atomic distances of the sample in a matter of seconds. One of the issues not discussed in previous sections was the fact that PZT motion alone is not large enough to move the tip away from the surface for easy access to the sample or tip. The PZT used here has a range of about 1.2 microns in Z and about 3 microns in X and Y. (The actual range of your scanner is saved in the software parameter page.) Given the range of motion of the PZT, then, how can the tip be brought close to the sample from macroscopic distances? This is accomplished using a stepper motor in combination with a motion-reduction lever mechanism similar to the one shown in Figure 3.5. The motion-reduction mechanism allows a finer motion than the step size of the motor allows. The tip is

stepped toward the sample automatically. The control electronics drives the motor and terminates this motion when a preset tunneling current is sensed. A mechanical indicator on the upper left-hand side of the head shows the tip position and its sense of direction (see Figure 3.2).

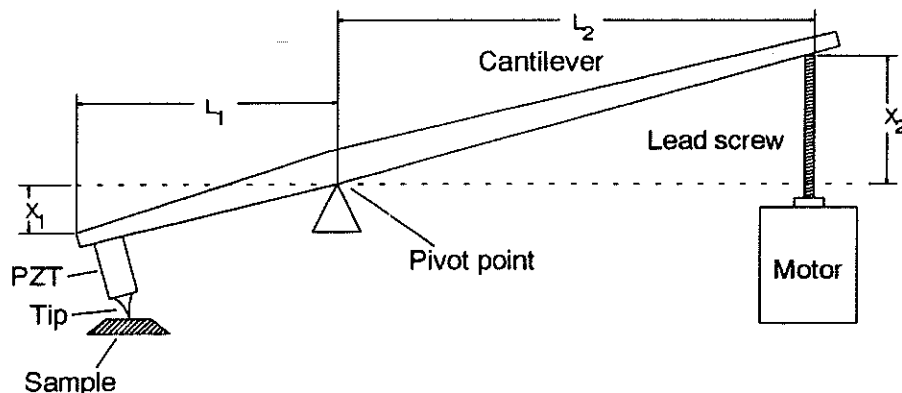


Figure 3.5. The tip coarse-reduction approach is controlled by a motor through a reduction of motion mechanism. The motion X_2 of the motor is reduced by a factor of L_2/L_1 in moving the tip.

The sample can also be moved toward or away from the tip by turning the Sample Position dial on the front of the head. Turning the dial counterclockwise moves the tip and sample closer together; turning it clockwise moves them apart. *Be careful when using this dial: you can easily run the sample into the tip and damage both sample and tip.* Observe the mechanical indicator on the lower right-hand side of the head showing the relative position of the sample to the tip. Do not attempt to go beyond the available range.

The vibration-isolation mechanism used in the ISTM Head consists of a stack of four metal plates with special rubber damping material between them, as discussed in Section 2.6. To achieve the best results, place the head on an optical table or vibration-isolation table. You can use a variety of techniques to decrease environmental effects. One of the easiest is to place a heavy metal plate on top of a small, partially inflated inner tube and then place the head on top of the plate. You should also avoid noisy environments for the operation of the ISTM. Acoustical noise can couple into the sample-tip junction, causing unwanted interference in the image, or possibly no image at all! Again, remember that the sample and tip are only angstroms away when tunneling. Even though the internal vibration-isolation mechanism of the ISTM is very effective, attention to reducing outside sources of vibration will result in much better images.¹

The head is connected to the control electronics via a connector on its side. The connecting cable carries the sample-tip bias voltage and the X, Y and Z PZT voltages to the head and returns the amplified tunneling current to the control electronics. Since the cable can conduct unwanted mechanical vibration into the head, try to position it with a slight loop or bend near the head to absorb vibrations.

3.2.2. Setting up the Head

To set up the head, first make sure the control electronics is turned off. At this point the sample carriage and/or tip may or may not be loaded into the head. Figure 3.2 shows the head with a sample and tip holder already loaded. If no sample is loaded, refer to Sections 3.2.2.1-4. If a sample and tip are already loaded, make sure you find out from your instructor what the sample and tip material are before proceeding.

A note about tools: you will need a pair of tweezers or needle nose pliers for the following operation. Since the head contains powerful magnets to retain the sample and tip, it is best to use non-magnetic tools. Unfortunately, non-magnetic tools may not always be available. If you must use magnetic (steel) tools, be careful that they are not pulled away from you, damaging the sample or tip. For best results, rest a thumb on the outside of the head and use it to support the tool.

To remove any preloaded samples and tips:

1. Watching the sample position indicator, located on the lower right-hand corner of the ISTM Head, move the sample down by turning the Sample Position dial clockwise. *Do not exceed the range of the indicator.*

NOTE: Do not turn the dial if you feel any resistance.

2. Stop when there is 1 - 2 mm space between the sample and tip.
3. Gently slide the sample carriage (Figure 3.3) out of the sample mount using your fingers (Figure 3.6).

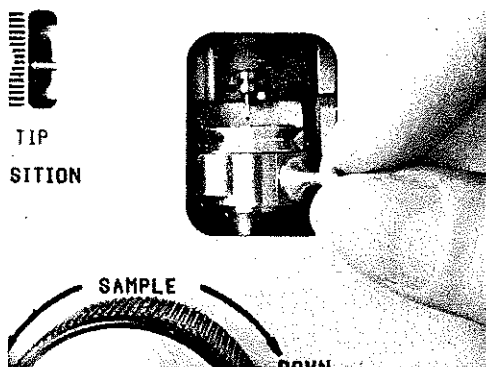


Figure 3.6. Use your fingers to take hold of the sample carriage handle and carefully slide out the carriage.

4. Avoid contacting the sample with the tip when removing the sample: this will scratch the sample and destroy the tip.
5. Set the sample aside in an upright position. Do not touch the surface of the sample: doing so will destroy the surface.
6. Hold the pliers or tweezers firmly and be sure that they are not pulled to the sample magnet while removing the tip holder (Figure 3.7). An optional pair of non-magnetic tweezers is provided with the sample-tip set.

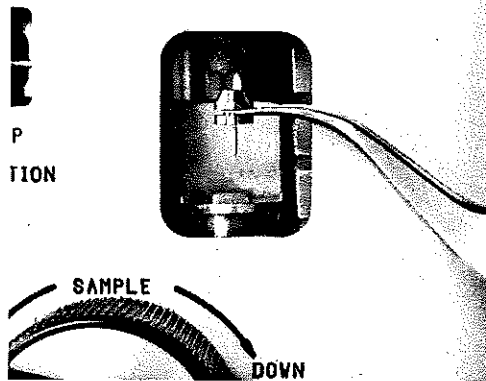


Figure 3.7. Use a pair of tweezers or pliers to remove the tip holder carefully.

7. Place the tip holder down on the table with the tip pointing up, to avoid damage.

Once the tip and sample are removed, you can load a new sample and tip.

3.2.2.1. Sample-Tip Set

For use as a teaching tool, the microscope is shipped with a prepared sample set. The sample set should be used as a starting point for the student/experimenter. Other sample surfaces should eventually be explored to better realize the capabilities of STM. The possibilities are by no means limited to the samples introduced here!

The sample-tip set includes:

- Highly-Oriented-Pyrolytic-Graphite (HOPG) sample, grade ZYH (Union Carbide Corporation)
- gold holographic grating on quartz
- molybdenite (molybdenum disulfide, MoS_2)
- liquid crystal (4'-n-alkyl-4-cyanobiphenyl, 8CB)
- n-alkane (dotriacontane, $\text{n-C}_{32}\text{H}_{66}$)
- extra HOPG samples for oxidation experiments
- platinum-iridium wire for tips (PtIr)
- tungsten wire for tips (W)
- conductive adhesive (GC Electronics Corporation — #22-201 Silver Print)
- tip holders
- hex key wrench to fix the sample holder in place
- cutting blade
- sample SEM plugs
- material safety data sheets
- fast drying, non-conductive glue
- non-magnetic tweezers
- platinum-iridium wire cutting tool

NOTE: The material safety sheets contain important safety information provided by the manufacturers of the above materials. These data sheets must, by law, be maintained on file in most facilities. Be sure to read and understand these data sheets before proceeding further. If you have any questions, please do not hesitate to contact Burleigh Instruments for clarification.

"The art & science of other aspects of making sharp tips"

A.J. Melmed, *J. Vacuum Science Technol.* B9, 601 (1991)

3.2.2.2. Mounting Samples

The samples are pre-mounted on SEM plugs. A protective cap is placed on top of the SEM plugs to prevent damage to sample surfaces. Prior to using the sample, remove the cap and retain it in the sample-tip set box. An extra SEM plug is also provided for your use. The HOPG and MoS₂ samples are mounted onto the SEM plugs using conductive adhesive. The conductive adhesive has a brush inside the cap which was used to paint the top of the SEM plug with a thin layer. The sample was then immediately set on the SEM plug and left to dry. The gold grating was glued using the non-conductive adhesive; then the conductive adhesive was used to make a conductive path between the sample surface and the plug.

We recommend using the conductive adhesive to glue samples requiring cleaving, such as layered compounds. These compounds are discussed in Chapter 4. Allow ample time (at least one hour at room temperature) for the glue to dry before using the sample for any experiments.

To mount any of the prepared samples or samples you have made, use the hex key wrench from the sample-tip set to loosen the set screw on the side of the sample carriage (Figure 3.3). Remove the desired sample from the sample set, insert the SEM plug stub into the carriage, and gently tighten the set screw to fix the plug in place. *Do not over-tighten the small set screw.* Place the wrench back in the sample-tip set box.

To examine samples with large periodic corrugation like the gold grating mount the samples in such a way that the grating lines are parallel to the sample carriage handle (Figure 3.3). The sample is rastered in such a way that the perpendicular direction to the sample carriage handle is the fast direction of scan (X) and parallel the slow direction (Y). Mounting the samples in the above arrangement allows large periodic corrugations to be better resolved.

3.2.2.3. Tip Preparation

A mechanically rigid tip with little surface contamination is one of the most important requirements for good imaging. The tip needs to be free of whiskers that are prone to acoustic noise and needs to be sharp enough that there is a reasonable chance for one atom to be closer to the sample than the other atoms on the tip. This is necessary to obtain good contrast on atomic features. There are two preferred tip materials for STM work. These are made from either tungsten (W) or platinum iridium (PtIr) alloy wire. The PtIr tips are the easiest to make and only require cutting the wire with a sharp pair of scissors or wire cutters. This tip seems to be better than tungsten tips for the study of adsorbed insulators on surfaces.

CAUTION: In this section you will be handling chemicals and will be cutting brittle wires that can be dangerous. Be sure to wear safety glasses and handle the chemicals with care.

We have provided you with 2" of PtIr and 12" of W wire. The tips must be made to a length between 0.2 - 0.4". Below we describe different techniques for preparing tips. After you make a tip you can mount it in the tip holder. Insert the tip from its uncut end into the tip holder, as

shown in Figure 3.4. Do not touch the sharp end of the tip or allow the tip to stick out of the back end of the tip holder. Note that the tip must be slightly bent so that it fits tightly in the holder.

The technique for making Ptlr tips is surprisingly easy. Hold 0.2 - 0.4" of wire with a pair of needle nose pliers and cut the tip off diagonally with ordinary diagonal cutters, pulling the tip and the rest of the wire apart from each other. You are not only cutting the wire, but shearing it to create sharp needles at its end. The tip can be mounted as explained above and shown in Figure 3.4.

NOTE: An optional pair of diagonal cutters is provided with the sample-tip set. Use this pair to cut Ptlr wire only. These cutters are specifically chosen for the purpose of preparing good Ptlr tips. Using these cutters to cut other material will damage them.

Although Ptlr wire preparation is very simple, Ptlr wire is considerably more expensive than tungsten. For this reason we include a brief description of the tip fabrication procedure for tungsten, in which the tip is electrochemically etched. This process should be performed under a ventilation hood for maximum safety. Figure 3.8 shows two different methods of electrochemical etching.

1. Prepare a concentrated solution of approximately 5 molar KOH using doubly distilled water. Wait for the solution to cool to room temperature.
2. Use tungsten wire as one electrode and platinum mesh as a counter electrode. Insert a small piece of tungsten wire (1 - 2 cm long) into a holder connected to a micrometer screw.
3. Adjust the screw to immerse 2.5 mm of the wire below the surface of the KOH solution.
4. Connect the tungsten wire and platinum counter electrode to an isolated source of 20 volts RMS at 60 Hz. With the supply turned on, observe the electrochemical etching of the tungsten tip as a bubbling action originating from the wire's surface. The bubbling action should stop within a minute when the wire is completely etched away to the solution surface.

NOTE: This operation is often done using an adjustable autotransformer (Variac, Powerstat, etc.). These devices are *not* isolated and present a severe shock hazard unless a separate isolation transformer is used. *Be absolutely certain that your power source is isolated from the line and is properly grounded!*

5. Turn the power supply off and rotate the micrometer to immerse approximately 100 microns of fresh tungsten. Set the supply to 25 volts and turn it on (only once) and off quickly. *Keep it in the "on" position for less than 5 seconds.*
6. Remove the tip from the holder with tweezers and rinse it in distilled water, followed by a rinse in clean methanol. The tip is immediately ready for use.

7. Insert the tip from the back into the tip holder (as explained above). If the tip is longer than 0.4", insert it so that the extra part sticks out from the back end of the tip holder, then trim the extra piece of wire with a pair of wire cutters.

NOTE: Tungsten wire is hard. It will destroy the jaws of expensive wire cutters instantly and with no regrets. Use cutters specifically designed for piano wire or "junk" cutters unsuitable for other purposes. "Flush Cut" diagonal cutters are extremely fragile and should never be used on tungsten wire or other hard materials.

The tip should be stored upright and should not be touched. Freshly made tips work the best since the KOH etching process removes the surface oxide layer which would otherwise act as an insulating layer. The oxide layer will develop with time and make the tip unsuitable. From time to time it will be necessary to change the KOH solution, which becomes saturated with insoluble tungsten oxides. To get an idea of the tip quality and to perfect your tip fabrication technique, it might be useful to examine the tip under a microscope. Long pointed tips with small cone angles are generally undesirable. Ideally, the tip should come to a sharp point with as large an angle as possible.

It may be desirable in certain experiments to obtain a fairly sharp tip, as, for example, in the determination of the holographic grating spacing. A very simple procedure we have used is to coat the last millimeter of the tungsten tip with a bead of glue (DUCO cement). The etching process eats away at the tungsten wire just above the cement. As the etching narrows the wire, a critical point is reached when the weight of the cement draws out the tungsten wire to a very fine tip. The etching process is stopped as soon as the cement bead is visibly seen to fall.

For more specialized applications, you may want to selectively shape the tip.² A very elegant procedure has been developed for field emission microscopy in which the platinum counter electrode is made into a loop and the etching solution is held by surface tension as a thin film in the loop. The tip can be selectively "machined" in this manner by monitoring the tip through a microscope and moving the tip in and out of the thin film etchant. As in the bulk solution etching procedure, a 1 molar KOH film is used for tungsten and KCN is used for PtIr wire tips.³

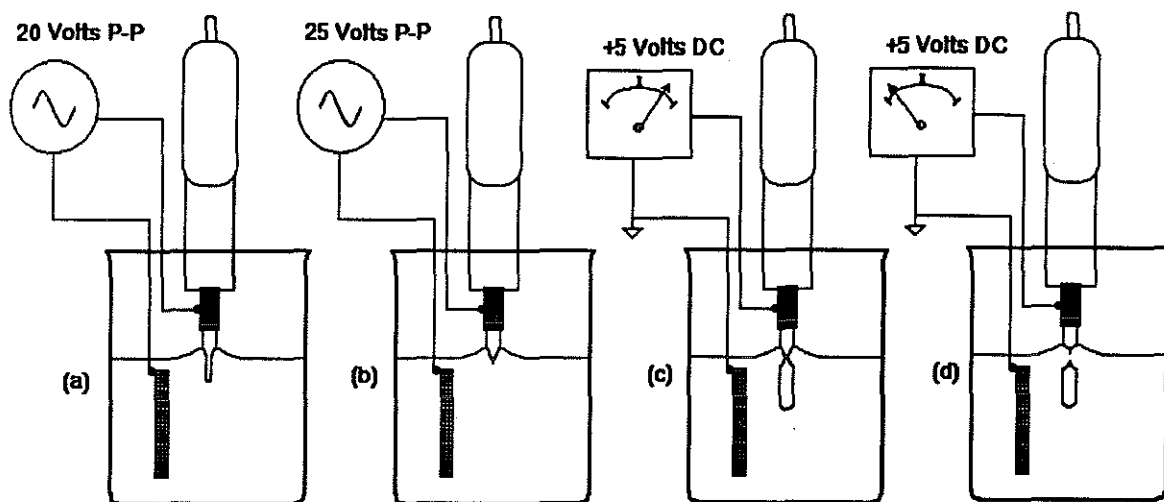


Figure 3.8. Electrochemical etching of tips. Using AC etching tip etches away from bottom to towards the surface. Fix the tip to a micrometer. Immerse the tip partially in a beaker of etching solution. Attach anode and cathode wires. This method can be used with for W and PtIr [a] and [b]. DC etching method can be used for W wires. The tip breaks off and leaves a sharp tip [c] and [d].

3.2.2.4. Loading the Sample and Tip into the Head

After the sample and tip are prepared, you are ready to load them into the ISTM Head. During handling of the tip and sample make sure not to damage the sharp end of the tip or the surface of the sample.

1. Check the sample position indicator. If it is not near the bottom of the range, turn the Sample Position dial clockwise to move the sample mount down.
2. Check the tip position indicator. If it is not above the middle, use the Coarse Retract button on the controller to reposition it.
3. With a pair of needle nose pliers or non-magnetic tweezers take hold of the tip holder. Make sure the tip is pointing down.
4. Carefully maneuver the tip holder into the ISTM tip mount until the magnet grabs hold of the tip. Be careful not to let the sample magnet attract the pliers (see Figure 3.7).

NOTE: It is important to examine the tip holder to make sure it sits properly in the tip mount by gently rocking it in its mount. Improper sitting of the tip holder would prevent getting images with atomic resolution.

5. Carefully hold the sample carriage handle with your fingers and slide the carriage into the sample mount. Make sure it clears the tip. *If it does not have enough room to clear the tip, do not insert it.* Check the sample and tip position indicators, and readjust the sample and tip position if necessary. The tip might also be too long. You can shorten it by removing the tip holder, pushing the tip further in, and clipping the excess from the back end; return to step 1.
6. After placing both the tip and sample holder in their mounts, turn the Sample Position dial counterclockwise until the sample is within 0.5 mm of the tip. You are now ready to set up the electronics for tunneling.

CAUTION: The PZT scanner is driven by high voltage so never insert any object into the tip mount. Additionally never touch the tip and sample when the unit is on. Doing so would send a large current surge to the sensitive preamp circuit which is designed to measure nanoamp currents.

3.3. ISTM Control Electronics

We will spend the next few paragraphs describing the tunneling process as it relates to the ISTM Control Electronics.

For tunneling to occur, it is necessary to apply a voltage between the sample and tip. This voltage is called the bias voltage. With voltage present, and the sample and tip in close proximity, a small tunneling current flows. The control electronics is designed to adjust the tip position so that constant tunneling current is maintained. If the tunneling current increases above the desired value, the controller will move the tip away from the sample, causing a reduction in tunneling current. If the tunneling current decreases below the desired value, the controller will move the tip closer to the sample causing an increase in tunneling current.

To keep the tunneling current constant within a small range, the controller must have a very high gain. That is, a small change in tunneling current will cause a rapid and large change in tip position. At the same time, it is essential to limit the gain; otherwise the system will oscillate violently as it attempts to make large corrections in response to small changes in tunneling current.

These contradictory requirements are met through two user-adjustable feedback paths within the controller. Adjustable feedback paths also allow data collection in two distinct modes, which we discuss in Section 3.5.

Figure 3.9 shows the front panel of the ISTM Control Electronics. The controls are divided into four basic areas: the Tunneling Controls, Scan/Offset Controls, Tip Approach Controls, and Monitor output signals. We will discuss each of the controls in order.

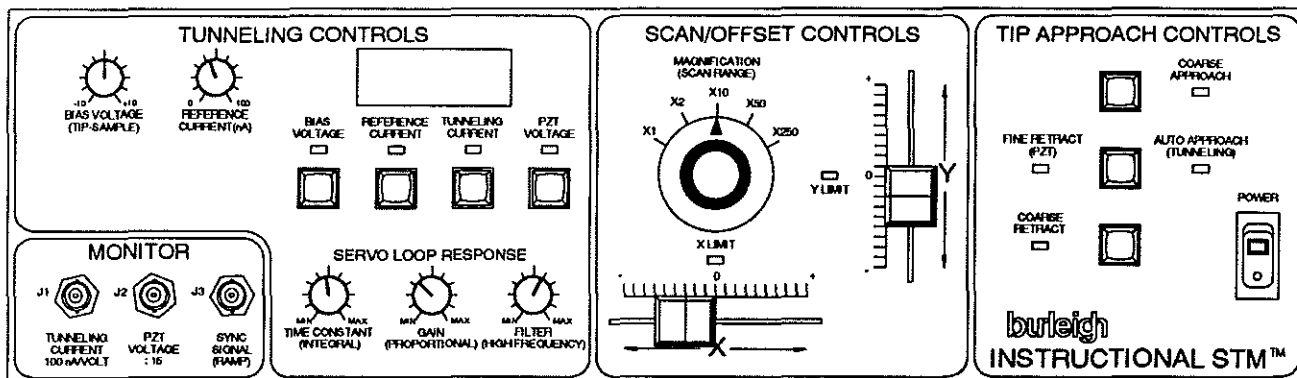


Figure 3.9. ISTM Control Electronics. The controls are divided into four basic areas: the Tunneling Controls, Scan/Offset Controls, Tip Approach Controls, and Monitor output signals.

3.3.1. Tunneling Controls

Tunneling Controls actually encompass three different functional areas. The first deals with operational controls for the head, the second with monitoring current and voltage parameters, and the third with servo loop response.

Bias Voltage sets the voltage bias between the sample and tip. This bias can be set from 0 to ± 10 VDC. Note that the bias is actually applied to the tip and the sample is connected to the current amplifier.

Reference Current is used to tell the ISTM Control Electronics the current at which it should tunnel. This current reference point can be adjusted from 0 to 100 nA. The sign of the current depends on the sign of the bias. If the bias is negative, the current is also negative and flows from the sample to the tip. If the bias is positive, the current is also positive and flows from the tip to the sample.

The **Current/Voltage Monitor**: four parameters may be read on the three-digit LED display. By pressing the appropriately marked button, you can read the value of **Bias Voltage**, **Reference Current**, **Tunneling Current**, or **PZT Voltage**. An indicator will show which parameter is being monitored. Do not press more than one button at a time.

The **Servo Loop Response** controls are used to optimize the servo loop response for a particular sample under test. When scanning across the surface terrain (see Figure 2.11) the feedback constantly monitors the tunneling current and makes adjustments according to how the servo loop is set. If the Time Constant is set to minimum, the servo loop will respond to any variations in the terrain very quickly. If the Gain is set high, the servo loop response to any tunneling current variation will be very large. If the Filter is set high, all the high-frequency variations in the current that the tip might see will be filtered out by the feedback loop. This circuit is shown schematically in Figure 3.10.

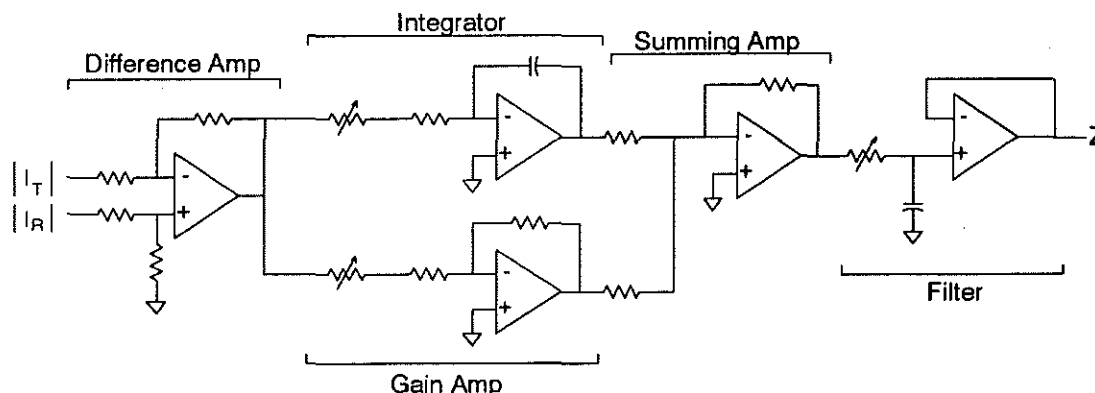


Figure 3.10. The measured tunneling current I_T and reference current I_R . The difference signal is used as "error" to adjust the Z output of the servo loop.

A description of each control follows; however, the overall strategy for operation will become more apparent with actual tunneling experience.

Time Constant (Integral): since no sample has a perfectly flat surface, it is necessary for the servo loop to follow its overall contours. This control is used to adjust the time constant of the contour tracing capability of the servo loop. You are actually controlling the time constant of a variable-time constant integrator. The "gain" of this stage is extremely high, but the effect is applied quite slowly.

Gain (Proportional) adjusts the signal gain within the servo loop and, in doing so, changes the proportional display of the resulting picture (in constant current mode). This feedback path is a simple variable-gain amplifier. As its gain is increased, the tip will make larger motions to correct for changes in tunneling current. This feedback path responds quickly, having a bandwidth of several kHz. Note that the system may oscillate if the gain is increased too high.

Filter (High Frequency) adjusts the frequency-response of the servo loop.

General information on electronic design for automatic controls can be found elsewhere.⁴

3.3.2. Scan/Offset Controls

These controls adjust the PZT voltages to the X and Y PZT elements. This enables you to look at different size areas or different locations on the sample.

The **Magnification (Scan Range)** dial is used to "zoom" in on a feature of the sample being tested. The X1 size is defined by the ISTM software. This control simply magnifies that view by reducing the overall distance scanned.

The X and Y controls allow the scan area to be shifted in both the X and Y directions. A limit LED indicator will light when the desired shift exceeds the available motion. The X and Y limits are also dependent on the current magnification factor. Note that no X and Y adjustment will be possible if the system is already scanning the full available range. At higher magnifications (with a tiny scan area) a relatively large degree of X and Y shift will be possible. Taking large X and Y scans (3 micron x 3 micron, for example) and large offsets of X and Y slides will cause the X-LIM and Y-LIM LEDs to light. This indicates attempts to move the PZT beyond its available range. Although the PZT will not be damaged, the image acquired in this mode will be clipped. The X and Y controls always correspond to the full range of the scanner independent of the magnification factor. So when imaging small areas to examine surfaces at an atomic scale do not move the X and Y controls large distances. The electromechanical properties of PZT may cause the image look distorted due to PZT drifts.

3.3.3. Tip Approach Controls

The ISTM Head contains two positioning systems: a precision stepping motor, lead screw, and lever system comprise the coarse positioning system; and the segmented PZT tube provides the final X, Y, and Z motions at atomic distances. These two systems must work together when the tip is retracted for sample exchange and to achieve tunneling.

The three tip approach buttons actually control five positioning functions, depending on the state of the controller when they are actuated.

Coarse Retract: before inserting a sample, the scanning assembly must be withdrawn to provide working space. This is the function of the Coarse Retract button. It is a momentary push button and only runs the stepper motor for as long as it is held down. Pressing and holding this button will move the tip away from the surface of the sample. The tip position indicator shows the relative position of the stepper system and must be kept within the marked range. Exceeding the stepper system range can jam the motor. You can use the Coarse Retract button at any time to withdraw the scanning tip from the sample. Note that pressing the Coarse Retract button also "arms" the controller in preparation for tunneling. *The Coarse Retract button must be pressed immediately prior to the initiation of tunneling.*

Coarse Approach advances the PZT scanning assembly toward the sample (exactly the opposite function of the Coarse Retract button). Again, be sure to keep the tip position indicator within its marked range. This control is rarely used, since tunneling is generally initiated from near the full retract position. It is included mainly to recover from excessive use of the retract button. To use this function the Auto Approach function (see below) should be activated first.

Fine Retract (PZT) / Auto Approach (Tunneling) has two functions, depending on the state of the controller. Pressing it immediately after the Coarse Retract button will cause the stepper motor to slowly advance the tip toward the sample until tunneling is achieved. During the approach the tunneling LED will blink until the tip reaches within tunneling distance from the tip. When tunneling, this LED will remain on. The stepper motor is then deactivated; it will not move forward again until it is rearmed by the Coarse Retract button. Pressing the Fine Retract (PZT) / Auto Approach (Tunneling) button a second time will withdraw the scanning tip, but will not affect the stepper motor. If the button is repeatedly pressed, it will toggle the system between the tunneling state and the PZT retract state.

NOTE: Brief stepper motor over-travel is usually not harmful, but, if allowed to continue, it may cause the advance mechanism to jam. Please keep watch on the travel indicators and do not exceed the marked range.

3.3.4. Monitor Outputs

The controller is designed to maintain precise tunneling currents with a minimum of attention. At the start of tunneling, however, various settings must be optimized. Since tunneling occurs on such a small physical scale, normal surface roughness can often exceed the ability of the tip to respond. In either case, the scan area or feedback parameters will have to be changed before useful data can be collected.

Access to three internal signals is provided via the front panel BNC connectors. The tunneling current and PZT Z drive voltage can be monitored with an oscilloscope, while the PZT scanning voltage can be used as a synchronization signal (trigger). This ISTM has a tunneling current range of ± 100 nA. The monitor BNC on the front panel (J1) has a scale of 10 nA/volt. The PZT voltage range (J2) has a scaling factor of +15.

3.4. True-Image™ Software Overview

The physical hardware necessary for scanning tunneling microscopy existed in the 1940s or even earlier, although the concept had yet to be imagined. Even the early STM experimenters used X-Y chart recorders or storage oscilloscopes to display images they acquired. However, it is modern computer technology that makes STM practical and allows those who are not specialists to acquire and manipulate meaningful images.

Burleigh True-Image software was written as a Microsoft® Windows™-based product, taking advantage of the ease of use provided by one of the most popular graphic-user interfaces (GUIs) and the inexpensive processing power of the latest generation of 386 and 486 PCs.

The True-Image software manages the scanning signals sent to the ISTM Control Electronics and displays the resulting images in close to real time. It also incorporates sophisticated image-processing functions specifically chosen for their applicability to STM images.

If the True-Image software is not installed, refer to the *Instructional Scanning Tunneling Microscope Operating Manual and Quick-Start Procedures*.

To start the True-Image software:

1. Type WIN at the Microsoft DOS® prompt.
2. Double-click on the Burleigh icon
3. Double-click on the STM icon.

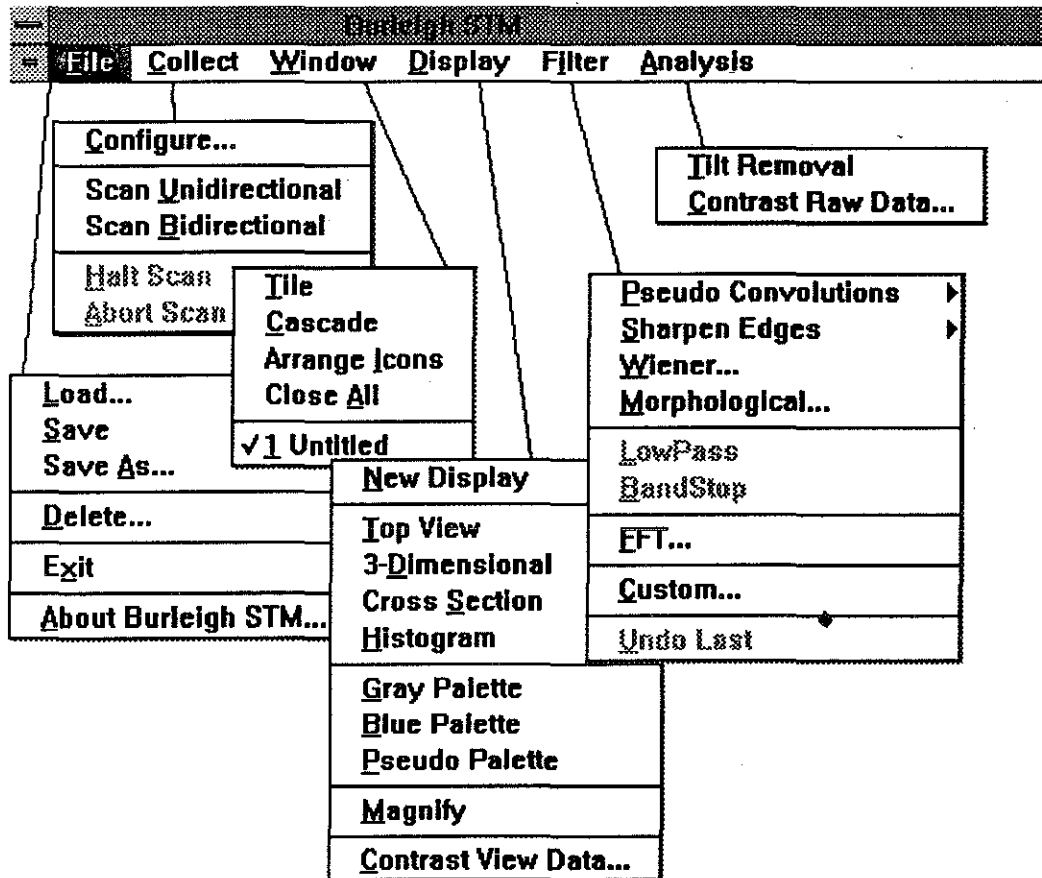
To shutdown the True-Image software:

1. Close the True-Image software by selecting Close from the File menu. You can also double click on the upper left-hand corner minus sign.
2. A menu box may appear prompting you to save your image data. If you wish to keep the image, choose YES and follow the prompts.
3. You will now be back in the Windows Program Manager. Double click on the upper left-hand corner minus sign to exit Windows.
4. One last message box will appear and Windows 3.0 will give you the option to keep any Windows changes. Windows 3.1 does this automatically. Choose the desired option. Note: do not "shell" out of Windows by choosing a DOS icon. You must fully exit Windows.
5. You should now be back at the standard DOS prompt. Almost all systems can be shut off at this point; however, very few may require manual head parking or cache flushing. See your system documentation.

NOTE: You need to make an orderly exit from both the True-Image software and Windows before turning off the computer. Failure to do this may result in loss of work, or even hard disk corruption, if the computer is shut off before data is properly updated.

3.4.1. Menu Structure

The True-Image software is a Windows program and operates according to the same general rules as all Windows software. For reference, the first two levels of the menu structure are shown below:



3.4.1.1. The File Menu

The File menu contains commands that are used to manipulate image files. The commands in this menu allow you to load existing files, delete existing files, and save new or existing files.

Load is used to automatically open an image window and load an existing image file into that window. If an image window is already opened and active, the Load command will allow an existing image file to be loaded into the opened window for analysis. To load an image from the image directory:

1. Click on the File menu.
2. Select and click on the Load submenu.
3. Another menu containing the directory and image files will appear.
4. Use the mouse to select one of the image files and double click on the desired name.
5. The image should appear on the screen.

Save is used to save the image file associated with the currently active image window. If the image file is already named, the file is saved under its current name. If the file is not already named, you will be prompted to enter a valid image filename under which the image file will be saved. The file extension used should be *.img*.

Save As can also be used to save the image file associated with the currently active image window. However, Save As always prompts you to enter a valid image filename under which the image file will be saved. This allows you to save a previously named file under a new name and to save a modified file without losing the original. The file extension used should be *.img*.

Delete allows existing image files to be deleted. You will be prompted to enter a valid image filename to delete from the disk. *Delete should be used cautiously: any files that are deleted by this command are unrecoverable by the system.*

Exit causes the Burleigh STM software to be terminated, sending control back to the operating system. Before performing this action, all valuable images in the system should be saved under appropriate filenames so they can be used in future sessions.

About Burleigh STM displays software version information about the current Burleigh STM software.

3.4.1.2. The Collect Menu

The Collect menu contains commands used for configuring data collection scans. To set up for a new page and scan:

1. Click on the Display menu.
2. Select the New Display submenu.
3. Select the Collect menu.
4. Select the Configure submenu. The parameter entry page will display.

Configure is used to set all of the available parameters pertaining to the scanning of an image. When this command is selected, a parameter entry dialog box is displayed. For a new display, the parameter values in the dialog box are set to default settings. For an image that has been loaded from disk, the parameters are set to the values that were entered when that particular image was scanned.

A description of each of the scanning parameters follows:

Data Points in X Direction is the number of actual samples (the number of data points) that will be taken as the microscope scans in the X direction. The number of samples can be powers of 2 up to 256.

Data Points in Y Direction is the number of actual scan lines (the number of data points) that will be taken as the microscope scans in the Y direction. The number of samples can be powers of 2 up to 256. The number of X and Y points should be equal.

Max Scanner Range in X is the maximum number of angstroms that the microscope can cover as it scans in the X direction. You may recalibrate and change this number. Your microscope is calibrated prior to shipment and the exact maximum scanner range in X is reflected in this menu.

Max Scanner Range in Y is the maximum number of angstroms that the microscope can cover as it scans in the Y direction. You may recalibrate and change this number. Your microscope is calibrated prior to shipment and the exact maximum scanner range in Y is reflected in this menu.

Max Scanner Range in Z is the maximum range of the motion of the PZT along the Z direction (perpendicular to the sample). The range of this scanner in Z is about 40 percent of the range in X and Y. Your microscope is calibrated prior to shipment and the exact maximum scanner range in Y is reflected in this menu.

Scan Range in X is the actual number of angstroms that the microscope will cover as it scans in the X direction is this number divided by the zoom factor. This value must not exceed the value for the Max Scanner Range in X. For a scan range of 5000 Å and zoom of 50 you scan a 100 Å area of the surface.

Scan Range in Y is the actual number of angstroms that the microscope will cover as it scans in the Y direction is this number divided by the zoom factor. This value must not exceed the value for the Max Scanner Range in Y.

Bias Voltage is the number of millivolts that is used to bias the microscope tip. This value should be set to match the bias voltage displayed on the front panel of the instrument.

Tunneling Current is the number of nanoamps that is flowing through the microscope tip. This value should be set to match the tunneling current displayed on the front panel of the instrument.

Scan Delay is the number of milliseconds that will elapse between each sample as the microscope scans in the X direction. This value can be set between 0 and 10 milliseconds. You need to adjust the scan speed depending on constant current or height mode of operation. This parameter can be changed with the slide ruler.

Zoom Multiplier is the value that is used to determine the actual number of angstroms encompassed when scanning in the X and Y directions. This value should be set to match the value of the zoom switch on the front panel of the instrument.

Scan Mode: selecting the **Single** option will cause the image to be scanned only once before stopping. Selecting the **Continuous** option will cause the image to be scanned continuously until you halt or abort the scan.

Data Type: the **Current** scan data option should be selected when the data that is being taken represents values in current. The **Topographic** scan data option should be selected when the data that is being taken represents values in angstroms.

Plane Removal: selecting this option will cause the raw data that has been scanned to be modified such that a plane is fit through the data and subtracted out to rectify any physical tilt of the sample material. The results of plane removal will only be seen after the current scan has been halted.

Line Removal: selecting this option will cause the temporary view data that is being displayed during a scan to be modified such that a line is fit through the data for each scan line and subtracted out to rectify any physical tilt of the sample material. This operation is done on a scan line by scan line basis, so the results will be seen as the image is being scanned. This operation does not affect the raw data of the image in any way.

OK will accept the current scan parameters for any subsequent scanning operations.

Cancel will abort any changes to the current scan parameters.

Default will save the current scan parameters to the application initialization file so that the current scan parameters will be used as the default scan parameters in the future.

After setting the parameters on the parameter page, you may initiate a unidirectional or a bidirectional scan. Type *A* or *Alt A* to abort the scan. Type *H* or *Alt H* to save the image in the memory.

Scan Unidirectional will cause an image to be scanned according to the current scan parameters. Each scan line will be sampled as the microscope moves in the X direction, from left to right, before retracing.

The **Scan Bidirectional** command will cause an image to be scanned according to the current scan parameters. The first scan line will be sampled as the microscope moves in the X direction from left to right and the next scan line will be sampled as the microscope moves in the X direction from right to left. The bidirectional mode operates twice as fast as the unidirectional mode.

Halt Scan will halt the scanning process after the current scan is complete. The results of the scan and any data manipulation will then be displayed. (This command may be accelerated by typing *H* during a scan.)

Abort Scan will stop the scanning process immediately. Any image data sampled will be lost. (This command may be accelerated by typing *A* during a scan.)

3.4.1.3. The Window Menu

You may have multiple images on the screen. Use the Window menu to select either the Tile or Cascade option to display multiple images on the screen. This is a standard Microsoft Windows option.

Tile displays all the opened displays on the screen in a mosaic fashion.

Cascade stacks all the opened displays on top of each other.

Arrange Icons rearranges the "minimized" displayed images on the bottom of the screen. To "minimize" an image, click one on the minus sign in the left-hand corner of the image, then select the "Minimize" option. Refer to your Microsoft Windows operations manual for further information.

Close All closes all the currently open displays.

3.4.1.4. The Display Menu

The Display menu contains commands that are used to modify only the view data for an image. The commands in this menu do not modify the raw data for the image in any way.

NOTE: When the software is first started, an opening screen will be displayed. You must first click Display on the menu bar, then select New Display.

New Display is used to open a new image window into which an image may be scanned or an existing image file may be loaded. All other commands in the Display menu are available only when a new image window has been opened or an existing image has been loaded from a disk.

Top View will cause the current image to be displayed in its default view which is as if looking at the sample from the microscope's point of view. The image is displayed from top with topographic or current data as a gray scale.

3-Dimensional View allows the current image to be viewed in perspective. A dialog box with parameters pertaining to the perspective view will be displayed. You can choose between a **Skeleton** view (low-resolution perspective) or a **Full** view (high-resolution perspective). Also the Z-axis multiplication factor may be entered as an integer from 1 to 20. Note that to use 3-Dimensional View, you should first normalize the data between its minimum and maximum (see Data View below).

Cross Section allows you to take a cross section of a top view image. With a top view display, a line may be stretched to indicate the boundary for the cross-sectional data.

Histogram the data for any image may be displayed as a histogram with this command. The resulting graph displays the number of actual samples at a particular data level.

The three **Palette** commands allow the system palette to be reset.

Gray Palette will display the current images in a monochrome range of grays with differing intensities.

Blue Palette will display the current images in a range of blue-green with differing intensities.

Pseudo Palette will display the current images in a pseudo coloring scheme that ranges from green to blue to red.

Magnify a portion of a top view may also be displayed magnified with the Magnify command. In top view a rectangle may be stretched to enclose a portion of the total image. The selected portion of the image will be displayed in a magnified form to further increase the detail that can be viewed within the selected region. (Note: only one level of magnification is supported.)

Contrast View Data provides the ability to change the contrast of the view data for an image in three different ways. A dialog box allows you to select the type of contrasting desired.

In **Minimum/Maximum** contrasting the view data for an image is scaled between the minimum and maximum data values in the image and then normalized to the range of colors in the selected palette. The minimum data value in the image is mapped to the darkest color in the palette and the maximum data value in the image is mapped to the brightest color in the palette.

In **Standard Deviation** contrasting the view data for the image is scaled between plus and minus two of the value obtained as the image data standard deviation and then normalized to the range of colors in the selected palette.

In **Manual** contrasting you can enter the minimum and maximum values to be used in the algorithm. The image view data may be scaled between any two values of image data before being normalized to the range of colors in the selected palette. The actual values that appear in the Minimum/Maximum edit fields are the values that correspond to the current minimum and maximum values of the view data. Therefore, after any of the three contrasting operations, the resulting values may be obtained by selecting Contrast View Data and viewing the values in the Minimum/Maximum edit fields.

3.4.1.5. The Filter Menu

The True-Image software package includes very extensive image-processing tools. The structure of the filtering allows user programs to interact directly with the program. Under the Filter menu you will find a set of image-smoothing routines.

The Filter menu contains commands that are used to modify the raw data of an image. Each of the commands in the Filter menu is available only when a new image has been scanned or an existing image has been loaded from a disk.

Pseudo Convolutions: Mean performs a convolution on the raw data of the image using the mean value of the data and an integer value for Strength between 1 and 500. A value of 1 has the minimal effect; a value of 500 has the maximal effect. Pseudo Convolutions Mean effectively performs a low pass filtration on the image.

Pseudo Convolutions: Median performs a convolution on the raw data of the image using the median value of the data within a user-specified window of samples and an integer value for Strength between 1 and 500. The median window can specify any number of samples by scantiness (X by Y) between two (1 by 2) and 81 (9 by 9). A value of 1 has the minimal effect; a value of 500 has the maximal effect. Basically this filter consists of a sliding window encompassing a matrix with an odd number of data points. The center data point of the matrix is replaced by the weighted median of the data points in the window. Pseudo Convolutions Median effectively performs a low pass filtration on the image.

Sharpen Edges: Gradient performs edge sharpening on the raw data of the image using a one-step Gradient mask on the data. Sharpen Edges Gradient effectively performs a high pass filtration on the image.

Sharpen Edges: Laplacian performs edge sharpening on the raw data of the image using a two-step Laplacian mask on the data. Sharpen Edges Laplacian effectively performs a high pass filtration on the image.

Unlike Pseudo Convolutions Mean and Median filtration, the Sharpen Edges Gradient and Laplacian filters have negative matrix elements. A typical mean filter would be:

1	2	1
1	4	1
1	2	1

while the Gradient and Laplacian Matrices used are:

-1	-1	1
-1	-2	1
1	1	1

0	-1	0
-1	4	-1
0	-1	0

Wiener Filter performs an optimal Wiener smoothing filter on the raw data of the image. The strength of the filtering algorithm is entered as the Wiener filter Strength, which can be any integer between 1 and 200. The Wiener filter used here removes the 1/frequency noise along the Y direction dominantly. This is particularly important in STM applications because the majority of uncorrelated noise is along the Y direction of the scan. The filter uses the Fourier transform of the image to find power spectra of image lines along the X direction for all the scan lines. These spectra are then averaged. The background on the average spectra is used as the optimal Wiener filter. The Wiener filter multiplies each pixel in the Fourier image by this filter. The effects of this filter can be very dramatic, so be careful in choosing the strength.

Morphological Filter performs a morphological filtering algorithm on the raw data of the image. You can choose between a filter that **Dilates** or **Erodes** the data. Each of the two filtering choices also has the option to use either a three-point or a five-point mask while filtering. The filtering is based on the degree that the masks fit the data. The points in the data that do not fit the mask are removed and replaced by it. The scheme of operation is graphically demonstrated in Figure 3.10. There are numerous advantages of this filter over Fourier transformation techniques. This filter does not distort the image during processing.⁵

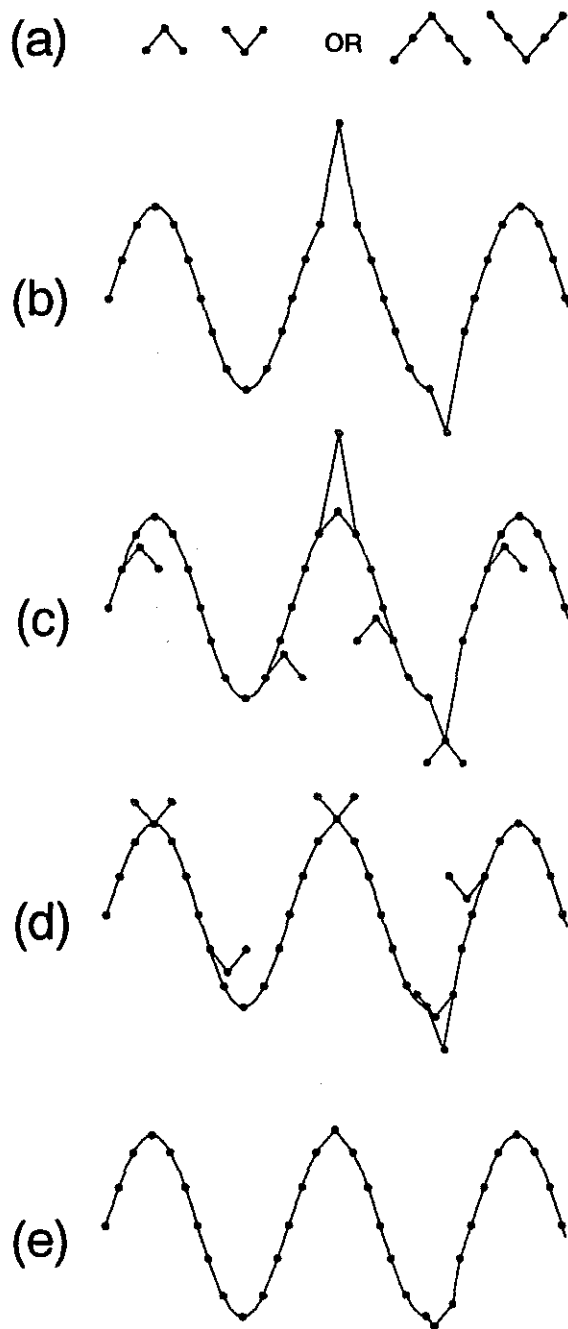


Figure 3.10. The masks are shown in [a] and the signal to be processed in [b]. The shape (slope) of the masks is determined by the strength factor. In [c] the erosion mask slides over the data points and removes all "positive" spikes. In [d] the dilation mask removes all the "negative" spikes. The resultant is shown in [e].

FFT (Fast Fourier Transform) transforms the raw data of the image into a representation of the spatial frequencies present in the image data. The resultant is the power image of the data. The lowest frequencies present in the data are at the center of the FFT image; the frequencies represented are higher as the image is traversed in both the X and Y directions out from the center. This image can be displayed in a linear or logarithmic gray scale. To see the details better, you should use logarithmic scale. Once an FFT has been executed, two other filtering operations become operational. These are the Low Pass and Band Stop Filter commands.

Low Pass Filter allows you to stretch a rectangle symmetrically about the center of an FFT image. The bounds of this rectangle represent the cutoff points for the spatial frequency filtering in both the X and Y directions. Since the lowest frequencies are at the center of an FFT image, this filtering operation will retain (pass) all spatial frequencies within the bounding rectangle and will exclude (attenuate) all spatial frequencies outside it. The results of the Low Pass Filter can be seen by performing an Inverse FFT on the filtered spatial image.

Band Stop Filter allows you to stretch a rectangle symmetrically about any point within an FFT image. The bounds of this rectangle represent the cutoff points for the spatial frequency filtering in both the X and Y directions. This filtering operation will exclude (attenuate) all spatial frequencies within the bounding rectangle and will retain (pass) all spatial frequencies outside it. The results of the Band Stop Filter can be seen by performing an Inverse FFT on the filtered spatial image.

Inverse FFT: after a transform, the FFT command changes to Inverse FFT. Selecting Inverse FFT after a filtering operation will transform the image back to a representation of discrete data values which will then show the results of the applied filter.

Custom Filter allows you to program a filter algorithm — specifically, a DOS executable file that conforms to the custom filtering specifications — to be performed on the raw data of an image. This executable file must reside in the Filters directory on the system's hard drive. When selected, the Custom Filter command will list all available filter algorithms that may be performed. After a custom filter is selected, the raw data will be modified by the selected algorithm and subsequently displayed as a filtered image. During the execution of a custom filter no other commands are operational. The program must wait for the algorithm to be completed before commencing any other functions. An example program written in "C" is given in this directory.

Undo Last Filter becomes operational after any filtering operation has been performed. Selecting this command will cause the previous raw data of the image to be restored. *The current filtered data will be lost.*

NOTE: Only one filtering operation may be executed before the original raw data of the image is lost. After this point (i.e. two consecutive filtering operations), the previous filtered data will become the new raw data for subsequent functions.

3.4.1.6. The Analysis Menu

The Analysis menu contains commands that are used to modify the raw data of an image. Each of the commands in the Analysis menu is available only when a new image has been scanned or an existing image has been loaded from disk.

Tilt Removal provides a means of fitting a plane to the raw data of an image and subtracting the value of each point on the plane from each corresponding data point on the image. This operation has the effect of modifying the raw data of the image such that the effects of any physical tilt of the original sample material are removed from the scanned data. The resulting image data is thus normalized to be relative to a flat plane (similar to Plane Removal in the Collect/Configure submenu). The best-fit plane constant is represented and can be changed by the user.

Contrast Raw Data has the same capabilities as the corresponding Contrast View Data command in the Display menu, except that Contrast Raw Data directly modifies the raw (rather than the view) data of the image.

3.4.2. Image-Processing with True-Image

We will now apply a series of transformations and filtrations to a noisy image. This will reveal just how much information can be extracted when the initial data is less than perfect. It is strongly recommended that you complete this exercise to understand the normal sequence in which the filters can be used.

1. Load the supplied image pic32.img by selecting Load from the File menu and double-clicking on the file name in the directory.
2. Perform a Fourier Transformation by selecting the FFT option from the Filter menu. Choose the Log method. The results should look like Figure 3.11. (We have combined images on the screen for comparison; however, it is not necessary for you to do so.)

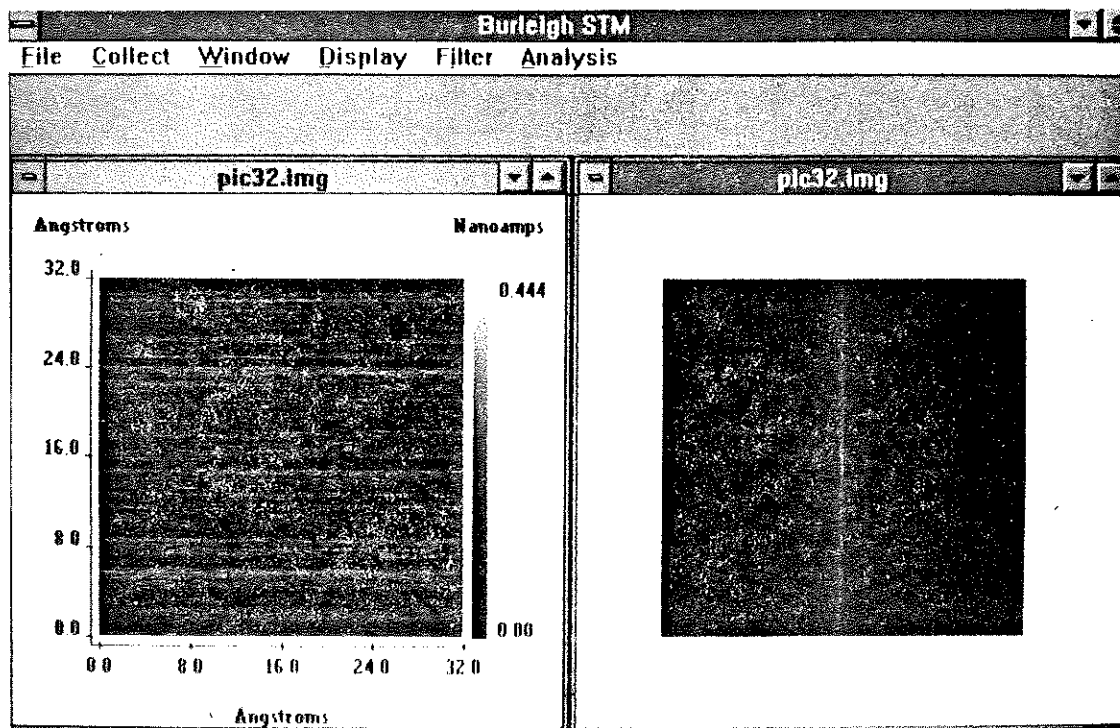


Figure 3.11. An STM image of NbSe and its Fourier transformation. This is a particularly noisy image selected to show the power of image processing.

3. Next, you will perform a Wiener filtration. Before this can be done, you must select Inverse FFT from the Filter menu. Perform the Wiener filtration by selecting Wiener from the Filter menu. Use the maximum filter strength of 200. Compare the resulting image with the original, then select FFT and compare the FFT with those done previously (see Figure 3.12).

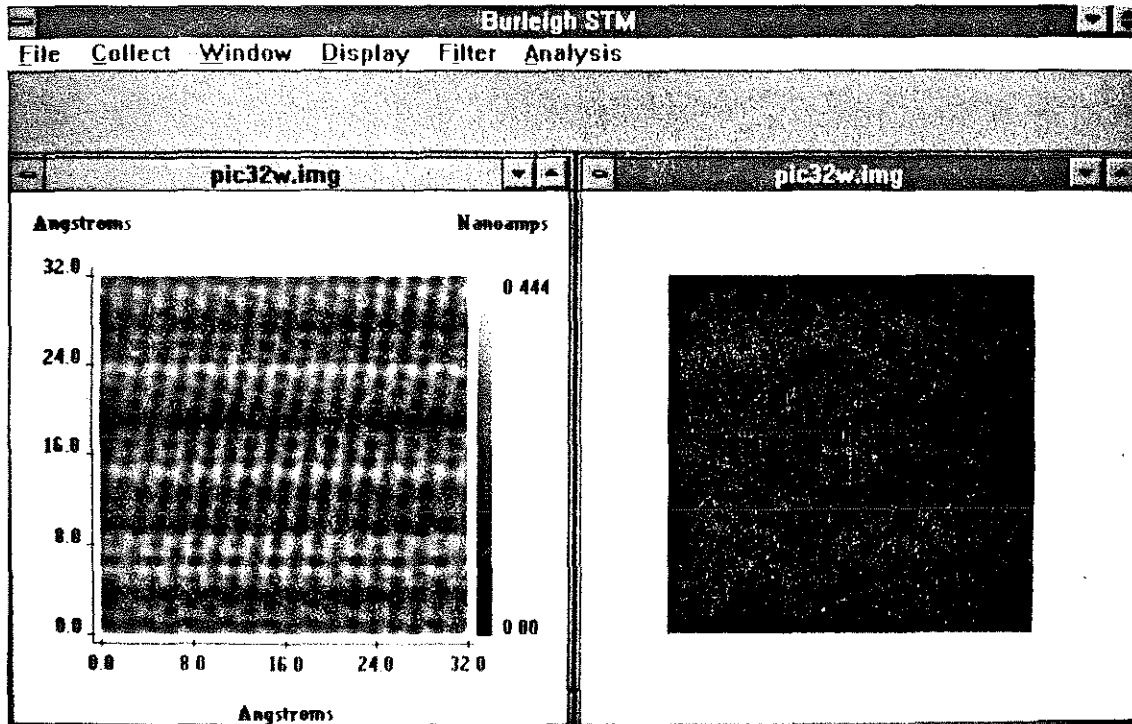


Figure 3.12. A Wiener filtered image of Figure 3.11 and Fourier transformation of the filtered image.

4. Perform a Low Pass Filter on the FFT image by selecting Low Pass Filter from the Filter menu. Place the window as shown in Figure 3.13a. The result should look like Figure 3.13b.

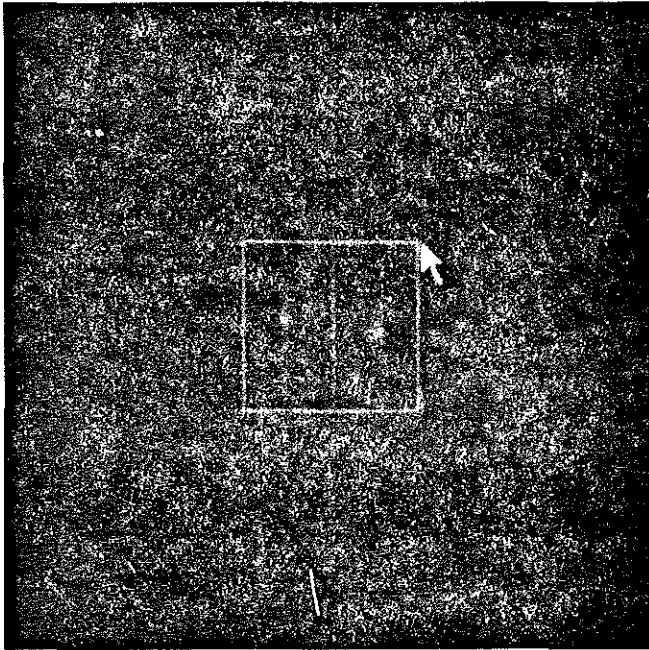


Figure 3.13a. Place the box on the Fourier transformation image for low pass filtration.

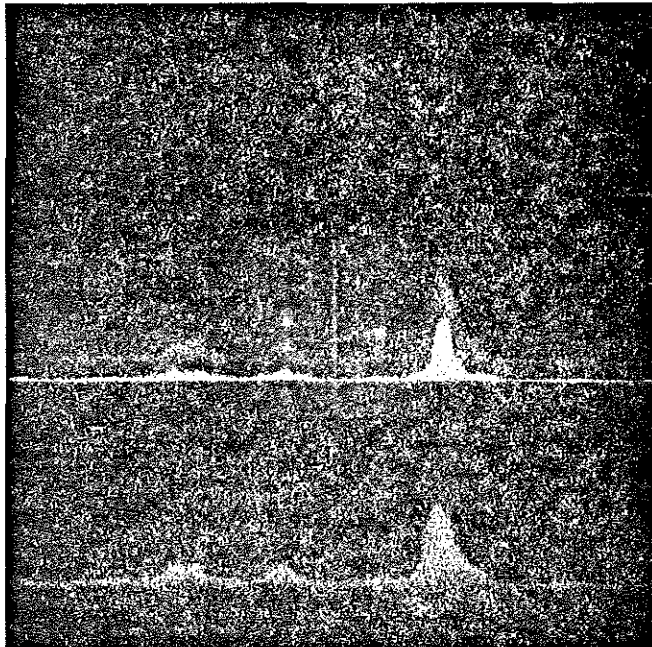


Figure 3.13b. The Low Pass Filter will smoothly zero the area outside the box.

5. Now perform a band stop filter in the same manner. Place the window as shown in Figure 3.14a and select the first point exactly in the center of the image.



Figure 3.14a. Select the first point in the center of the image and the second point as shown in the figure.

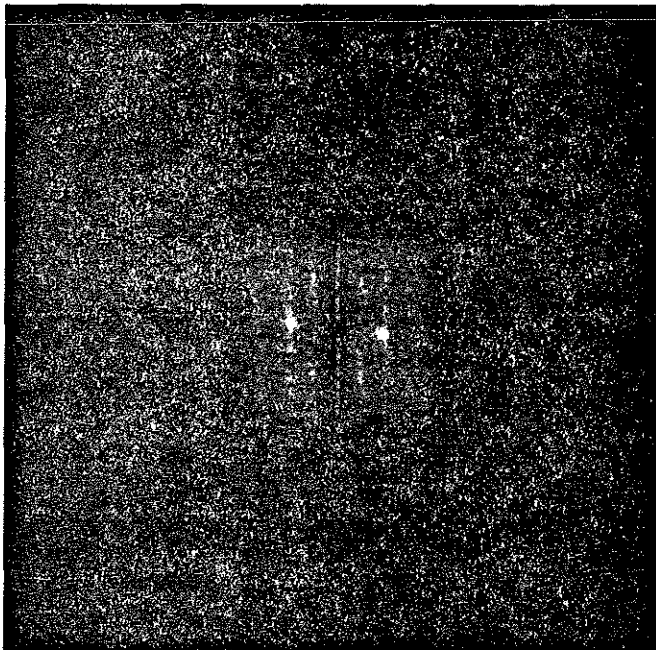


Figure 3.14b. The low frequency noise will be filtered out.

- The FFT image should now look like Figure 3.14b. All data in the center and the outer area should be cleared. Select Inverse FFT from the Filter menu and examine the image. It should closely resemble Figure 3.15.

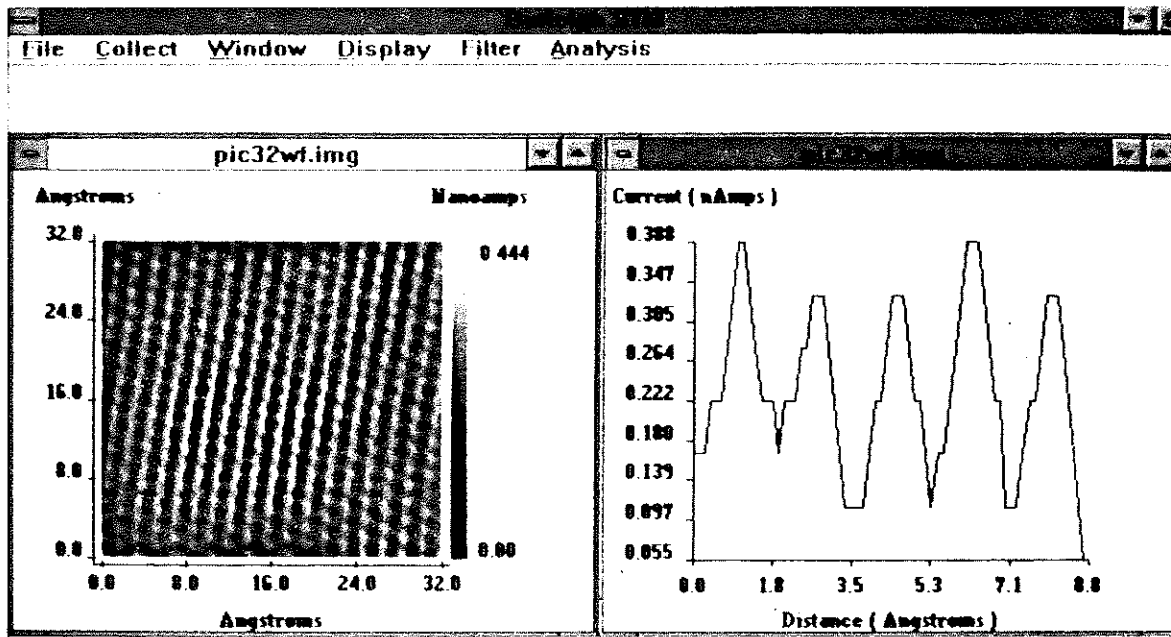


Figure 3.15. The image is reconstructed after filtration by inverse Fourier transformation. The cross section of the data is also shown.

- You can display a graph of the cross-section values by selecting Cross Section from the Display menu. Place the section line as shown in Figure 3.15. Note the digitization of the cross-section values in the graph.
- Finally, select Pseudo Convolutions Mean from the Filter menu. Display the cross section in the same manner as above and note the reduction of digitization in the image (as shown in Figure 3.16).

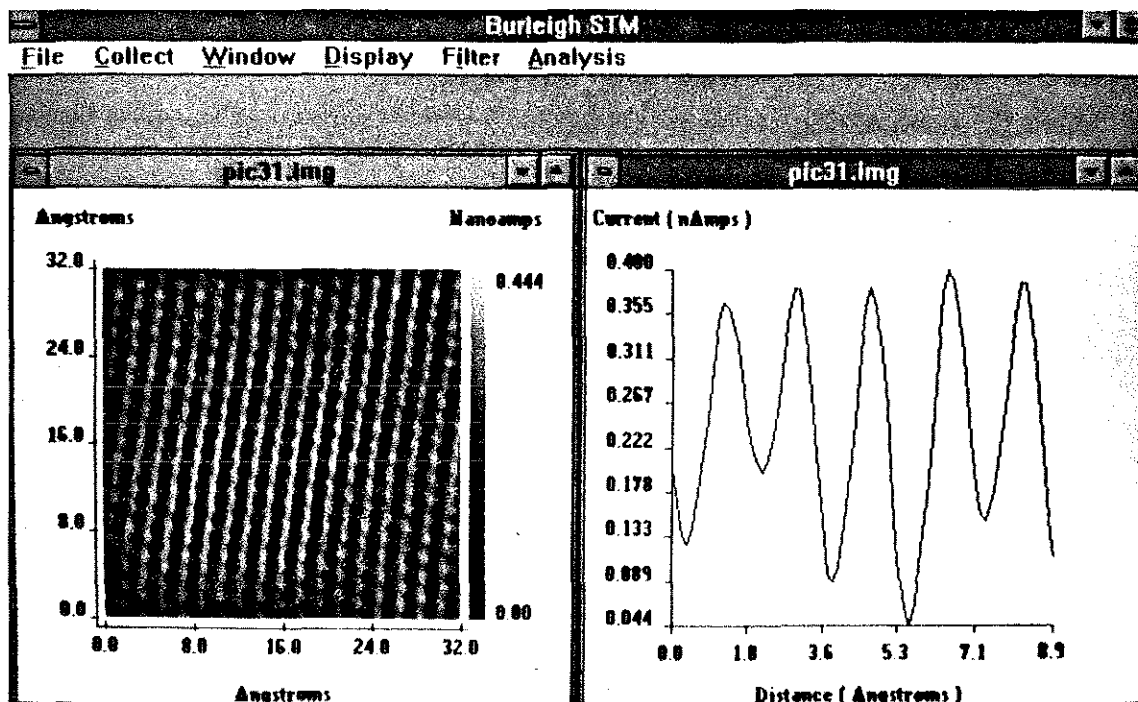


Figure 3.16. The smooth image of NbSe shows the power of filtration. Compare this figure to Figure 3.11.

This completes our image-processing demo. The True-Image software is not intended to be a full featured image-processing and analysis package, but the functions provided are extremely powerful. Hint: you may wish to keep detailed notes on your processing of images; you will then be able to recreate the results and fine-tune your overall filter strategy.

3.5. Data Collection Modes

A solid understanding of this section will make operation of the system much more logical. The explanation of various control settings usually starts with the data collection mode. The problems encountered with tips, surfaces, and loop stability will differ depending on your mode of data collection.

3.5.1. Constant Height Mode

In this mode the goal is to scan the tip over the sample surface at a constant average height. Surface features on the sample will cause the tunneling current to fluctuate about the set point. The tip will not attempt to follow every detail of the surface. At the same time, the tip must follow the average surface height, otherwise it would move out of tunneling distance or crash into the surface.

Typically the Gain control will be set to minimum and the Time Constant to maximum in this mode. If the surface is not relatively flat, it may be necessary to increase the Gain slightly. This will improve the ability of the controller to respond to surface defects and reduce crashes. The setting of the Filter control is not normally critical, but experimentation may be beneficial with some surfaces.

In this mode, surface information is derived from the tunneling current and the software should be set accordingly (set the Tunneling Current in the Collect/Configure submenu). The PZT Z voltage is relatively constant in this mode.

Monitoring the tunneling current with an oscilloscope can be very useful. Use the synchronization signal for trigger. It will be immediately apparent if the surface is uneven or if the controller is in oscillation.

Ideally, one should observe a relatively flat trace, with a small amount of ripple representing atomic structure. In reality, expect a somewhat noisier signal, with atomic detail only occasionally visible. If the signal reaches zero volts, or exceeds about one volt, the surface flatness is sub-optimal. You should attempt to find a smoother location on the sample.

3.5.2. Constant Current Mode

In this mode the tip should follow the sample surface as closely as possible. As the tip moves over atomic features, the controller will adjust the position of the tip to maintain constant tunneling current. Surface information will not be seen in the tunneling current, since the controller is making every effort to keep it constant. The surface information is thus contained in the PZT drive voltage, which must be read by the data acquisition system.

Precise tracking of the sample surface requires the Gain to be set as high as possible without oscillation. A certain amount of high frequency filtration will help prevent oscillation; adjusting the Filter control to just below its maximum value will allow this. Normally, the Time Constant control should be set to minimum.

If the surface profile and scan speed combination require tip deflections beyond the abilities of the controller, image degradation will occur. This usually appears as a smearing effect, often changing rapidly as debris is collected by the tip. A tip crash and surface damage are also likely. To prevent this, the scan speed should be reduced significantly. You will have to make a trade-off between experiment duration, thermal drift, PZT drift, and scan quality.

When working in constant current mode you may also want to monitor the PZT Z voltage on the second channel of the oscilloscope. Note that the signal is effectively AC coupled, though at a very low cutoff frequency. The surface height data will therefore appear centered near ground if the sample is relatively flat. Adjust the vertical sensitivity of the oscilloscope as required. The Gain, Time Constant, and Filter can be adjusted for the most stable tunneling current. Be sure to watch the tunneling current signal for oscillation, but also be aware that good images are often obtained when the system is in a condition of marginal stability.

3.5.3. Basic Tunneling Instructions (Constant Height Mode)

1. Complete the installation of the tip and sample. (For detailed instructions see Sections 3.2.2.1-4.)
2. Adjust the sample height for a distance of about 0.5 mm between the tip and sample.
3. Set the Bias Voltage to 0.2 volts.
4. Set the Reference Current to 2.0 nA.
5. Set the Gain to maximum.
6. Set the Time Constant to minimum.
7. Set the Filter to maximum.
8. Briefly press the Coarse Retract button.
9. Briefly press the Auto Approach (Tunneling) button; note that the LED lights.
10. The stepper motor will run and the tip will approach the sample. Monitor the actual tunneling current, which should be close to zero. When tunneling is achieved, the current will jump to a value near the reference value. The Auto Approach (Tunneling) Led should also light.
11. Set the Gain to minimum.
12. Set the Time Constant to maximum
13. Congratulations, you are now tunneling and setup for constant height mode of tunneling!

4. LABORATORY EXPERIMENTS

This chapter describes a number of experiments based on the STM with an emphasis on obtaining meaningful results within the time constraints of a normal undergraduate teaching lab. These experiments seek to convey various concepts of molecular and electronic structure in a very direct manner. There are seven laboratory experiments, involving five different classes of material, described in this section. The experiments include:

- imaging of gold surfaces
- graphite
- two-dimensional semiconductors (MoS_2)
- molecular ordering of liquid crystals (8CB, to be defined below) and alkanes ($\text{C}_{32}\text{H}_{66}$) on surfaces
- the phenomena of charge density waves (TaS_2 ; not provided with the prepared sample set)

The prepared sample set is used in applications of electron tunneling to metals, semimetals, and semiconductors. All of the materials and the experiments suggested below were chosen because they are relatively straightforward, require little sample preparation, and had high success rates. Our experience at the University of Rochester and Burleigh Instruments has been that approximately 80 percent of students obtain atomic resolution images of graphite, all students get good, though not atomic, images of gold, 80 percent of students get images of MoS_2 with reduced clarity relative to graphite, and 30 to 50 percent of students get reasonable images of liquid crystals or alkanes on graphite. These percentages give some guideline as to which experiments might be more suitable for a particular course.

In this regard, the distinctive properties of graphite, gold, and semiconductor surfaces can be studied and each material can be related to the electronic band structure of the crystal. In particular, the ordering of liquid crystals and alkanes gives a good example of the cooperative effects between molecules that can lead to self assembly and overcome entropic barriers; and the charge density wave exhibited by TaS_2 provides a very dramatic example of the effect of small bond distortions on electron density and band structure. The set of experiments using adsorbed liquid crystals and alkanes also demonstrate how electron tunneling can be modified by insulators.

Each sample is discussed in detail below as a self-contained experiment with example data and general instrument settings to get started. Figures from prior experiments are also provided for your reference. Together these experiments can be incorporated into a full laboratory course on materials based on the STM alone.

4.1. Gold Surfaces — An Example of a Metal

Based on their relative resistance to conducting electricity, solid state materials are broadly classified as metals, semiconductors, and insulators. Metals have very low resistance due to the availability of a continuous distribution of electronic levels to transport electrons, i.e. a conduction band. The resistance of a metal is determined primarily by lattice vibrations that impede the electrons' motion. Insulators have very large resistance and basically do not conduct electricity; this high resistance results from the large energy gap between valence molecular orbitals and the conduction band of unoccupied states. The valence orbitals of insulators are completely filled with electrons. Since no two electrons can occupy the same orbital (i.e. electrons are fermions) there can be no *net* motion of electrons in an electric field. The resistivity of semiconductors falls between that of metals and insulators. For semiconductors, conduction occurs through the thermal promotion of electrons, which creates unoccupied electronic levels that enable net electron motion. These three classifications are shown schematically in Figure 4.1.

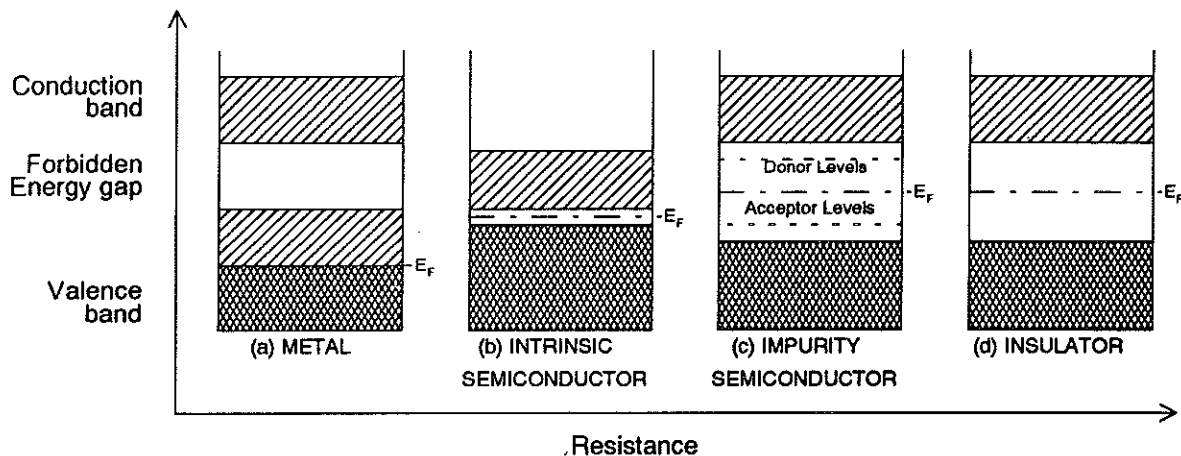


Figure 4.1. Schematic band models of solids classified according to electronic properties.

The element gold (Au) exists at room temperature as a metal that is extremely inert. Most metals, such as iron, aluminum, and alkali metals, react rapidly with oxygen in the air to form an insulating metal oxide on their surfaces. This oxide layer makes these metals unsuitable for STM studies under ambient conditions. Gold, on the other hand, does not tarnish (oxidize) and retains its metallic luster for years, which is one of the main reasons for its prominent role in history in coinage, jewelry, and art. Gold, silver, and platinum are referred to as the noble metals because of their relatively low reactivity with oxygen. Of the noble metals, gold is the most inert.

The general definition of a metal is that it is shiny, ductile, and highly conductive. All of these material properties can be understood from the atomic structure and the nature of the atomic orbitals defining the bonding between atoms. The metal shine comes from the extremely high index of refraction at virtually all wavelengths, from the visible to the infrared. The conduction band electrons can absorb light and be promoted to higher-lying unoccupied levels at virtually

any wavelength. These optical transitions, and the enormous concentration of electrons that can interact with light, impart the high index of refraction that makes metals highly reflective. The metal's gold color originates from variations in absorption in the blue and red regions of the visible spectrum (it is not perfectly reflective). The ductile property of gold and other metals arises from the strong overlap of the valence atomic orbitals, which leads to the formation of electronic bands. The curvature of their interatomic potential, which defines the interatomic forces that hold the lattice together, is smaller than that of an insulator. Basically, as a force is applied to increase the interatomic spacing, there is still enough orbital overlap to maintain a degree of bonding between the lattice plains. However, the ductile nature of metals actually comes from dislocations in the lattice. No crystal is perfect; there will always be locations where the lattice has a break in its symmetry that essentially increases the structural void space of the lattice. Any stress applied to a metal deforms the dislocations of the crystal as the atoms maintaining a net bonding interaction move past one another. The ductile nature of metals is much like rolling out air pockets in dough to stretch the dough. It is this property that enables metals to be pulled into wires. In the absence of defects, most metals would have a tensile strength 10^2 to 10^4 higher than naturally occurring crystals.

High conductivity is the primary characteristic of metals. An atomic level understanding of this phenomena requires a discussion of how atoms bond together to form solids. Whether or not a material is conductive depends on the relative energy positions of the interacting valence atomic orbitals that bond the lattice of atoms together. To understand this point, consider what happens when two atoms are brought together spatially, as shown in Figure 4.2. If the energy of the two orbitals is similar, the two levels will combine to form a lower energy (bonding) molecular orbital and a higher energy (antibonding) molecular orbital. This coupling between two levels is a classic problem in quantum mechanics. In the bonding molecular orbital, a build-up of electron density occurs between the two atoms (the atomic orbitals add constructively). The two-atom system enters a condition of quantum resonance in which the electrons are shared by both atoms. In this manner, the electrons experience the coulombic attractive forces of both nuclei and the total energy decreases to form a lower energy bound state referred to as a molecular bond.

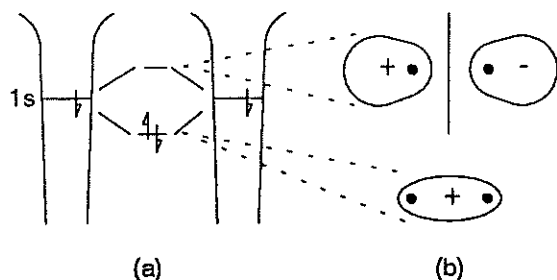


Figure 4.2. The creation of two new molecular orbitals from the spatial overlap of two 1s hydrogenic orbitals.

Now, consider the case in which, instead of two atoms interacting, n atoms are interacting, where n is a very large number. The atoms can again be defined to have a minimum energy point at some characteristic interatomic separation or bond length. Each atomic orbital contributes one electronic level to a highly congested overlap of electronic levels that merge to form a *band*, as shown in Figure 4.3.

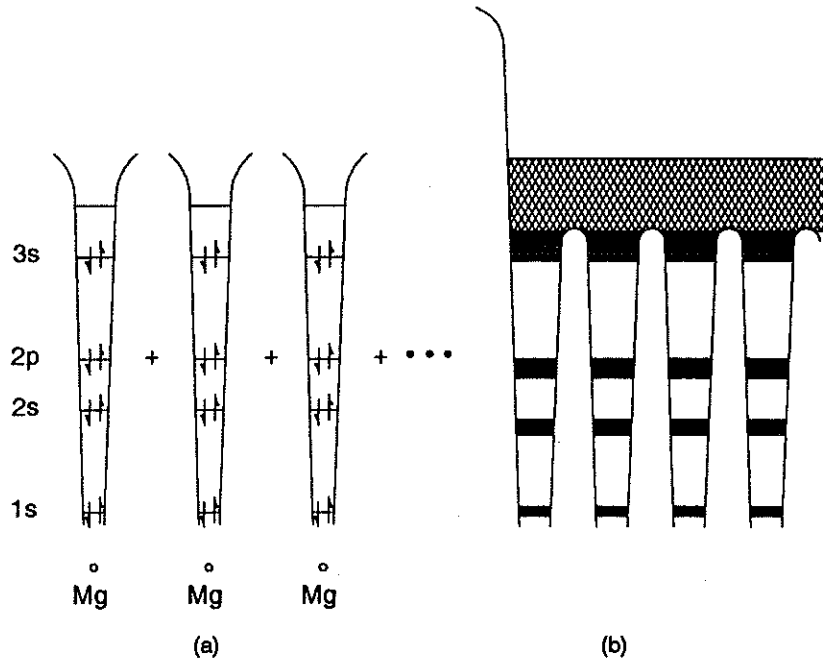


Figure 4.3. Energy levels in magnesium: [a] isolated atoms; [b] section of crystal. The sharp energy levels in the atoms have merged to form bands in the crystal. Double arrows represent filled levels.

One other important feature of the solid state that merits discussion before proceeding is the nature of the electronic wavefunctions. As opposed to atoms in which the electron experiences a coulombic attractive potential from a single nucleus, electrons in the solid state experience a periodic potential of period a , the dimension of the crystal unit cell, $U(r + a) = U(r)$, where the vector $r = x + y + z$. The wavefunctions must reflect this symmetry. Refer to Schrödinger's equation in Chapter 2.5. The wavefunctions would have the form:

$$\psi(r + a) = e^{ik \cdot a} \psi(r), \quad k = \frac{2\pi}{\lambda} \quad (4.1)$$

where k is referred to as the momentum vector and λ is the effective wavelength of the electron. The electrons would have a periodic wavefunction, governed by the periodic potential of the crystal. Wavefunctions expressed in this form are known as Bloch wavefunctions and can be understood by considering a simple particle in a box problem of length L where L corresponds to the length of the crystal. This is a fairly good analogy. There are no barriers between the atoms as the atoms are covalently bonded and the electron behaves as if it were a free electron within the confines of the crystal dimensions. The quantum mechanical solution

to this problem gives $k = n\pi/L$ where n is an integer. Larger n integers have shorter effective wavelength and thus higher energy, i.e.,

$$E = \frac{p^2}{2m} \quad (4.2)$$

where p is the momentum and m is the electron mass. From the de Broglie relation equating the correspondence between particle and wave properties: $p=h/\lambda$ or alternately $p = \hbar k$ the energy relation can be rewritten in terms of the momentum vector as:

$$E = \frac{\hbar^2 k^2}{2m} \quad (4.3)$$

This is the usual manner for depicting the different energy levels in a solid. An isotropic solid would give a parabolic dependence of energy on momentum, as shown in Figure 4.4[a]. There are discrete steps in the energy, just as in a molecule's energy diagram. However, the steps are so small (10^{-20} times smaller than kT at room temperature for a 1 cm^3 crystal) that the conduction or valence band appears as a continuous function or a continuum (of states).

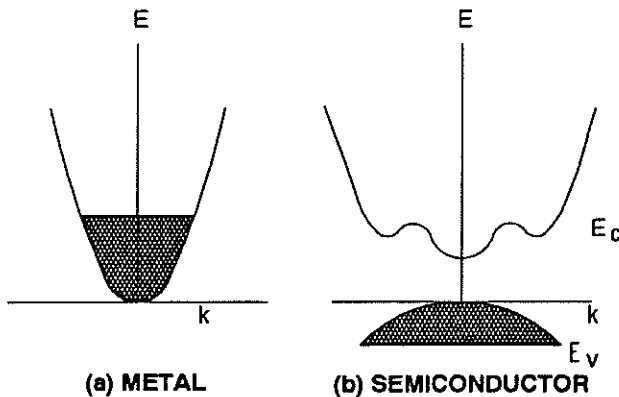


Figure 4.4. In [a] the free-electron-like behavior of electrons in metals compared to [b] the more complex behavior of electrons in semiconductors.

The nature of electrons is such that they would occupy lowest possible energy states. Finite increases of temperature excites these electrons to higher energy states. Since the electrons defined by k states are fermions, the probability that a particular level is occupied is given by Fermi-Dirac statistics:

$$P(E) = \frac{1}{1 + e^{(E-E_F)/kT}} \quad (4.4)$$

where E_F is called the Fermi energy, the energy at which there is a 50 percent probability of finding a state occupied by an electron. This distribution is shown in Figure 4.5. For a metal, E_F and the position of the highest occupied molecular orbital coincide.

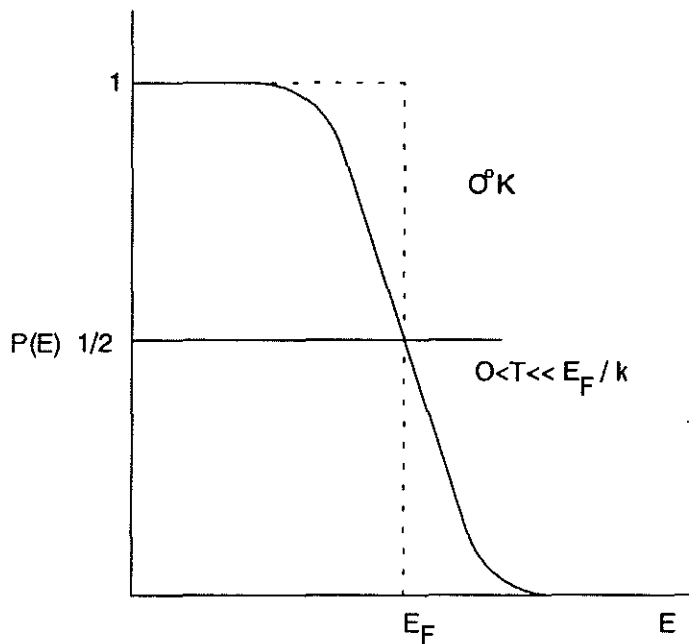


Figure 4.5. The Fermi-Dirac distribution function for energies of electrons in metal.

The property of electrical conductivity requires that the electron be free to move spatially throughout the crystal in response to an applied field. This is only possible when there are close-lying, unoccupied orbitals that enable the electron to move spatially and pick up translational energy from the applied field. In this regard, the bands from the core orbitals are comprised of closed-shell atomic orbitals and are completely filled states. The electrons from these states do not contribute to the conduction process. Only the bands formed from the valence orbitals can meet this condition. It is the energy level of these bands that defines the Fermi energy, as explained above.

The high electrical conductivity for a metal such as sodium (Na), whose electronic configuration is $1s^2 2s^2 2p^6 3s^1$, is easy to understand. The valence band is only half occupied, leaving accessible higher-lying levels for electron motion. The case of magnesium (Mg) is more difficult to understand. Because its atomic electronic configuration is $1s^2 2s^2 2p^6 3s^2$ one would expect the valence band to be filled. However, the higher-lying conduction band, formed primarily by the 3p orbitals, overlaps energetically with the valence band to form a continuous band of states capable of supporting conduction. This is shown schematically in Figure 4.3.

It should be noted that the above picture is somewhat oversimplified. In the case of diamond, for example, the valence band is formed by a combination of both carbon 2s and 2p orbitals and there is a large gap between the valence and conduction bands for the interatomic separation characteristic of the diamond structure (which we discuss further, below). This large band gap makes diamond a very good insulator, even though it has open shell 2p levels for

the constituent atoms. This latter point is made to illustrate that the exact nature of the solid state electronic levels depends on the details of the interatomic spacing (lattice structure) and extent of wavefunction overlap. Nevertheless, this discussion points out that a metal can be formed through either partially filled valence band states or the overlap of the valence band with higher-lying molecular orbitals referred to as conduction bands.

In STM experiments you are measuring the spatial variations in the electron density of the highest occupied levels in the band. These are the states near the Fermi level of the metal. The electrons near the Fermi level have the lowest barrier and can tunnel to unoccupied states in the tip. Gold has a valence electronic configuration $6s^1 5d^{10}$. The conduction band of this metal is formed primarily from these 6s and 5d atomic orbitals, as shown schematically in Figure 4.6. The STM images the spatial modulation in electron density associated with these band states.

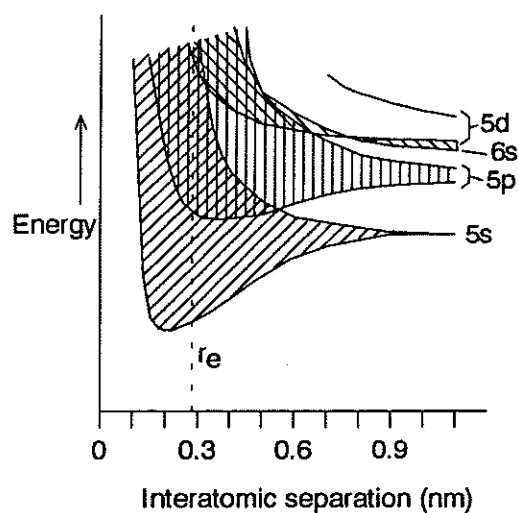


Figure 4.6. Approximate quantum mechanical calculation of the formation of energy bands as atoms are brought together into a crystal.¹

The minimum energy crystal structure for gold is a simple face-centered cubic structure with an average interatomic separation of 2.9 Å. There are several different surfaces that can be studied with the STM. The different surface orientations relative to the lattice structure are defined by the orientation of a vector perpendicular to the plane using Miller indices for the nomenclature. The different crystal structures and surface orientations are shown in Figures 4.7 and 4.8. Au(100) was the first surface studied by the STM² and Au(111) was the first metal surface to be observed with atomic resolution.³ Since then, other orientations have been studied and a variety of phenomena have been observed. Atomic resolution has been obtained in air³ and even in electrochemical environments.⁴

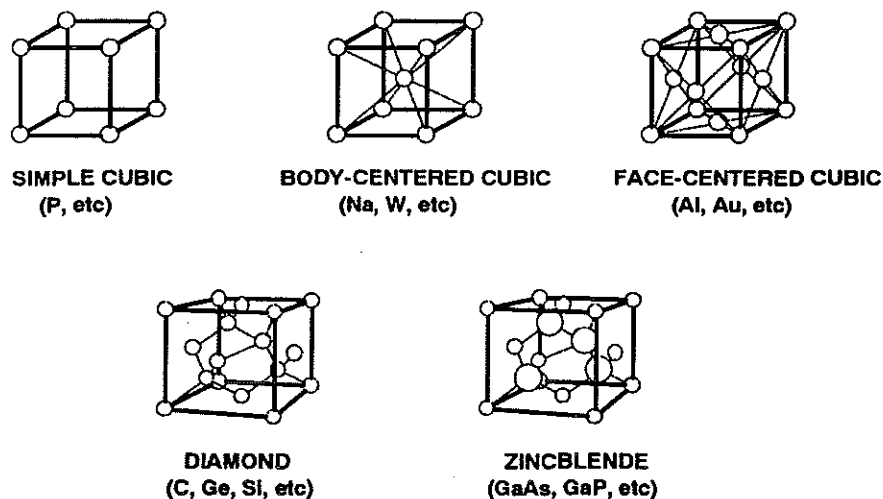


Figure 4.7. Some important unit cells (direct lattices) and their representative elements or compounds.

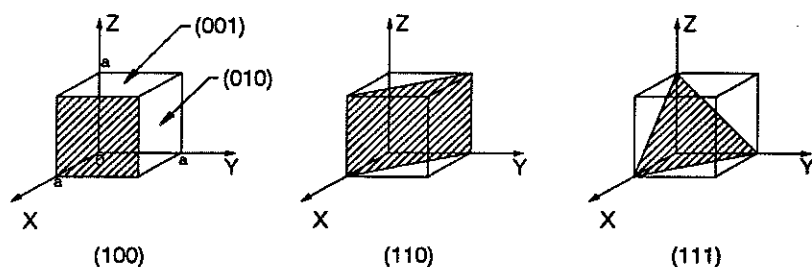


Figure 4.8. Miller indices of some important planes in a cubic crystal.

4.1.1. Experiment

To attain atomic resolution for gold, the STM signal has to be particularly low in noise. The very nature of the metal means that the electrons will be strongly delocalized between the atoms and there will only be small variations in the electron density with atomic position. The periodic modulations are typically on the order of 0.1 \AA , so one should not expect to image gold atoms in normal room conditions. The purpose of this lab is to introduce the concepts of tunneling and the extremely delocalized nature of electrons defined by the metallic state.

4.1.1.1. Holographic Gold Grating: STM Magnification

The first sample to examine is the gold-coated holographic grating. This sample is a single-period hologram with a sinusoidal spacing. A hologram of the type seen on credit cards is composed of many such sinusoidal patterns of varying periods and orientations, which recreate the original image when viewing the diffracted or scattered light off the surface. This sample illustrates the piezoelectric tube scanner range and reinforces the level of magnification possible with the STM. The reference images are: grating1.img, grating2.img, grating3.img, grating4.img, and grating5.img. These are images of a grating with spacing of $0.2 \text{ }\mu\text{m}$ (2000 \AA). The grating you are provided with has a spacing of 2400 lines/mm or about $0.4 \text{ }\mu\text{m}$ (4000 \AA) line spacing. It is easier to obtain high quality images with this grating.

Procedure:

Head Preparation

1. Prepare either a PtIr or W tip and mount the tip.
2. Select the gold grating from the sample set. To determine the direction of the grating lines. Look at the surface of the sample along one of its edges. Light would diffract by the grating along a direction perpendicular to the grating lines. Mount the sample so that the grating lines are parallel to the sample carriage handle.
3. Turn the Sample Position dial until the sample range indicator is close to the middle of the range or the sample-tip spacing is less than 0.5 mm . Be careful not to damage the tip and the sample. You may have to use the Coarse Retract button to reposition the tip. By moving the tip with the controller make sure there is enough range for the tip to reach the sample during approach.

Software Preparation

4. Load grating3.img (File/Load). This image is shown in Figure 4.9.

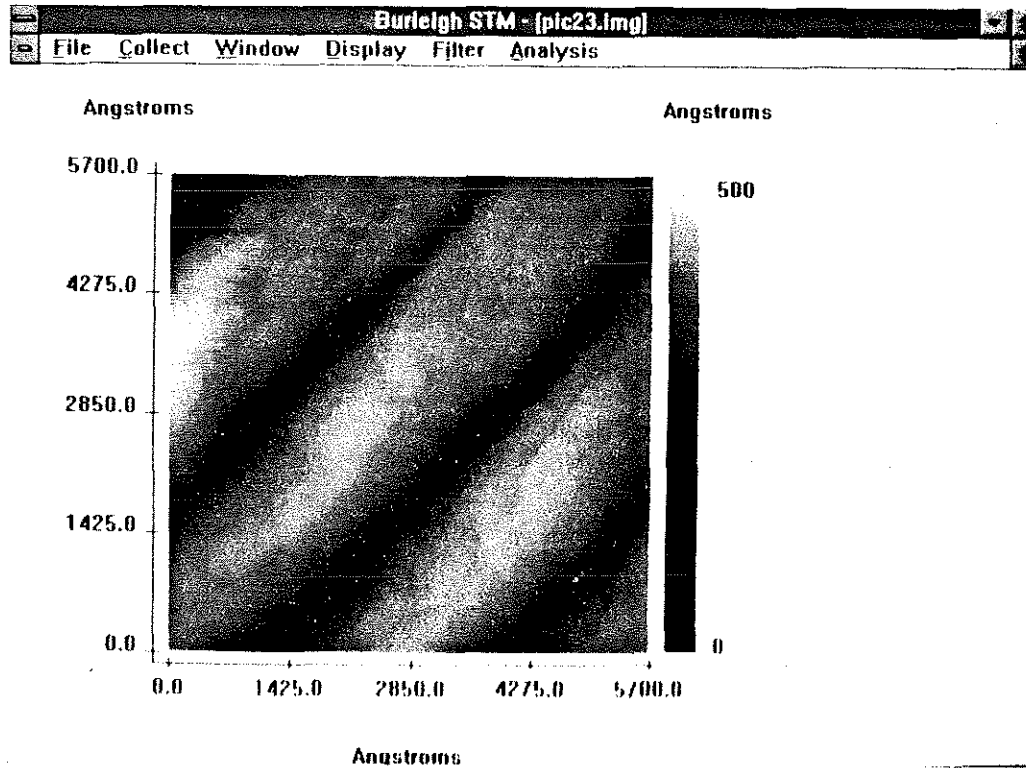


Figure 4.9. An ISTM image of a 5700 Å x 5700 Å area of gold grating obtained in constant current mode.

5. Set the Scan Delay (Collect/Configure) to 0.2 mS/Sample.
6. In this scan you are monitoring height variations, so set the Data Type to Topographic (Collect/Configure).

Electronics Preparation

7. Set the Bias Voltage to about 1 volt.
8. Set the Reference Current to 8 nA.
9. Set the Servo Loop Response for constant current mode of operation. Set the Gain close to maximum. Set the Filter close to maximum. Set the Time Constant to minimum.
10. Set the magnification to X1.

11. Set the X and Y offset slides at their middle range.
12. Press the Tunneling Current button to monitor tunneling current (it should read about zero).

Tunneling

13. Press the Coarse Retract button momentarily to reset the motor controls.
14. Press the Auto Approach (Tunneling) button for approach and wait.
15. Monitor the tunneling current until it reaches about 8 nA (equal to the reference current). If the tunneling current oscillates, reduce the Gain and Filter or increase the Time Constant to stop the oscillation. Oscillation manifests itself as periodic variations of the PZT voltage (J2 BNC on the front panel of the controller) which you may monitor on an oscilloscope.
16. Once tunneling is achieved, start a unidirectional scan (Collect/Scan Unidirectional).
17. Collect images and save one at this range.

NOTE: Typing (ALT C then A) or just A will abort the scan without saving the image. Typing (ALT C then H) or just H will stop at the end of the image and save it in the computer memory.

18. Change the scanner range by turning the magnification dial. Set the software size correctly in the menu by setting the zoom factor (Collect/Configure). Collect an image at each setting.

The large scan range should reveal a sinusoidal pattern on the surface with a period of 4000 Å and height variations of 400 - 500 Å. Figure 4.10 shows large scans of a grating with a periodic spacing of 2000 Å. As you zoom in, the details of the gold crystallization process on the hologram should become apparent. The evaporated gold tends to rapidly diffuse to form random crystallites with grain sizes of approximately 60 - 100 Å. You can prepare a montage of all the collected scans (from the Windows display mode) to visualize an overall factor of magnification of $\sim 10^8$ at the highest magnification (such as in the images grating1.img through grating5.img).

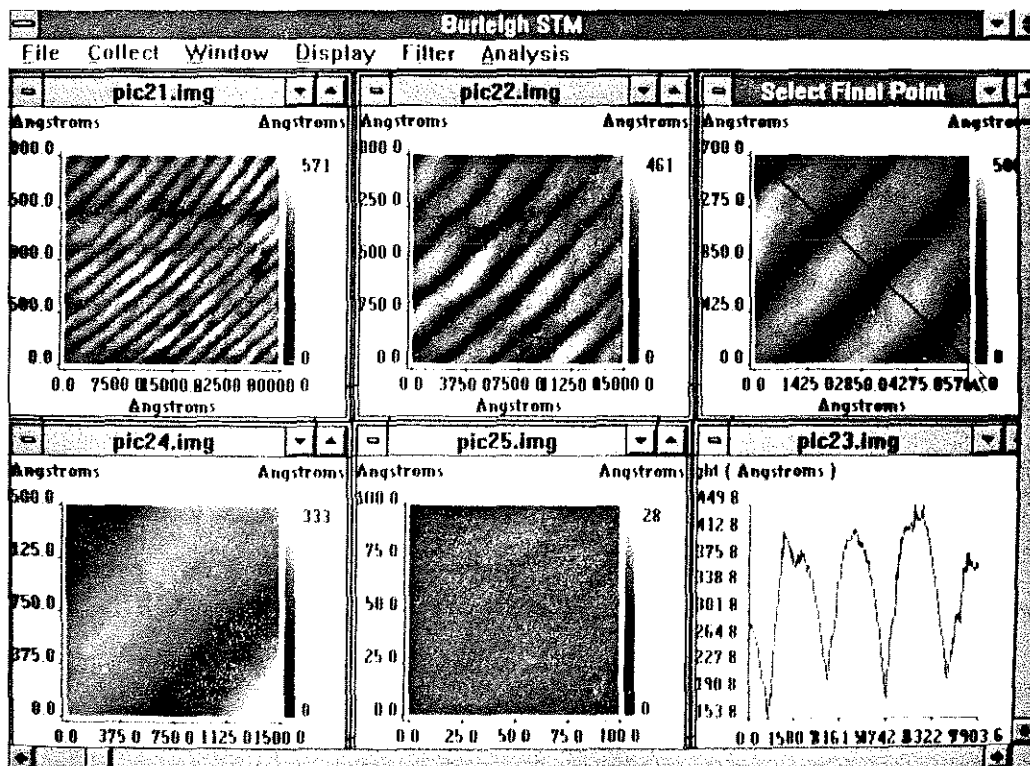


Figure 4.10. STM images of gold grating at different magnification settings. It should be possible to take images of atomic steps in extremely quiet tunneling conditions.

You may use the grating spacing to calibrate the range of the PZT motion. The grating has 2400 lines/mm (Your sample kit may indicate a different number of lines/mm, use that number for calibration). This corresponds to a line spacing of about 4167 Å, the perpendicular distance between center of the lines. To calibrate the PZT acquire images of the grating with the following software settings (Collect/Configure): Set Scan Range in X equal to Max Scanner Range in X, and set Scan Range in Y equal to Max Scanner Range in Y. Set the Zoom Multiplier to X2. Take an image with the magnification set to X2 on the control electronics.

From the image calculate the scale in X and Y directions. The sample may be oriented to give only vertical grating lines on the display. You may assume the scan to be square, and just count the number of grating lines you see on the screen. Then, multiply this number by 4167. Set the Max Scanner in X and Y equal to this number multiplied by 2. The Max Z Range is typical 40% of the Max Range in X.

Only for extremely quiet tunneling conditions will it be possible to discern atomic features. The best chance of obtaining atomic features is from the constant height mode at high scan speeds. Set the tunneling current to 4 - 5 nA and use a bias voltage of ~100 mV. You should compare this image to the constant current scans. The constant current mode cannot operate at as high a scan speed because it is limited by the response-time of the feedback loop; it is also more prone to acoustic noise than the constant height mode. The tip is extremely important in this regard, so you may want to try different tips. However, you should not expect to attain atomic resolution in this experiment. The main point here is to get an approximate determination of the maximum periodic variation in the electron density across the surface.

Load a representative image (File/Load). Use the cursor and draw a line through the data to visualize the fluctuations in tunneling current (Display/Cross Section). The current should be fairly constant across the surface, with variations of less than 0.1 Å in the tip position, to maintain constant current. The noise on your data may exceed this value, so you may want to filter the data to reduce the noise level in the image. The main point is that the low degree of current variation across the surface illustrates the highly delocalized nature of electrons in metals. This study should be contrasted to that of graphite in the next section.

NOTE: Be sure to store the images you want to keep on a diskette as backup. You may want to analyze or filter the images later and put them into perspective view or other formats. You should also make a hard copy for your reports. These can be made by either photographing the computer monitor or using a video printer, if available.

4.1.1.2. Questions

1. Sometime during the use of the STM, the tip may have "crashed." This is observable as a sudden large change in the current. This occurs when there is a change in the surface topology to which the feedback loop does not respond quickly enough and the tip touches the surface. Calculate the effective resistance of the tunneling gap for the conditions used in your experiment and compare that to the expected resistance if the tip was in direct ohmic contact with the surface. The resistivity of gold is $10^{-8} \Omega/\text{cm}$. This comparison should graphically illustrate the tunneling effect you are observing.
2. As the temperature of metals is raised, the resistance to current flow increases. Discuss the mechanism of resistance in metals and compare this mechanism to electron tunneling. How would the temperature-dependence of the two mechanisms differ?

3. Because these experiments were conducted in air, adsorbed water, solvents, and gases are undoubtedly on the surface. How do these molecules affect the tunneling process and how might the tip perturb their distribution? Contaminants on the tip are also likely problems. Explain how this would affect the noise on your STM experiment.
4. Consider the problem of the electron source in these experiments. If the tip is not scanned but left stationary over the surface, at a fixed distance that corresponds to a tunneling current of 1 nA, calculate the number of electrons/second that flow through the atoms that participate in the tunneling process between the gold and tip surfaces.
5. Calculate the expected variation in tunneling current for workfunction of 5 eV and sample height variations of 0.1 Å.

4.2. Graphite — Semimetals

The most striking images taken with an STM have been of semiconductor surfaces prepared in an ultra high vacuum environment. If one can create a flat, clean surface in vacuum, it will remain clean long enough to image with an STM. If the vacuum is not of a high enough quality, contaminant molecules will start to adsorb onto the surface. They will perhaps agglomerate on the surface or move under the surfaces, degrading the ability of the STM to resolve atoms. Given enough time, some contaminants may form a thin layer on the surface that may be insulating, thus preventing the tunneling process.

Because of the presence of contaminants, it would seem amazing for the STM to work in air.⁵ However, some materials are resistant to contaminants adsorbing onto the surface in destructive quantities. Graphite is one of these materials; gold, as previously discussed, is another. In this section, we consider some properties of Highly-Oriented-Pyrolitic-Graphite (HOPG), more commonly referred to as graphite. We will also learn how these properties relate to the STM images that are measured.⁶

The atomic structure of graphite, as determined by other methods, such as X-ray diffraction technique, has been known for a number of decades. A ball and stick model is shown in Figure 4.11[a]. An important feature of graphite is that it is highly anisotropic. It is a layered material: the atoms can be grouped into planes, where the distance between nearest-neighbor atoms in the plane is 1.42 Å and the distance between the planes is 3.35 Å. The planes of atoms in the graphite structure are staggered. This can be seen clearly from the side-view shown in Figure 4.11[b].

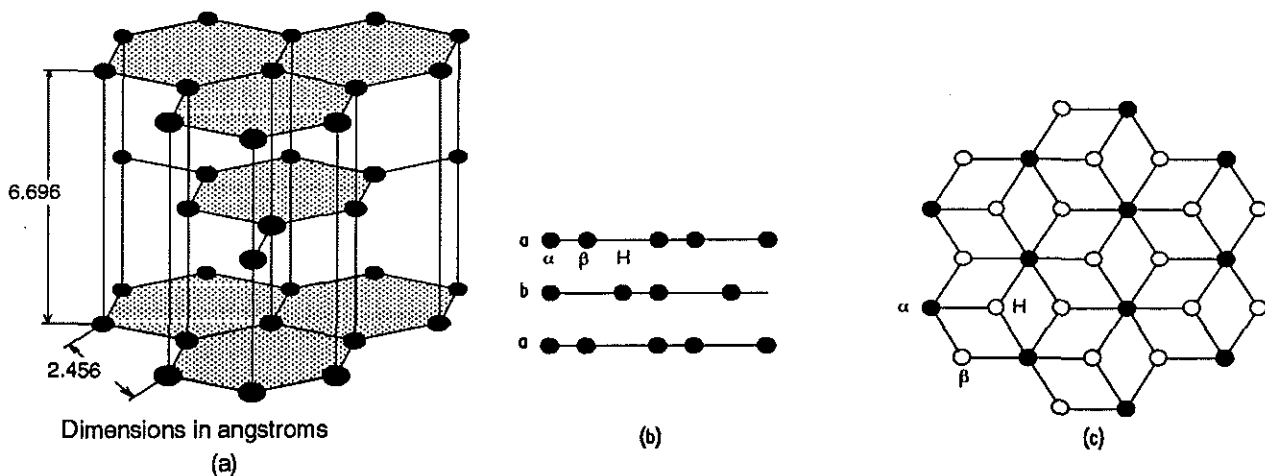


Figure 4.11. Crystal structure of graphite. This structure is peculiar in that the separation between lattice planes is almost 2.4 times the nearest-neighbor distance within planes [a]. Note the two different atomic sites α and β indicated in side [b] and top view [c].

Because of the staggering of the planes, there will be two types of atoms on the top surface layer, which we call α atoms and β atoms. An α atom on the top layer is right above a β atom on the layer below it, while a β atom on the top layer is above a hollow site. The two different types of carbon atoms can be distinguished with the STM.

As illustrated in Figure 4.11, the graphite surface can be thought of as a network of benzene molecules bonded together covalently. Covalent bonding refers to the chemical model in which atomic orbitals of similar energy overlap and form bonding combinations that are occupied and make up the valence band and antibonding combinations that are normally empty (and hence form the conduction band). It is also likely that this interstitial electronic distribution will be localized in certain preferred directions, leading to what are known in the language of chemistry as "bonds" (see Figure 4.12). The carbon atoms are sp^2 hybridized in the graphite crystal structure. The atomic s-orbitals mix with p_x and p_y . The bond angles are 120° , which leads to the formation of a hexagonal surface structure. Each carbon atom is bonded to three other carbons, which uses up three of the four valence electrons. This leaves a residual p orbital and an extra electron for each carbon atom. The p orbitals overlap to form an electronic band similar to the delocalized π orbitals in benzene (see Figure 4.13). The carbon bond length of 1.42 \AA is also close to that of benzene, half way between a single and double carbon bond. The bonding overlap of the p orbitals ties up all the valence electrons. There are no non-bonding orbitals exposed at the surface that would be susceptible to electrophilic reactions with contaminants; and there are few molecular reactions in which it would be energetically favorable to break up the resonance stabilization of the carbon lattice. This makes graphite highly inert.

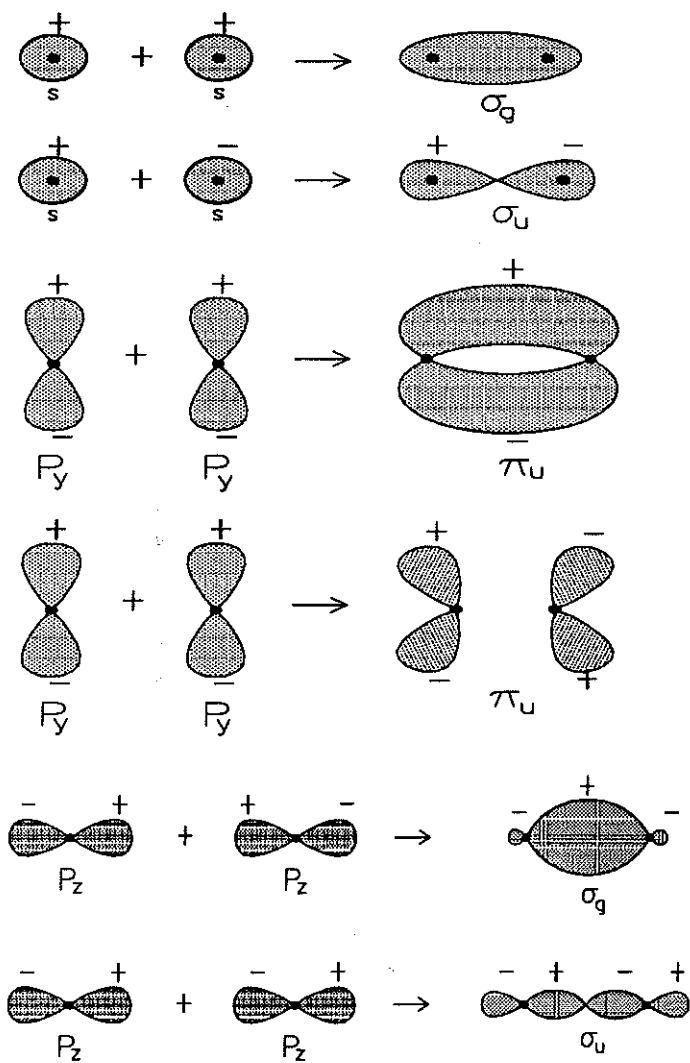


Figure 4.12. The description of σ and π bond formation by overlay of p orbitals. A σ orbital is symmetrical around the bond direction, but a π orbital has a planar node in the bond direction.

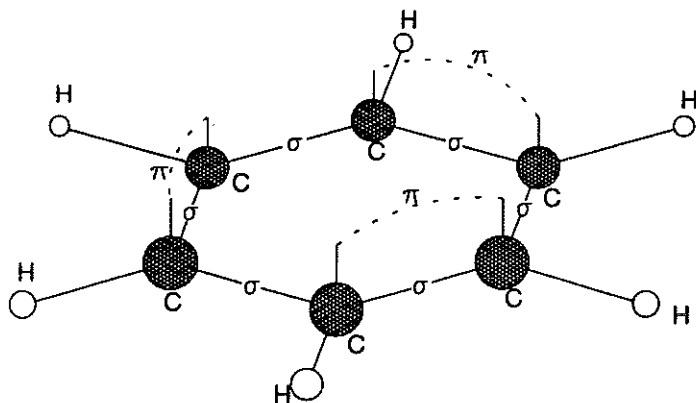


Figure 4.13. The C-H and C-C bond orbitals formed by a set of sp^2 hybrid orbitals on each carbon atom are shown here only as lines. The "sideways" overlap of two p orbitals gives a π orbital.

The anisotropy in the structure of graphite (see Figure 4.11) is significant for understanding its mechanical and conductive properties. Since all the valence electrons are tied up in bonding orbitals, most of the interatomic interactions involving the graphite surface involve weak van der Waals forces. This weak interaction leads to very low surface friction and is responsible for the excellent lubricant properties of graphite. In addition, since all of the bonding orbitals in the two-dimensional hexagonal structure of graphite are "saturated," only a relatively weak van der Waals bonding exists between the planes in the lattice. The very weak bonding between the planes relative to the strong covalent bonding within the plane causes the crystal to fracture along the planes. A very simple method of cleaving the crystal is to apply transparent tape and peel off a layer of graphite to expose a very clean surface suitable for STM studies (see Figure 4.14).

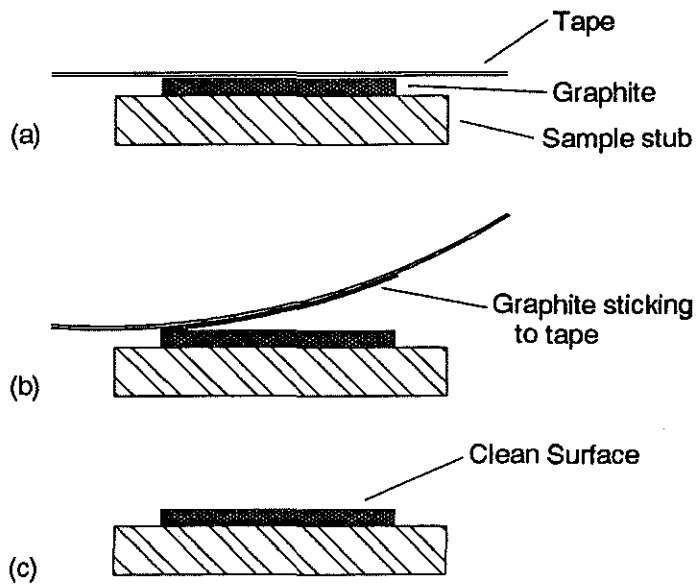


Figure 4.14. The weak bonding between the planes allows for a simple method of cleaning. Place a piece of clear tape on the surface and gently peel a layer off.

The highly anisotropic conductivity of graphite can also be understood from its atomic structure. The electronic coupling between atoms is related to the wavefunction overlap or degree of sharing of electron density between carbon atoms. This degree of coupling between two atoms determines the ease of motion of the electron from one atom to another. Electronic coupling or wavefunction overlap is much stronger within the plane than it is perpendicular to the surface. Thus, the resistance is much higher perpendicular to the surface; for this reason graphite is classified as a semimetal.

4.2.1. Atomic Resolution Images of Graphite

As discussed earlier, the image taken by the STM is not exactly the atomic topography but the density of the cloud of electrons around the atoms of the surface. In addition, it is only the highest energy electrons in the well and the extent of those electron clouds in space that is responsible for the tunneling (see Figures 4.15 and 4.16). Because a α atom of the top plane can couple to another α atom of the plane below, the energy of the electrons in the α atoms will be lowered. Thus the highest energy atoms in the top plane will only be on the β atoms. To the STM, it is as if the α atoms have disappeared. Therefore, an ideal STM image should only be of the β atoms. One should see a triangular lattice of β atoms rather than the honeycomb lattice of all the surface atoms, as shown in Figure 4.17.

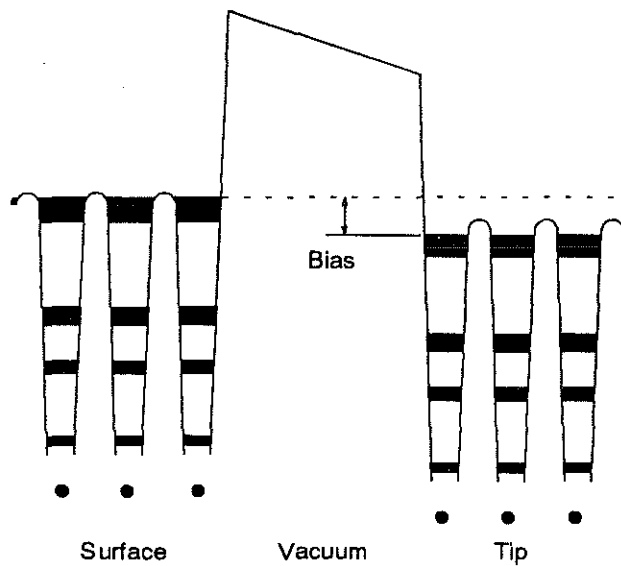


Figure 4.15. An energy diagram of the sample-tip tunnel junction. The sample is biased negatively with respect to the tip.

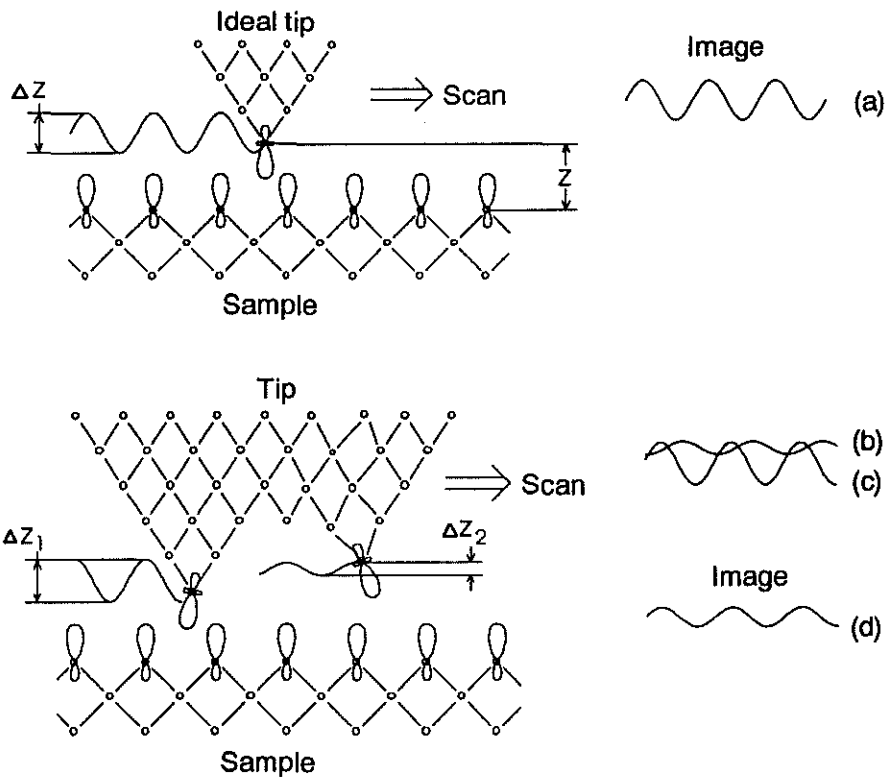


Figure 4.16. The overlap of the tip and sample electron clouds as the tip is scanned over the surface leads to the creation of an atomically resolved image of the surface [a]. Multiple tips can produce overlapping images [b and c] which may ultimately yield faulty results [d]. Refer to the text for more details.

However, images are not always seen for graphite surfaces, as shown in Figure 4.17. By adjusting the bias voltage and the tunneling current, sometimes the image appears to change to another structure. These anomalous structures are caused by multiple atomic tips.

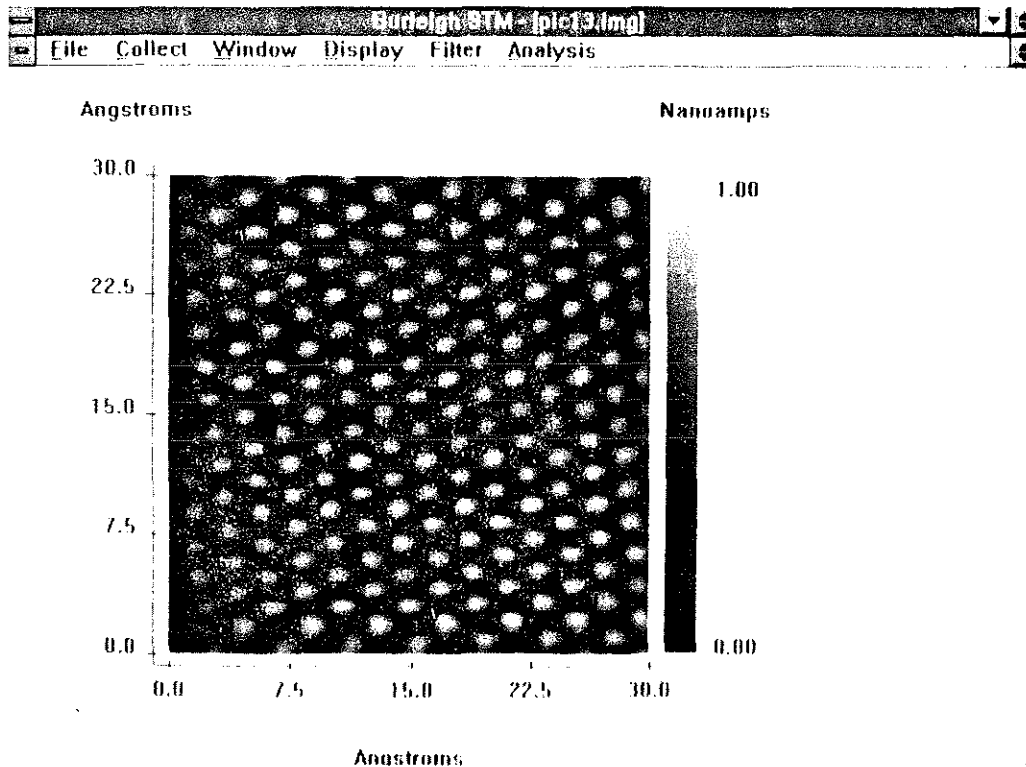


Figure 4.17. A 30 Å x 30 Å image of graphite acquired in a constant height mode.

4.2.1.1. Distortions in Images Caused by Multiple Atomic Tips

To understand how multiple atomic tips can distort images, one must first look at the path the tip takes as it scans over a series of atoms. This path is shown by the sinusoidal lines in Figure 4.16. Because the atoms are so close together, the atom that protrudes from the end of the tip cannot reach in between surface atoms. Instead of tracing out the round shapes of the atoms, the tip takes a path more like a sine wave.

Because of the high electric field that exists between the tip and sample, atoms will sometimes move around on the tip. It is possible that a tip might have two or more atoms that are about the same distance from the surface, as illustrated in Figure 4.16[b]. If the two tip atoms are approximately the same height above the surface, significant tunneling current will flow through both atoms. Because of the exponential dependence of the tunneling current on sample-tip separation, the exact configuration of the other atoms that comprise the macroscopic tip is not significant.

The effect of a multiple tip is that both scan the surface but their image of the surface is shifted relative to one another. Thus one obtains a ghost image, i.e. two images of the surface are shifted relative to one another and superimposed. For surfaces that have atoms that are far apart, we should see this superposition as a doubling of atoms. Figure 4.18 shows a 1000 Å x 1000 Å area of gallium phosphate (GaP) surface decorated with bismuth (Bi) islands of different heights (gray and white dimples) imaged with STM. A second scan of the surface has clearly revealed the effect of two well-separated tips tunneling and imaging the same surface.

The microscope "sees" everything doubled. You can easily correlate the islands between two images to recognize the double tip effect. The multiple tip effect can be very severe when the tip is "blunt" (a few tips stick out and tunnel simultaneously). The tip may be so blunt that the flat atomic corrugations on the surface might not be imaged, as Figure 4.19 suggests.

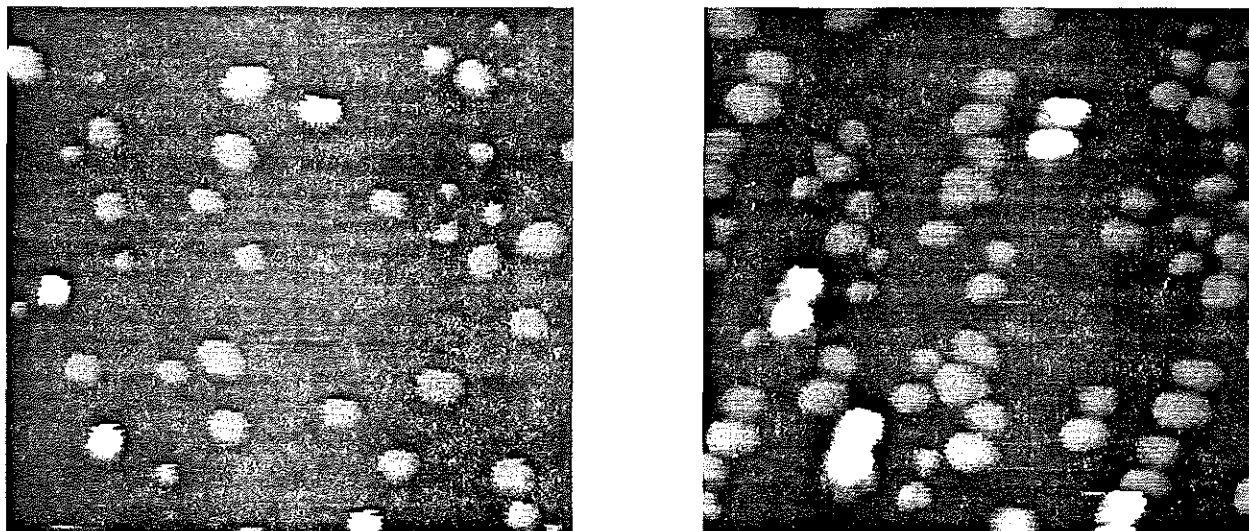


Figure 4.18. Multiple tip effect is dramatically evident when comparing the STM images of bismuth islands on gallium phosphate.

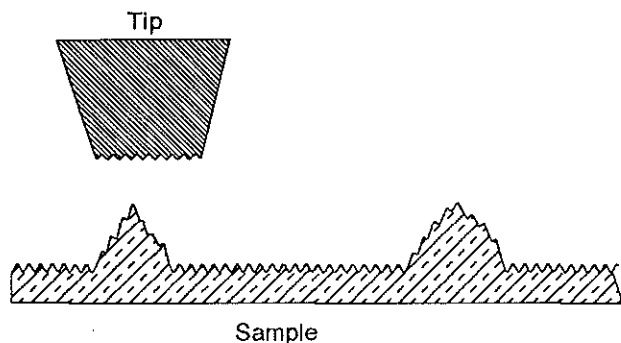


Figure 4.19. Severe multiple tip effect. The tip is so blunt that the surface images the tip!

For materials like graphite that have a periodic array of atoms, the superposition takes on a different form. When two tips image the surface, the resulting image is a superposition of two periodic images that can appear as having larger or even different periodicity. The effect of combining these images can be seen by shifting around the transparencies of three sine waves with different phases provided with this manual. If one slides the top transparency slowly to the right, one can make the triangular array of atoms turn into a honeycomb lattice of atoms. The number of atoms appears to have doubled, even though the same periodic structures are being combined. These distortions are due to multiple tips over a periodic structure. Another interesting case can occur when multiple tips scan over multiple grains of same periodicity. Use the transparencies of graphite images now and move these transparencies with respect to each other. A number of ghost images with different periodicity can be produced this way. In terms of optics this is a Moiré-like effect.⁷

4.2.2. Experiment

This lab should provide direct observation of atomic features of the graphite surface. It should also serve to contrast the difference in the spatial variation of electron density at the Fermi level between metals and semimetals. This reflects the nature of and the degree of overlap in the atomic orbitals involved.

4.2.2.1. Imaging Graphite

Procedure:

Head Preparation

1. Prepare either a PtIr or W tip and mount the tip.
2. Select the HOPG (graphite) from the sample set and mount the sample. You might want to use transparent tape to cleave the sample (see Figure 4.14).
3. Turn the Sample Position dial until the sample range indicator is close to the middle of the range or the sample-tip spacing is than less than 0.5 mm. Be careful not to damage the tip and the sample. Place an optically flat portion of the sample under the tip. You may have to adjust the tip position using the Coarse Approach or Retract on the control electronics. Use the control electronics to make sure there is enough range for the tip to reach the sample.

Software Preparation

4. Load graph1.img (File/Load).
5. Set the Scan Delay (Collect/Configure) to 0.0 mS/Sample.
6. In this scan you are monitoring current variations, so set the Data Type to Current (Collect/Configure).

Electronics Preparation

7. Set the Bias Voltage to about -20 mV.
8. Set the Reference Current to 5 nA.
9. For approach always setup the Servo Loop Response for maximum rate of response. This corresponds to setting the Gain close to maximum, the Filter close to maximum, and the Time Constant to minimum.

10. Set the magnification to X250.
11. Set the X and Y offset slides at their middle range.
12. Press the Tunneling Current button to monitor tunneling current (it should read about zero).

Tunneling

13. Press the Coarse Retract button momentarily to reset the motor controls.
14. Press the Auto Approach (Tunneling) button for approach and wait.
15. Monitor the tunneling current until it reaches about 5 nA (equal to the reference current). Adjust the Gain, Time Constant, and Filter, if necessary, to stop any tunneling oscillation. Oscillation manifests itself as periodic variations of the PZT voltage (J2 BNC on the front panel of the controller) which you may monitor on an oscilloscope.
16. Once tunneling is achieved, set the Servo Loop Response for constant height mode of operation. Set the Gain close to minimum. Leave the filter at its maximum. Set the Time Constant to maximum. Start a unidirectional scan (Collect/Scan Unidirectional). Scan over a few areas of the surface by using the X and Y slide bars to find a relatively flat region. The tip needs some conditioning to remove contaminants, so it may take a while for the tunneling current to settle.

NOTE: You may have to use the X and Y slides to find flat areas on the sample. When using these slides note that the image on the screen moves accordingly. However, it may take a few minutes for the tip to settle and for the drifts to become small. Be careful when using the X and Y slides. The total range of the slides always corresponds to the maximum scanner size. Moving the slides for large distances and frequent times will cause the images look distorted. This is due to electromechanical properties of PZT.

17. Collect images and save one at this range.

NOTE: Typing (ALT C then A) or just A will abort the scan without saving the image. Typing (ALT C then H) or just H will stop at the end of the image and save it in the computer memory.

18. Change the scanner range by adjusting the magnification dial. Set the software size correctly in the menu by setting the zoom factor (Collect/Configure). Collect an image at each setting. Acquire images with effective sizes of 1000 Å x 1000 Å, 500 Å x 500 Å, 100 Å x 100 Å, and 20 Å x 20 Å.

19. Attempt to acquire images in the constant current mode by setting the Gain close to maximum. Set the Filter close to maximum. Set the Time Constant to minimum. Set the scan delay (Collect/Configure) to 0.10 mSec and collect topographic data. Usually the best images are obtained in the constant height mode. Tips which are not sharp and give unstable results in constant height mode usually will not give atomic resolution images in the constant current mode.

If the above procedures (steps 16-19) do not work, back off the tip and change tips. You should also cleave the surface again if repeated attempts don't bring out atomic details.

It should be possible to obtain images of graphite like those shown in Figure 4.17. If you get very stable graphite images, you should collect a number of scans, as a function of bias, to see how the appearance of the graphite lattice changes with bias. For a select scan, go into the display mode and use the cursor feature to determine the spatial variation in the constant current position of the tip. You may want to filter your data before you do this. Your data should show variations in surface topology of 1 - 2 Å. Variations may be larger in certain cases because of surface-tip interactions.

Contrast this result to the earlier study of gold surfaces (Section 4.1.1). For most images it should be possible to determine the hexagonal surface structure bond angles and approximate bond lengths of graphite. You should keep in mind the α and β types of carbon atoms in making your assignments. Multiple tip effects may also be observable. From your lowest noise image, it is particularly interesting to look at the surface structure using the 3-Dimensional perspective view display mode in Display. Again, be sure to store your data on a disk for later analysis and backup and to make a hard copy for your report.

4.2.2.2. Observation of a Chemical Reaction: Oxidation of Graphite

This experiment enables direct observation of how chemical reactions proceed. Graphite will oxidize in air at elevated temperatures. The reaction is $C_{\text{graphite}} + O_2 \rightarrow CO_2$. The activation is endothermic by 393.5 KJ/mole, which necessitates the elevated temperature. It is interesting that the reaction initiates at discrete locations on the surface. Dislocations and defects in the surface structure represent lower activation barriers to the process than the ideal flat surface. These sites tend to initiate the reaction, which then further develops from the vacancy left by the CO_2 that thermally desorbs. The result is that the oxygen drills craters into the surface. If the reaction is arrested, the reaction process can be monitored at various stages. One can anticipate in the future being able to watch in real time as a molecular bond is being made or broken.

This experiment is based on the work of Chang and coworkers.⁸ At the time of writing this manual, the results were highly dependent on the oven temperatures. Please be sure to determine the satisfactory parameters for your laboratory conditions.

NOTE: A second sample of graphite has been included for this experiment. This sample is not mounted on an SEM plug.

Procedure:

1. Make a fresh cleave of the graphite surface and place it in an oven. Heat the graphite up to a temperature of 900°C and leave it at that temperature for 5 - 10 minutes. Bring the sample out and let it cool.
2. Repeat the procedure for imaging graphite described above. The degree of oxidation is somewhat variable and depends on how well the graphite temperature can be monitored. You may have to extensively scan the surface to find evidence of oxidation.

The oxidation of graphite leads to some interesting reaction craters. You should try to correlate the sites of oxidation to any observable defects in the vicinity. This experiment gives insight into the initiation of reactions and the process of reactions at the surface. It may be possible to correlate reaction rates at specific sites by observing the depth and diameter of the oxidation crater.⁸

4.2.2.3. Questions

1. A common observation for graphite is that the surface corrugations associated with its atomic features are unusually large, i.e. greater than 2 Å. This determination must be made in the constant current mode. Such large corrugations result from additional contributions other than the electronic structure of graphite. Provide an explanation of this effect.
2. When you change the current set point to lower values, does this bring the tip closer to or farther from the surface? When you change the bias voltage to lower values, how does it affect the relative position of the tip to the surface?
3. In the solid state, carbon exists in either the graphite or diamond lattice structure. Diamond is the hardest material known. The diamond structure is tetrahedral with each carbon sp^3 hybridized. The formation of bands as a function of interatomic separation in the diamond structure is shown in Figure 4.20. Explain the differences in conductivity and hardness between diamond and graphite in terms of their atomic and electronic structure.

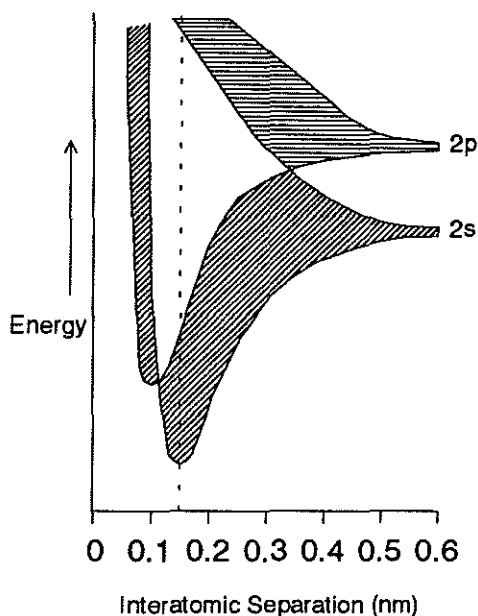


Figure 4.20. Energy bands of the diamond structure formed from s and p orbitals hybridizing.

4. A new form of carbon, referred to as a fullerene structure, has been recently discovered. This form of carbon is really an extremely large carbon molecule, but it does approach some solid state properties (recall that a solid state lattice can also be thought of as a giant single molecule). A particularly stable fullerene is C_{60} , which is shaped like a soccer ball. Each carbon is 120° apart to form a perfect icosahedron. If this molecule was crystallized in a closed-pack lattice, predict whether or not it would be conductive and whether or not it would be a good lubricant.

4.3. Molybdenum Disulfide — Semiconductors

Semiconductors are characterized by a full valence band and an energy gap between the valence band levels and the conduction band (see Figure 4.1.).⁹ This class of materials can take on conducting properties from either thermally promoted electrons from the valence band or from electron impurities. The impurities or dopants can act as electron donors, in which case the donor levels must be very close in energy to the lowest energy level of the conduction band. In this case, the semiconductor is said to be n-type because the current is carried by the electrons (negative charge carriers) thermally promoted to the conduction band. Impurities that have unoccupied electronic levels very close in energy to the highest occupied valence band level can pick up electrons. This leaves a vacant level or hole in the valence band. Electrons can move into this vacancy and cause the hole to move in the opposite direction. In this case, the current is carried by the hole carriers and the semiconductor is referred to as p-type (positive charge carriers).

Silicon is the most technologically important semiconductor. The growth of silicon crystals doped with phosphorous produces an n-type semiconductor because phosphorous has an extra electron relative to silicon and the position of this occupied level is 0.045 eV below the conduction band. Approximately 20 percent of these electrons will be thermally promoted to the conduction band (i.e. $e^{-\Delta E/kT}$). Similarly, boron can be doped in silicon crystals. In this case, boron has one less electron than silicon, which leaves a vacant level at the boron site, also 0.045 eV above the valence band. Silicon becomes p-type with this dopant. Selectively doping different regions so that an n-type region is adjacent to a p-type region creates a field as the dopants exchange electrons. The electrons from the n-type dopants fill the vacant levels of the p-type dopants, which leaves the n-type dopants positively charged and the p-type impurities negatively charged. This structure is called a p-n junction. The field that develops gives the semiconductor interface its rectifying properties, i.e. current can only flow in one direction. By applying an external bias, as in the STM experiment, the electrons can be "pumped" back to switch the junction to a conducting state. Clever alternations of n-p interfaces have enabled the development of a number of important solid state devices. For example, the first semiconductor device was the bipolar transistor (*transfer resistor*), which has an n-p-n or p-n-p doping profile. This doping profile enables operation as an amplifier or a fast current switch. There are numerous other structures that impart special properties for switching and amplifying currents. These developments have had an enormous impact in the technology base — from computers to communication.

As explained above, semiconductor devices operate on modified interfacial properties. This aspect makes the surface chemistry very important. In this regard, one of the simplest reasons silicon has played such a prominent role in the semiconductor industry is that it is the only semiconductor that forms a stable oxide at its surface (SiO_2 , i.e. quartz). This Si/SiO₂ interface does not have a large number of defect levels in the semiconductor gap at the interface or surface states. Midgap surface state levels created by surface reactions deteriorate the device performance because these levels complicate the doping of p or n donors needed to obtain a certain function. All other semiconductors either form oxide layers in contact with air that create a high surface-state density or form an unstable (continuously reacting) interface.

The first semiconductor bipolar transistor was discovered in 1947. This device was barely operational, but it demonstrated the basic operating principles of transistors. It took nearly two decades and thousands of work-years to solve the material purity and interfacial problems that have made semiconductor devices so widely used today. The surface properties of semiconductors have been and remain an important area of research. The STM has already played a very important role in this area by helping to elucidate the relationship between the structure and function of semiconductor interfaces (e.g. the Si(111) 7x7 surface reconstruction problem).¹⁰ The future will certainly be directed toward developing smaller and smaller devices providing more functions per unit area at higher speeds. Current devices are on the micron scale and the push is towards 100 nm devices, which would place us in an era of nanotechnology. STM provides the needed tool to look at what we design and it very likely will be used to fabricate certain devices. There is already a great deal of discussion about the possibility of using STM tips to pick up atoms and place them selectively on a surface as a method of digital data storage.¹¹ This would enable the storage of up to 10^{16} bits of information per cm^2 compared to today's highest storage capacity of $10^5/\text{cm}^2$. The fabrication of 10 nm masks by drilling away material with an STM has already been demonstrated.¹²

In this lab, we will examine the structural and electronic properties of molybdenum disulfide (MoS_2). This material occurs naturally in a mineral known as molybdenite. MoS_2 is a semiconductor with a band gap of .75 eV. It can be doped either p- or n-type so that it is conducting enough for STM studies.¹³ Like graphite, MoS_2 is a layered material in which all the valence orbitals within a single layer are involved in bonding orbitals. In general, the termination of the lattice at a surface leaves valence orbitals exposed that are not involved in covalent bonds with other atoms in the structure. These occupied non-bonding orbitals are referred to as dangling bonds. They are particularly prone to reactions with adsorbates on the surface that have different energy levels in their electronic structure. For semiconductors the result is the formation of the midgap surface states. For MoS_2 there are *no* non-bonding orbitals that arise at the surface. The very nature of a layer compound is that all the orbitals in a plane are involved in bonding. The crystal structure is quasi two-dimensional, with only weak van der Waals forces holding the planes together in the three-dimensional crystal structure. As with graphite, this property of MoS_2 makes it relatively free of contaminants and stable (two necessary conditions for ambient STM studies). In fact, examination of the MoS_2 surface in an ultra high vacuum shows that the surface picks up only trace amounts of carbon and oxygen even after immersion of the surface in a liquid.

The strong two-dimensional character of the lattice also means that the MoS_2 surface layer is not strongly perturbed and does not undergo surface reconstruction, i.e. does not need to undergo relaxation of the surface atoms to minimize the surface energy. Thus STM studies should provide representative results of the bulk lattice atomic and electronic structure of this material.¹⁴ The surface structure of MoS_2 is shown in Figure 4.21 for the (100) surface,¹⁵ as inferred from X-ray diffraction data.¹⁶ Figure 4.22 shows an actual STM image of the MoS_2 surface. The material consists of alternating layers of molybdenum between two layers of sulfur. The sulfur atoms form a diamond pattern on the surface with a lattice constant of 3.16 \AA . There is a similar pattern of molybdenum atoms in the next atomic row, but these are laterally displaced. It is interesting to note that the different atoms (Mo and S) occupy distinctively different sites in the lattice. With this information it is possible to identify the different atomic species on the surface.¹⁷ Approximate electron tunneling contours are shown in Figure 4.23 for the (100) and (110) directions. Theoretical calculations of the band structure of MoS_2 find that there is a significant contribution to both the valence band levels and conduction band levels by the Mo 4d and 5s orbitals. Even though the Mo atoms are not in the surface plane, it is possible to detect the Mo atoms from the symmetry of the tunneling contours. Figure 4.24 shows a $12 \text{ \AA} \times 12 \text{ \AA}$ area of this surface. The cross-sectioned area of the surface shows Mo and S atoms distinctly. The height distribution of the surface atoms also shows the existence of two distinct surface sites. These results should be reproducible in this experiment. molybdenum tellurite (MoTe_2) exhibits very similar characteristics to MoS_2 . Tellurium and molybdenum atoms can also be distinctly resolved in STM images.

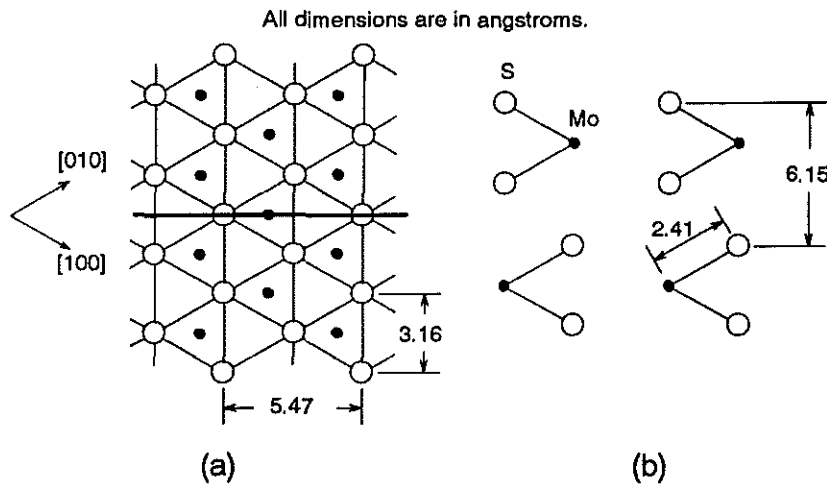


Figure 4.21. The (100) surface structure determined from X-ray diffraction studies [a] and the (110) cross section (along the dashed line in [a]) of MoS_2 [b]. (Adopted from reference 15).

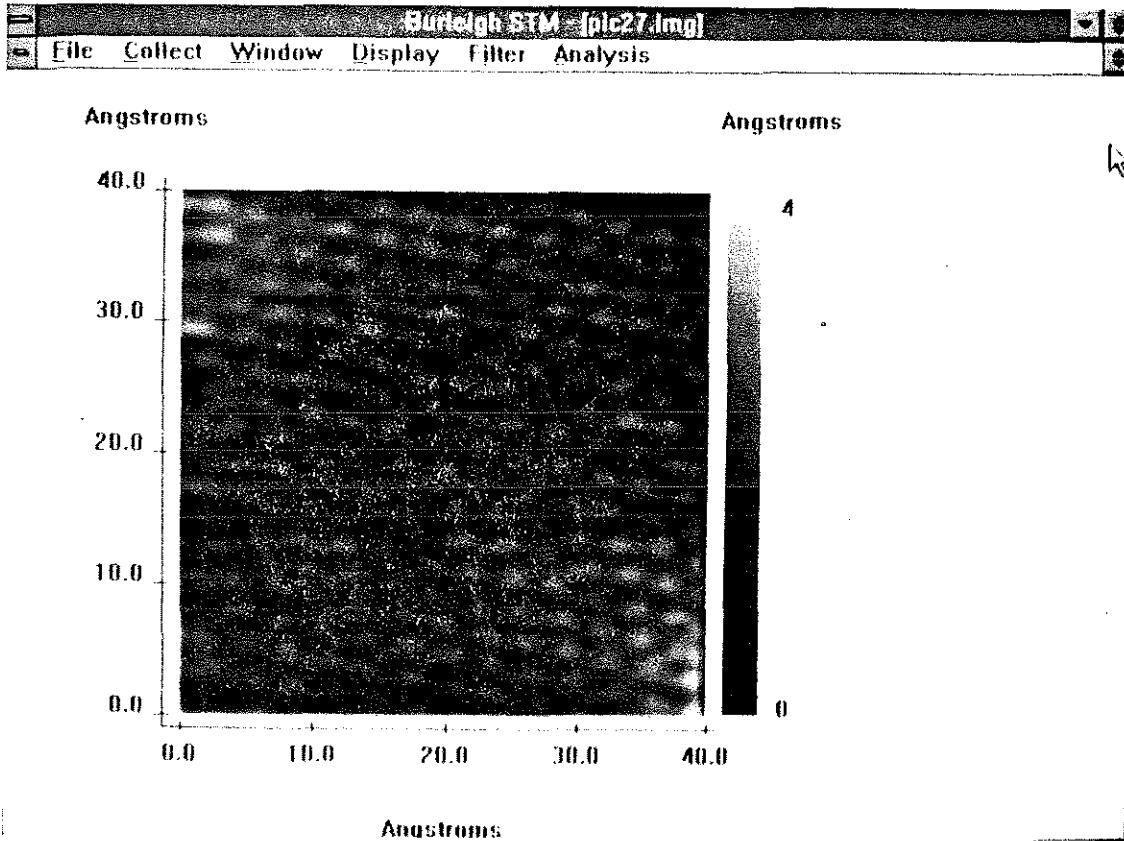


Figure 4.22. An STM image of natural MoS₂ showing a 40 Å x 40 Å area.

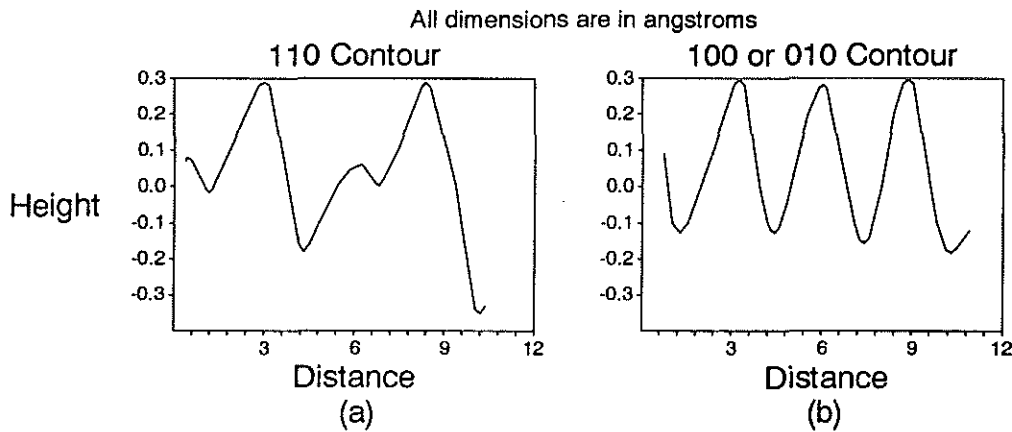


Figure 4.23. Anticipated cross sections from the data of Figures 4.21 and 4.22 along the (110) cell diagonal [a] and the (100) cell edge [b].

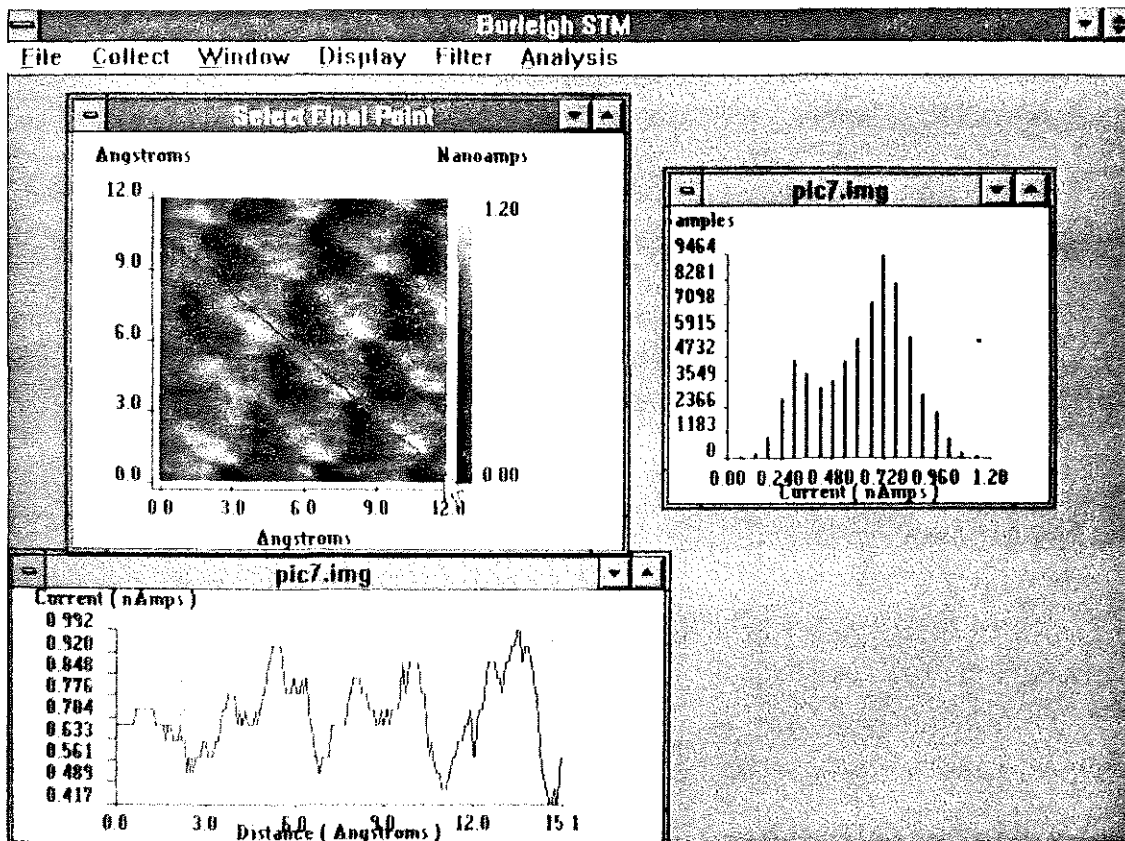


Figure 4.24. A 12 Å x 12 Å area of MoS₂ -imaged in constant height mode. The current variations along the surface clearly indicate the existence of two surface sites.

The MoS₂ crystal provided in this experiment is a naturally occurring mineral. These crystals can form near hot-springs and under water, where bacteria and other living organisms often contribute to mineral formation. Figure 4.25 shows a 500 Å x 500 Å scanned area of this crystal. It is interesting to note the ring-like structures on this surface. These structures have typical radii of 15 Å and 40 Å. A synthetically grown MoS₂ structure does *not* display any ring structures. Figure 4.26 shows a close-up of one of these ring structures. Secondary Ion Mass Spectroscopy (SIMS) technique shows a concentration of 0.5 percent carbon-12. This is in the same range as the size and density of these ring-like structures, if they are attributed to carbon based structures. One could think of carbonated chemical or molecular fossils as organic molecules that have survived unchanged or slightly altered from their original structure when they were part of organisms that have long since vanished. Scanning Electron Microscopy studies of larger particles of condensed spheroidal organic matter attributed these particles to early forms of life. The above interpretation, although still not clearly proven, may indicate early evolution of life on earth originating in geological time 3×10^9 years ago, marking the boundary between chemical and biological evolution.

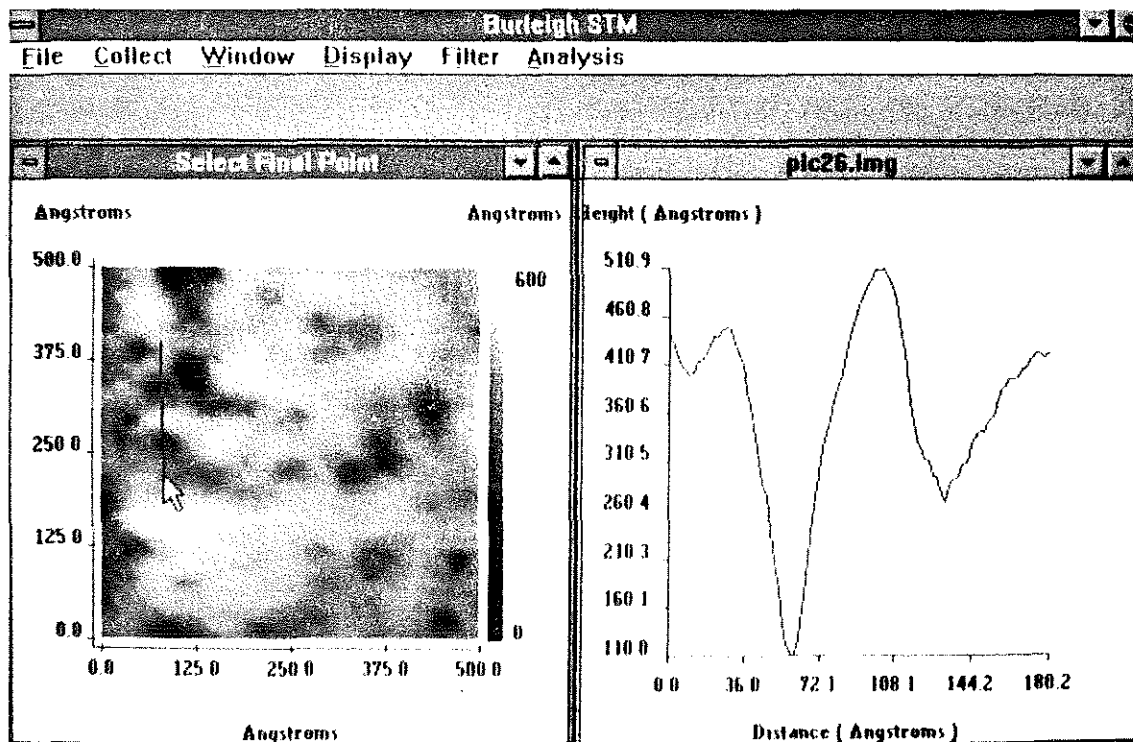


Figure 4.25. An STM image of natural MoS₂ showing ring structures with a radius of about 15 - 40 Å. This image was taken with a bias voltage of 25 mV and a tunneling current of 2 nA in constant current mode.

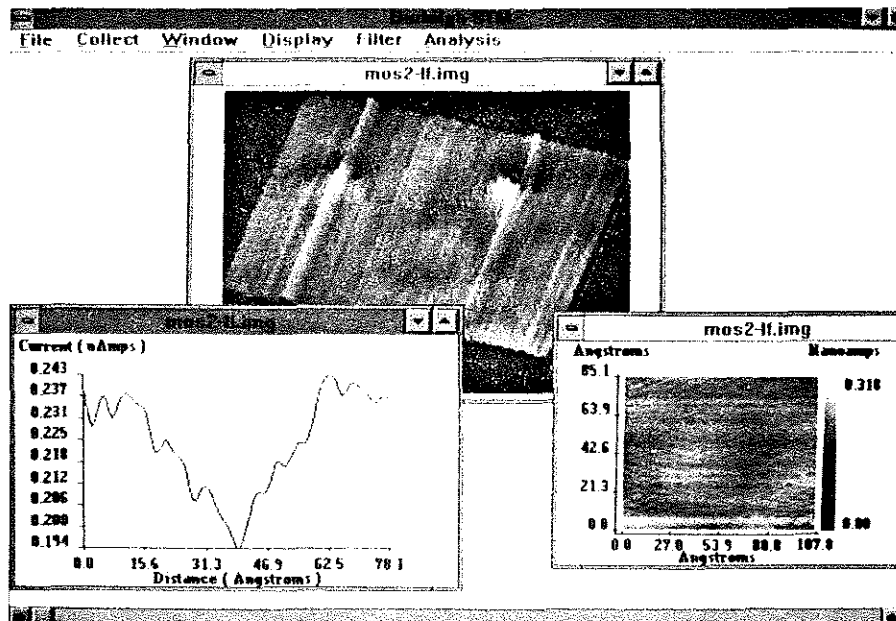


Figure 4.26. A closer view of the ring structures on MoS₂. The atomic corrugations of sulfur atoms can be clearly seen.

4.3.1. Experiment

4.3.1.1. *Imaging MoS₂*

MoS₂ can be cleaved like graphite by using the tape method. It cleaves along the van der Waals planes exposing the (100) surface.

Procedure:

Head Preparation

1. Prepare either a PtIr or W tip and mount the tip.
2. Select the MoS₂ from the sample set and mount the sample. You might want to use transparent tape to cleave the sample (see Figure 4.14).
3. Turn the Sample Position dial until the sample range indicator is close to the middle of the range or the sample-tip spacing is less than 0.5 mm. Be careful not to damage the tip and the sample. Make sure the tip is on a mirror flat portion of the sample.

Software Preparation

4. Load mos1.img (File/Load).
5. Set the Scan Delay (Collect/Configure) to 0.20 mS/Sample.
6. In this scan you are monitoring height variations, so set the Data Type to Topographic (Collect/Configure).

Electronics Preparation

7. Set the Bias Voltage to about 50 mV.
8. Set the Reference Current to 2 nA.
9. Set the Servo Loop Response for constant current mode of operation. Set the Gain close to maximum. Set the Filter close to maximum. Set the Time Constant to minimum.
10. Set the magnification to X10.
11. Set the X and Y offset slides at their middle range.

12. Press the Tunneling Current button to monitor tunneling current (it should read about zero).

Tunneling

13. Press the Coarse Retract button momentarily to reset the motor controls.
14. Press the Auto Approach (Tunneling) button for approach and wait.
15. Monitor the tunneling current until it reaches about 2 nA (equal to the reference current). Adjust the Gain, Time Constant, and Filter, if necessary, to reduce any servo loop oscillation.
16. Once tunneling is achieved, start a unidirectional scan (Collect/Scan Unidirectional). Scan over a few areas of the surface by using the X and Y slide bars to find a relatively flat region. The tip needs some conditioning to remove contaminants, so it may take a while for the tunneling current to settle down.

NOTE: MoS₂ does not provide as large a region of atomically flat cleavage planes as graphite. You will need to scan the surface to find a relatively flat region using X and Y slide bars. Once you find a suitable region, zoom in on the scan range to 20 - 30 Å. It may take a while for the tip to settle down to produce atomic images.

17. Collect images and save one at this range.

NOTE: Pressing (ALT C then A) or just A will abort the scan without saving the image. Pressing (ALT C then H) or just H will stop at the end of the image and save it in the computer memory.

18. Change the scanner range by turning the magnification dial. Set the software size correctly in the menu by setting the zoom factor (Collect/Configure). Collect an image at each setting. Acquire images with effective sizes of 1000 Å x 1000 Å, 500 Å x 500 Å, 100 Å x 100 Å, and 20 Å x 20 Å.
19. Acquire images in the constant height mode, setting the Gain at minimum. Set the Filter close to maximum. Set the Time Constant to maximum. Set the Scan Delay (Collect/Configure) to 0.00 mSec and collect current data. Usually the best images are obtained in the constant height mode.

With reasonable signal-to-noise, it should be possible to assign the surface structure. A representative STM image is shown in Figure 4.24. Using the cursor feature (Display/Cross Section), examine the different crystal directions and try to discern if there is evidence for the underlying Mo atom contributions to the tunneling current.

4.3.1.2. Questions

1. The first identification of individual atoms using the STM was accomplished for n-GaAs surfaces (also a compound semiconductor). At high positive bias, the As atoms appeared to occupy the positions of highest tunneling current. At low negative bias, the Ga atoms appeared brightest. Discuss this effect and how the different atoms could be assigned based on the bias-dependence for the image.
2. Discuss how you would perform spectroscopy on a semiconductor surface, i.e. what would a determination of dI/dV at a fixed position look like for MoS_2 . How would the appearance of surface states alter the dI/dV signal?
3. MoS_2 strongly absorbs light with wavelengths shorter than $1.5 \mu\text{m}$. The light promotes an electron from the valence band to the conduction band, producing an electron in the conduction band and a hole in the valence band. These states are referred to as electron hole pairs. Discuss how irradiating a surface of MoS_2 with light at $1.5 \mu\text{m}$ or shorter would affect the tunneling current.
4. How would you go about implementing the dV/dI capabilities of your STM to enable spectroscopic studies? To properly answer this question, consider what would happen to the tip as the voltage is scanned through the semiconductor gap region.
5. One of the hallmark differences between metals and semiconductors is that the resistivity of metals increases with increasing temperature and that, in contrast, the resistivity of semiconductors decreases with increasing temperature. Explain this difference.

4.4. Molecular Ordering on Graphite — Liquid Crystals and Long Chain Alkanes

STM studies under ambient conditions undoubtedly involve surfaces with adsorbed molecules. The molecules on the surface can affect the tunneling current in two ways: they can 1) act as a physical barrier to the tip's approach to the surface (mechanical effect) and 2) modify the height of the tunneling barrier (electronic effect).

In the first case, the intervening molecules may block the tip from approaching the position at which it normally would be for vacuum tunneling. The tip-approach mechanism will still advance the tip until it establishes the selected current value. The tip will literally push the molecule into the surface or squeeze the molecule out of its path. Normally the intervening molecules do not strongly adhere to the surface and are swept aside by the tip. The only effect is an increase in the noise of the experiment. However, in certain cases the intervening molecule is strongly adsorbed and can't be swept aside. The closer approach of the tip will cause the sample's surface to deform. The edges around the surface region depressed by the tip will raise and new electron tunneling pathways to the tip can form (see Figure 4.27). This is one possible mechanism that enables the STM to image individual molecules adsorbed to surfaces.

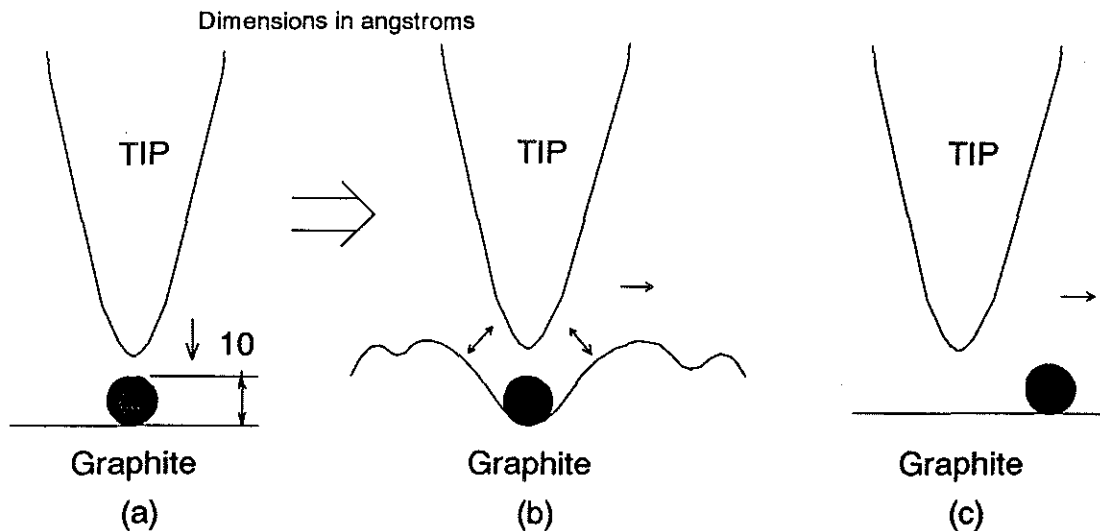


Figure 4.27. Adsorbate mechanical effects: Sample-tip interaction through an intervening molecule may cause the tip to actually deform the surface to keep a constant tunneling current between them, or push the molecule out of its path.

In the second case, the electronic levels of the intervening molecule can affect the tunneling current. The molecule's unoccupied levels will modify the effective barrier the electron experiences between the tip and surface. This effect is shown schematically in Figure 4.28. The net effect is the reduction of the barrier height. The enhancement effect of higher-lying energy levels on electron transmission probability is well known in molecular electron transfer processes. If one considers that the electron tunneling process depends exponentially on barrier height, this effect can have a significant impact on the observed tunneling current.

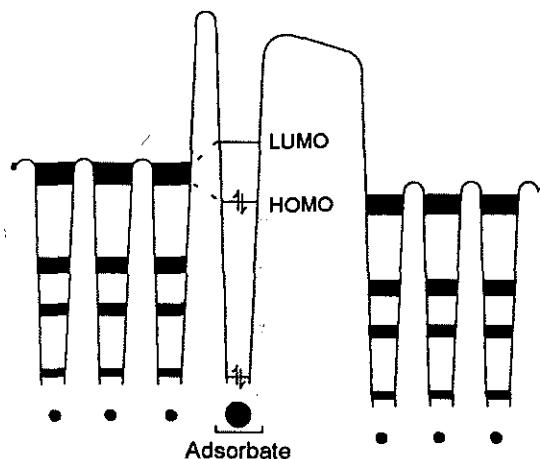


Figure 4.28. Adsorbate electronic effect: The effective barrier height is modified in the presence of an adsorbate. This can drastically change the tunneling current between the sample and tip.

In principle, either mechanical or electronic factors can provide a contrast mechanism that would enable the STM to image individual molecules. In fact, individual molecules and even adsorbed atoms have been imaged. The main problem is attaching the molecule or atom to the surface so the tip doesn't sweep it out of its path. Covalent bonding of molecules to surfaces or low temperatures so the molecule or atom is "frozen" to the surface have been successful.

The ability of the STM to study individual molecules is very important. There has been a great deal of research on how molecules orient and move themselves on surfaces. These are important issues related to the mechanisms of surface reactions. The STM is being used to answer these questions. In addition, if one can identify individual molecules, it is possible to use the STM tip to selectively initiate chemical reactions or pick molecules up and move them around like a pair of "atomic tweezers."¹¹

In the following series of experiments, we will examine the effect of intervening molecules between the STM tip and a conducting surface. The main focus of the experiments will be on molecular ordering using liquid crystals and long chain alkanes that strongly adsorb to the surface. Under the right conditions, these molecules form a two-dimensional lattice on the surface that exhibits a high degree of symmetry. This two-dimensional "crystallization" prevents the tip from pushing the molecules out of the way. In addition, it is generally difficult to assign STM images of individual molecules since there are not well-defined criteria for determining whether they are the molecule of interest, a contaminant, or a surface defect. The periodic nature of the molecular lattice permits unambiguous assignment of the molecular structures.

4.4.1. Liquid Crystals

Liquid crystals are familiar molecules to all of us. These molecules are commonly used in displays such as watches. By appropriate choice of structure, it is possible to convert these molecules from random orientations, which strongly scatter light (giving a frosted appearance), to aligned orientations with an electric field, for polar molecules, which are clear. This property allows the control of a display. As the name implies, these molecules have properties that are on the border between liquid and crystal. The basic structures of liquid crystals are all similar.¹⁸ They are generally rod shaped and the long axis of the molecule acts to accentuate its intermolecular interactions. The long axis hinders rotation and provides more exposed area to increase the van der Waals attractive forces that lead to the ordering of molecules, even in the liquid state. There are two specific phases unique to liquid crystals: the nematic phase, which is a short-range ordered fluid (semi-liquid state), and the smectic phase, which is a layered phase in which long-range order is established in a layer to give a two-dimensional liquid or solid (semi-solid state).

The ordering property of liquid crystals makes them ideal for studying the delicate energy balance of molecular self-assembly that is at the heart of living organisms. This property also enables the formation of a rigid layer on top of graphite that can be imaged with the STM without displacing the adsorbed liquid crystal molecules.

The first liquid crystal imaged with the STM was 4'-n-octyl-4-cyanobiphenyl (8CB).¹⁹ This liquid crystal has a convenient low temperature crystal-smectic phase-transition temperature. At room temperature, the material in contact with graphite crystallizes through the interaction with the graphite lattice and the material farther away remains fluid enough to permit tip approach. The structure of 8CB and a representative STM image are shown in Figures 4.29 and 4.30. Most striking in the STM image is the high degree of symmetry in the way the molecules order on the surface. There is a head-to-tail arrangement in which the lowest energy structure is with the two biphenyl groups next to each other. In addition, it is possible in certain cases to discern the individual biphenyl rings. Since the initial 8CB study, many other types of liquid crystals have been imaged. If the alkyl chain is changed, the length of the lamellar structure seen in Figure 4.29 changes. The period of the lamellar structure changes, as expected for the increase or decrease in the alkyl chain length. If the biphenyl head group is changed or substituted, there is a similar change in the interface region. These observations demonstrate that the STM can obtain enough contrast to directly study molecules at interfaces.

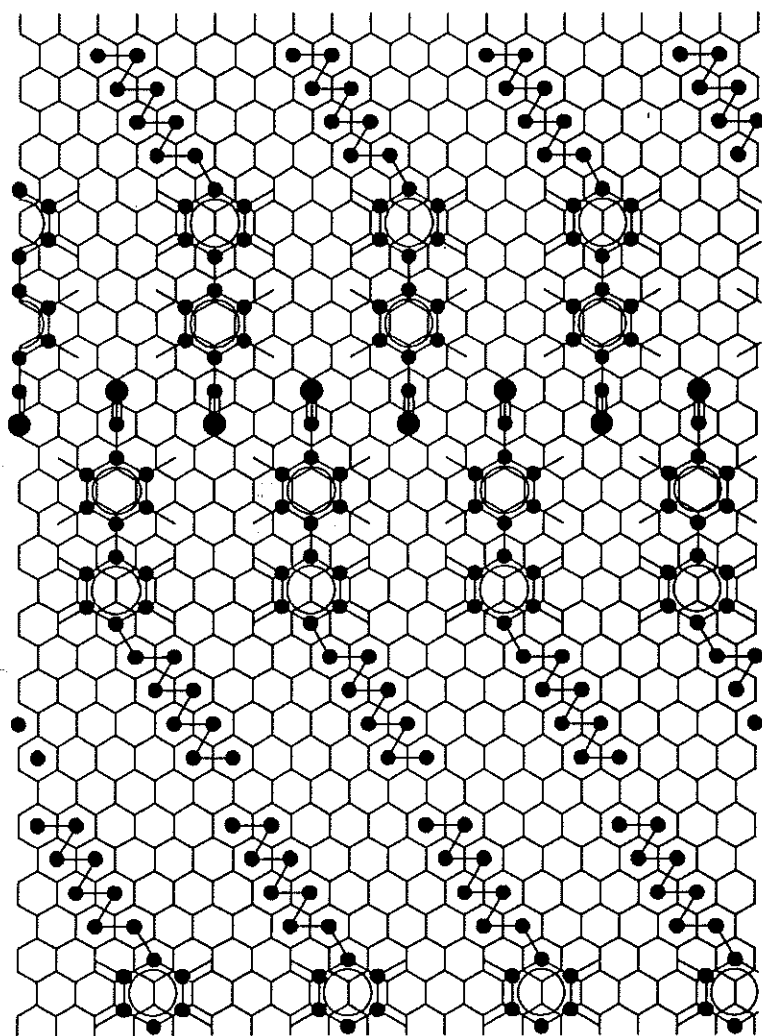


Figure 4.29. A schematic representation of 8CB chains on graphite. The length of the molecule is about 20 Å. It consists of a cyano group (nitrogen is the larger filled circle) to a biphenyl ring and a chain of carbon atoms attached to a second biphenyl ring.

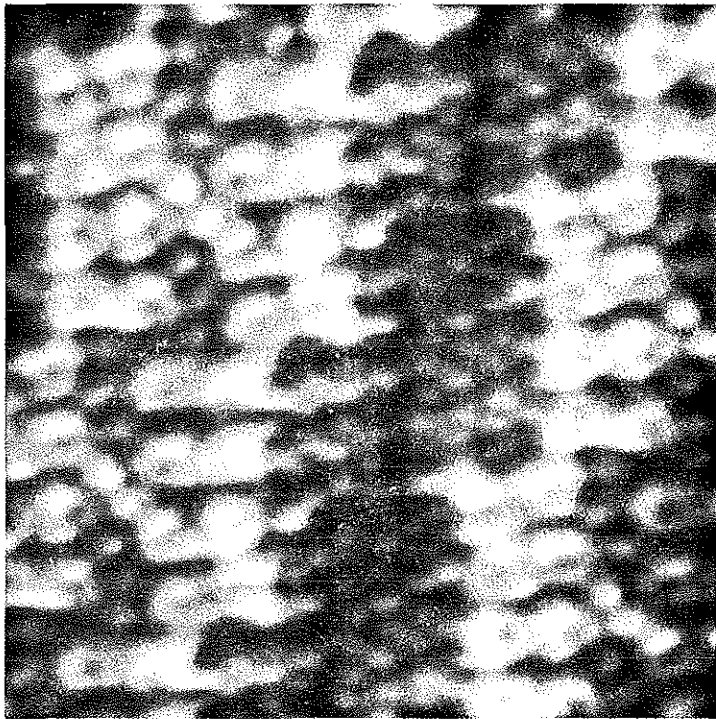


Figure 4.30. A detailed image of 8CB molecules adsorbed on graphite showing clearly the biphenyl rings. The 8-atom carbon tail appears dark in STM images. (Photo courtesy of D.P.E. Smith.)

4.4.2. Alkanes Adsorbed on Graphite

Long chain alkanes have been instrumental in determining the effect that adsorbed molecules can have on electron tunneling.²⁰ These saturated hydrocarbons are generally considered to be fairly flexible and usually form disordered solids at room temperature (such as paraffin wax). If carefully annealed, well-ordered crystals can be grown. It has been known for a number of years from calorimetric measurements that long chain alkanes adsorb quite strongly to graphite. It was believed that the graphite lattice acted like a template that ordered the adsorbed molecules into their lowest energy crystal structure.²¹ It was also known that the ordering phenomena, which was speculated to give rise to the strong adsorption, only pertained to the first monolayer on the surface.

Recent STM studies have found just that. Dotriacontane, $C_{32}H_{66}$, is one of the strongest adsorbed alkanes on graphite, with a surface adsorption energy of 209 KJ/Mole.²² This molecule was a natural starting point and was the first alkane successfully imaged on graphite.²³ A representative scan is shown in Figure 4.31. The molecules line up parallel to each other forming 40 Å wide stripes of molecules or lamellar regions. The different rows of molecules are separated by 4.5 Å and the spacing between the 40 Å lamellar patterns is 5 Å. This study directly demonstrated that this alkane preferentially adsorbs to the graphite surface in registry with the graphite carbon atoms (i.e. it is commensurate). The bright spots in this figure show the high tunneling regions that correspond to graphite atom locations. The alkane structure itself, if imaged alone, would consist of a zig-zag structure with 1.6 Å alternations in height. This result indicates that the adsorbed molecules are imaged primarily through their effect on the tunneling barrier, i.e. electronic factors dominate the contrast.

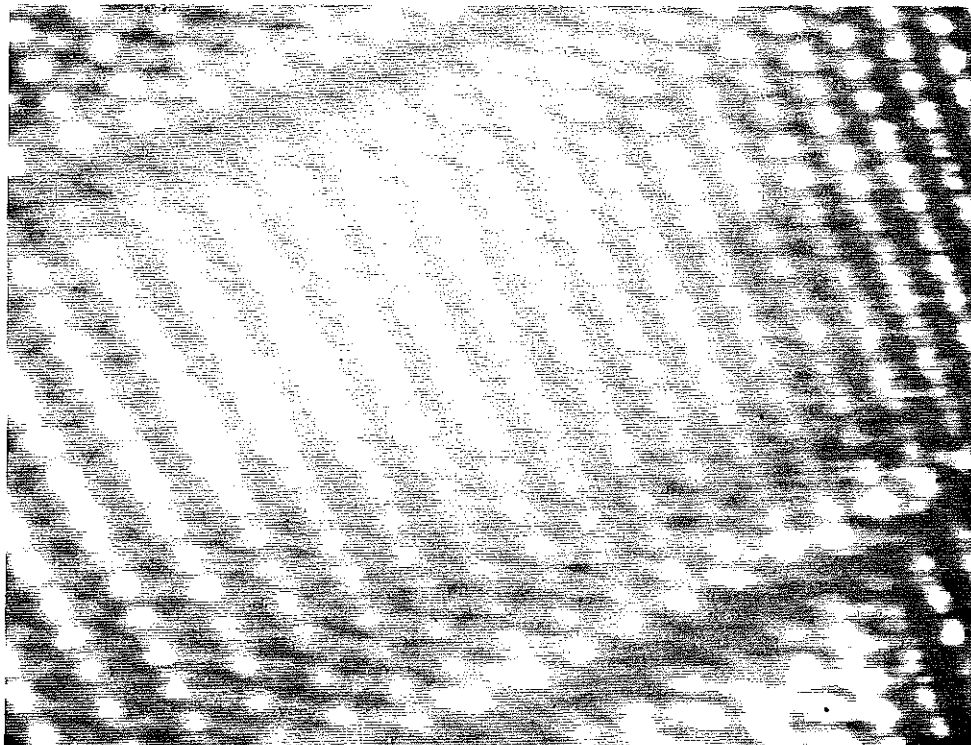


Figure 4.31. An STM image of dotriacontane ($C_{32}H_{66}$) monolayer on HOPG. (Photo courtesy of J.P. Rabe.)

It is fascinating to contemplate how these molecules and the above liquid crystals can possibly develop such highly symmetric structures. What are the forces that drive this self-ordering and how does the system find its way into the lowest energy pattern? Since the original work on n-C₃₂H₆₆, a number of other alkanes, long chain alcohols, and fatty acids have been imaged.²¹ If the structure cannot line up with the graphite lattice, it does not form a commensurate structure with graphite. Also, it has been possible to follow in real time how the molecules move with respect to one another, allowing motion of whole domains of lamellar structures to move with respect to one another. STM studies of both the structure and motion of self-assembling molecules should play an important role in understanding this phenomenon.

4.4.3. Experiments

4.4.3.1. Imaging Surfaces Under Liquids

This experiment is designed to illustrate that atomic resolution of surfaces can be achieved even under liquids. This observation can be made only if the tip displaces the intervening molecules as it scans.

Procedure:

Head Preparation

1. Prepare either a PtIr or W tip and mount the tip.
2. Use the mounted graphite sample provided. Cleave the surface and place a drop of n-decane on the surface of the sample. Place the sample onto the STM sample mount.
3. Turn the Sample Position dial until the sample range indicator is close to the middle of the range or the sample-tip spacing is less than 0.5 mm. Be careful not to damage the tip and the sample.

Software Preparation

4. Set the scan size to 10,000 Å x 10,000 Å and the zoom factor to 50 (Collect/Configure).
5. Set the Scan Delay (Collect/Configure) to 0.00 mS/Sample.
6. In this scan you are monitoring current variations, so set the Data Type to Current (Collect/Configure).

Electronics Preparation

7. Set the Bias Voltage to about 1 volt.
8. Set the Reference Current to 2 nA.
9. Set the Servo Loop Response for the maximum rate of response for approach. Set the Gain close to maximum Set the Filter close to maximum. Set the Time Constant to minimum.
10. Set the magnification to X50.
11. Set the X and Y offset slides at their middle range.
12. Press Tunneling Current button to monitor tunneling current (it should read about zero).

Tunneling

13. Press the Coarse Retract button momentarily to reset the motor controls.
14. Press the Auto Approach (Tunneling) button for approach and wait.
15. Monitor the tunneling current until it reaches about 2 nA (equal to the reference current). Adjust the Gain, Time Constant, and Filter, if necessary, to stop any servo loop oscillation.
16. Once tunneling is achieved, set the Servo Loop Response for constant height mode of operation. Set the Gain the minimum, leave the Filter at maximum and set the Time Constant to maximum. Start a unidirectional scan (Collect/Scan Unidirectional). Scan over a few areas of the surface by using the X and Y slide bars to find a relatively flat region. The tip needs some conditioning to remove contaminants, so it may take a while for the tunneling current to settle down.
17. Collect images and save one at this range.

NOTE: Typing (ALT C then A) or just A will abort the scan without saving the image. Typing (ALT C then H) or just H will stop at the end of the image and save it in the computer memory.

18. Change the scanner range by turning the magnification dial. Set the software size correctly in the menu by setting the zoom factor (Collect/Configure). Collect an image at each setting. Acquire images with effective sizes of 1000 Å x 1000 Å, 500 Å x 500 Å, 200 Å x 200 Å, and 100 Å x 100 Å.

19. After you acquire several images, carefully back the tip away from the surface without damaging the tip. Press the Fine Retract button, then use the Coarse Retract to back off the tip. Cleave the surface again and place a drop of water on it. Repeat the above procedure (steps 1-18) and attempt to acquire atomic resolution images of graphite.
20. Replace the drop of water with a 0.1 mole electrolyte solution (KCl, KClO_4 , or any convenient salt) and repeat the above procedure.

It should be possible to image graphite and obtain atomic resolution with the non-polar fluid. As the liquid is made more polar, other contributions to the current appear. These contributions include current conduction through ion migration to the oppositely charged tip and surface (Faradaic currents) and orientation of polar molecules in the field created by the tip. The alignment of a molecule with a dipole moment is equivalent to the motion of positive and negative charge. The drop of water can be replaced by ethanol to get a qualitative determination of the magnitude of the current contributions from orientational effects. You should compare the surface image obtained in air and in the presence of the different liquids and discuss the differences.

4.4.3.2. Imaging Alkanes on Graphite

This experiment has a higher success rate than liquid crystals in obtaining atomic details. You should be able to obtain images of surface-adsorbed alkane at least half the time you try a tip approach. $\text{C}_{32}\text{H}_{66}$ is supplied with your samples. The solution needs to be made up in the lab. The important thing to note is that this molecule is similar to the non-polar liquid examined in the above experiment but much longer.

Procedure:

Head Preparation

1. Prepare either a Ptlr or W tip and mount the tip.
2. The best results are obtained using a 10 percent saturated solution of the alkane. A saturated solution is made up in phenyloctane. Aliquots from these solutions are taken and diluted by a factor of ten. Place a drop of 10 percent saturated solution on a freshly cleaved surface of graphite. Another solution that works well is 16 mg of alkane dissolved in 10 mil iso-octane. Place a drop on the surface and allow it to evaporate. Follow this with a drop of 16 mg of alkane dissolved in n-decane.
3. Turn the Sample Position dial until the sample range indicator is close to the middle of the range or the sample-tip spacing is less than 0.5 mm. Be careful not to damage the tip and the sample.

Software Preparation

4. Set the scan size to 10,000 Å x 10,000 Å (Collect/Configure) and the zoom factor to 10.
5. Set the Scan Delay (Collect/Configure) to 0.00 mS/Sample.
6. In this scan you are monitoring current variations, so set the Data Type to Current (Collect/Configure).

Electronics Preparation

7. Set the Bias Voltage to about 600 mV.
8. Set the Reference Current to 1 nA.
9. Set the Servo Loop Response for maximum rate of response for approach. Set the Gain close to maximum. Set the Filter close to maximum. Set the Time Constant to minimum.
10. Set the magnification to X10.
11. Set the X and Y offset slides at their middle range.
12. Press the Tunneling Current button to monitor tunneling current (it should read about zero).

Tunneling

13. Press the Coarse Retract button momentarily to reset the motor controls.
14. Press the Auto Approach (Tunneling) button for approach and wait.
15. Monitor the tunneling current until it reaches about 2 nA (equal to the reference current). Adjust the Gain, Time Constant, and Filter, if necessary, to stop any servo loop oscillation.
16. Once tunneling is achieved, set the Servo Loop Response for constant height mode of operation. Set the Gain to minimum. Leave the Filter at maximum. Set the Time Constant to Maximum. Start a unidirectional scan (Collect/Scan Unidirectional). Scan over a few areas of the surface by using the X and Y slide bars to find a relatively flat region. The tip needs some conditioning to remove contaminants, so it may take a while for the tunneling current to settle down.

A highly-ordered alkane layer on the surface isn't normally apparent as you first approach a flat region. The molecules need time to find the right structure (the lowest energy configuration) and the tip needs time to establish equilibrium and/or remove contaminants. You should change the scanner settings to a 100 Å range. The best images are obtained in constant height mode with a 1 nA current and bias voltage of approximately 1 volt. It takes a bit of patience to obtain good images. You need to try different currents between 0.5 - 1 nA and bias voltages between 0.4 - 1 volt. It sometimes helps to raise the bias voltage momentarily to 2 volts to initiate either tip cleaning or ordering of the layer. The most reliable procedure is to provide several short pulses of 4 volts and 1 microsecond duration to the tip bias.²⁴ The tip needs to be moved over after pulsing. This procedure almost always works and is probably related to tip cleaning. If you don't have this pulsing option available, you should try different tips. Eventually you will get a tip to work. You might have to scan the surface to find a relatively flat region using X and Y slide bars. After you move the X or Y slides, it may take a while for the tip to settle down to produce atomic images.

17. Once you obtain good images, they are generally very stable. You may want to zoom in on certain regions, depending on what you find, and change the current and bias levels to optimize the contrast. At certain current values you should be able to see both the graphite lattice and the alkane ordering. Collect images and save them for different scan ranges.

NOTE: Typing (ALT C then A) or just A will abort the scan without saving the image. Typing (ALT C then H) or just H will stop at the end of the image and save it in the computer memory.

18. Change the scanner range by turning the magnification dial. Set the software size correctly in the menu by setting the zoom factor (Collect/Configure). Collect an image at each setting. Acquire images with effective sizes of 1000 Å x 1000 Å, 500 Å x 500 Å, 200 Å x 200 Å, and 100 Å x 100 Å.

You should analyze the images you find and compare them to the known structure of C₃₂H₆₆. In particular, if the image quality is good enough, you should discuss the registry of the periodic structures with respect to the graphite lattice. Discuss whether the current is enhanced and consider how the alkane is influencing the tunneling current. In addition, you should compare these results to those obtained for n-decane in the above experiment.

4.4.3.3. Imaging Liquid Crystals

This experiment is similar to the one above, except that the biphenyl group of the molecules to be studied makes a large difference on the energetics that are responsible for the self-assembling nature of these molecules relative to alkanes. In addition, the biphenyl group is relatively large and provides a good landmark for assigning the images.

Procedure:

Head Preparation

1. Prepare either a PtIr or W tip and mount the tip.
2. Use the mounted graphite sample provided. Cleave the surface and place a drop of 8CB on the surface. Note that the liquid crystal might not be liquid, depending on the room temperature. If it is not liquid, simply hold the bottle in your hand, or heat the container to about 30° C, until the crystal liquefies. It helps to slightly heat the surface up to 60° C and let it cool slowly. We've found that scraping a razor blade across the surface makes a thin layer and helps induce ordering. Use the knife provided in the sample kit to scrape the surface and remove the excess liquid crystal. The images for 8CB are best observed at 18° C. After the sample is prepared, place the sample onto the STM sample mount.
3. Turn the Sample Position dial until the sample range indicator is close to the middle of the range or the sample-tip spacing is less than 0.5 mm. Be careful not to damage the tip and the sample.

Software Preparation

4. Load the 8cb1.img (File/Load), shown in Figure 4.32.

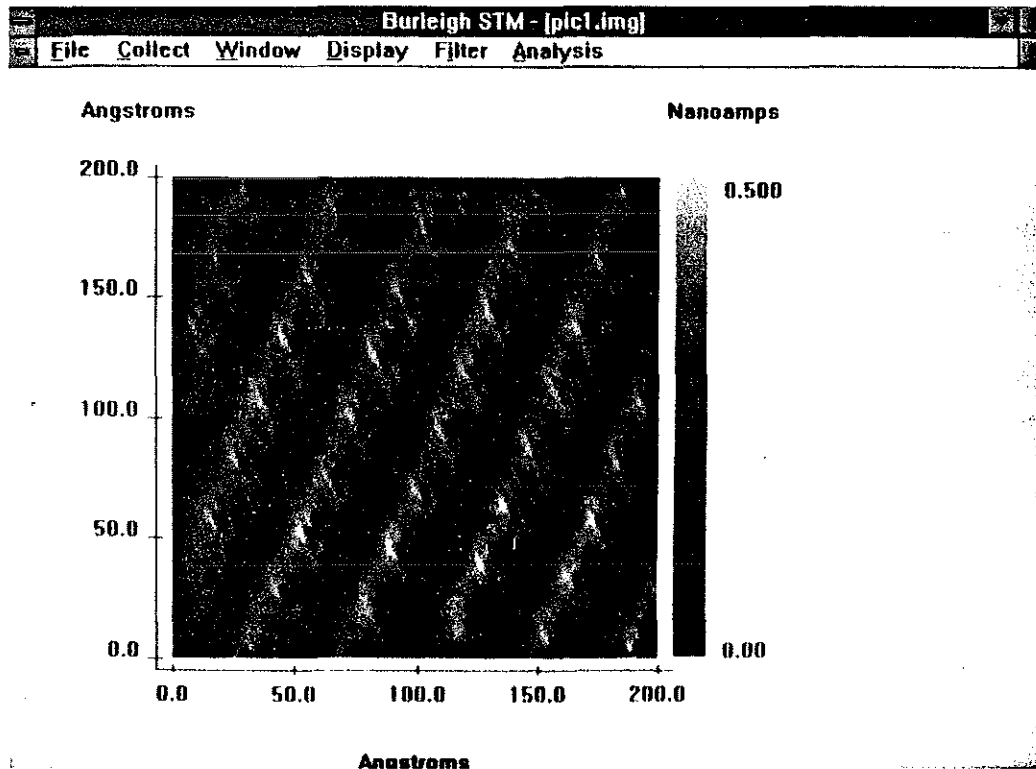


Figure 4.32. A typical STM image of 8CB taken using the Burleigh ISTM. A careful examination of the figures reveals the alignment of the two biphenyl groups.

5. Set the Scan Delay (Collect/Configure) to 0.00 mS/Sample.
6. In this scan you are monitoring current variations, so set the Data Type to Current (Collect/Configure).

Electronics Preparation

7. Set the Bias Voltage to about 1 volt.
8. Set the Reference Current to 1 nA.
9. Set the Servo Loop Response for maximum rate of response for approach. Set the Gain close to maximum. Set the Filter close to maximum. Set the Time Constant to minimum.

10. Set the magnification to X50.
11. Set the X and Y offset slides at their middle range.
12. Press the Tunneling Current button to monitor tunneling current (it should read about zero).

Tunneling

13. Press the Coarse Retract button momentarily to reset the motor controls.
14. Press the Auto Approach (Tunneling) button for approach and wait.
15. Monitor the tunneling current until it reaches about 1 nA (equal to the reference current). Adjust the Gain, Time Constant, and Filter, if necessary, to minimize any servo loop oscillation.
16. Once tunneling is achieved, set the Servo Loop Response for constant height mode of operation. Set the Gain to minimum. Leave the Filter at maximum. Set the Time Constant to maximum. Start a unidirectional scan (Collect/Scan Unidirectional). Scan over a few areas of the surface by using the X and Y slide bars to find a relatively flat region. The tip needs some conditioning to remove contaminants so it may take a while for the tunneling current to settle down.

It should be possible to find very large flat areas of ordered liquid crystal on this surface, as shown in Figure 4.33. Use the X and Y slide bars to find relatively flat areas. After you move the X and Y slides, it may take a while for the tip to settle down to produce atomic images. The conditions for studying the graphite/8CB interface are the same as the alkane study described in Section 4.4.3.2, except that the current should be kept around 0.1 nA, with a bias of approximately 1 volt.

17. Once you find a good area showing ordered regions of 8CB, you should adjust the Servo Loop Response settings to higher currents. This will cause the tip to move closer to the surface. Under these conditions it is possible, with a stable image, to see the registry of 8CB with the lattice. Again, good images require some patience; and you should try different currents, biases, and tips to get a good image. Pulsing the tip also helps. Collect images and save one at this range.

NOTE: Typing (ALT C then A) or just A will abort the scan without saving the image. Typing (ALT C then H) or just H will stop at the end of the image and save it in the computer memory.

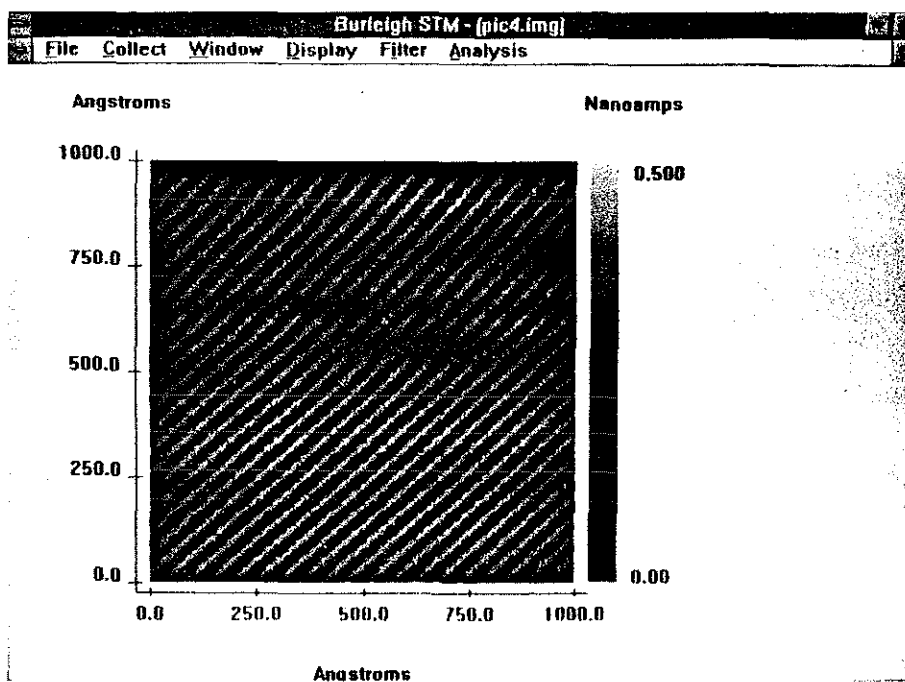


Figure 4.33. A 1000 Å X 1000 Å area of the sample showing the long range ordering of 8CB on graphite.

18. Change the scanner range by turning the magnification dial. Set the software size correctly in the menu by setting the zoom factor (Collect/Configure). Collect an image at each setting. Acquire images with effective sizes of 1000 Å x 1000 Å, 500 Å x 500 Å, 200 Å x 200 Å, and 100 Å x 100 Å.
19. It is possible to acquire liquid crystal images in constant current mode as well. Try acquiring and saving some images in this mode.
20. If a polarization microscope is available, it is useful to observe the liquid crystal form in its smectic phase by observing the color contrast as the liquid crystal orders into the smectic phase and becomes birefringent. This is a highly visual effect. STM images are not obtained unless the smectic phase is observed.²⁵

This experiment is interesting in that the biphenyl group shows clearly in the images. It has been possible in exceptional images to make out the individual rings and functional groups. The phenyl group of 8CB enables a determination of the structure of the liquid crystal with respect to the graphite lattice and an appreciation of the forces that lead to ordering. Figure 4.33 shows typical data. Image processing will more clearly bring out its bilayer structure.

A nice additional experiment is to repeat the experiment with an MoS₂ substrate. On graphite, 8CB should appear as a bilayer structure with the two biphenyl rings of different molecules arranged in a head-to-head fashion. On MoS₂ the structure appears linear, rather than as a bilayer, in which the biphenyl is sandwiched between two alkyl groups of adjacent molecules.²⁶

4.4.2.4. Questions

1. The biphenyl rings of 8CB have been found to enhance tunneling relative to the alkyl side chains. One explanation is that the phenyl groups lower the effective barrier more than the alkyl groups. Another is that the phenyl groups affect the electron density near the Fermi level of the substrate. Discuss these two mechanisms with respect to the approximate position of the energy levels of phenyl groups relative to graphite.
2. Discuss what forces exist at the graphite surface that would favor a commensurate structure for C_{32} on its surface.
3. For exceptional STM scans it is possible to image individual atomic rings. The hexagonal structure appears visible. The highest occupied molecular orbitals (HOMO) and lowest unoccupied molecular orbitals (LUMO) for benzene should approximate that of the phenyl group which is a substituted benzene ring. If the imaging mechanism is assumed to arise from electronic effects, explain how the image seems to conserve the hexagonal ring structure, using the molecular orbitals of benzene as a basis.
4. One of the most exciting prospects of scanning probe microscopy would be to use either STM or AFM to sequence DNA. Some experiments have given encouraging results, but this possibility still remains controversial. Based on the above experiments and discussion, explain what needs to be accomplished experimentally before the sequencing of DNA could be achieved.

4.5. Lattice Distortions

Band theory is concerned with the behavior of electrons in a periodic solid. In some ways it is like putting the cart before the horse since the arrangement of atoms in a crystal is itself determined by the bonding interactions of the electrons. Although the existence of regular crystal structures shows that bonding forces often produce a periodic lattice, this is not always the case. Some electron configurations produce forces that distort the lattice from its ideal regular configuration. The presence of electrons may sometimes cause a distortion that destroys simple periodicity of the lattice. This in turn disrupts the band structure and may have an important influence on the electronic properties of the solid.

Usually one- and two-dimensional solids are used to introduce the concepts of band theory. In fact, many real solids with a one-dimensional electronic structure are now known, but their properties are much more complicated than simple band theory would suggest. The study of such compounds is an active research field.

In this section we will introduce the concept of charge density wave (CDW) in a very simple system and show you STM images of a more complicated two-dimensional system. Crystals for this set of experiments are individually grown and are expensive and rare. If you are interested in actually examining the nature of CDW with your STM, contact Burleigh Instruments for more information.

4.5.1. Periodic Lattice Distortions and Charge Density Waves

One of the best-known one-dimensional conductors in the partially oxidized platinum chain compound, $K_2Pt(CN)_4Br_{0.3} \cdot 3H_2O$, which, for simplicity, is usually known as KCP. The metal atoms form chains along one axis of the crystal and the top band is composed principally of platinum $5d_z$ orbitals overlapping along the chain. The presence of Br^- ions leaves 0.3 holes per platinum in this band, which would otherwise be filled. At room temperature there is good metallic conductivity, occurring predominantly along the chain directions. Reflectivity is observed only with light polarized parallel to the chains. Crystals of KCP are quite transparent to visible light polarized perpendicular to the chain axis. But KCP is not a true metal, since its conductivity declines sharply at temperatures below $150^\circ K$. Although KCP has a band gap at lower temperatures, it seems to disappear as the temperature is raised. Diffraction experiments reveal an interesting feature: the spacing between atoms in each chain is not regular below about $250^\circ K$, but displays a periodic lattice distortion. This is exaggerated in Figure 4.34[a]. In fact, the maximum displacement observed in KCP is only about 0.5 percent of the regular lattice spacing.

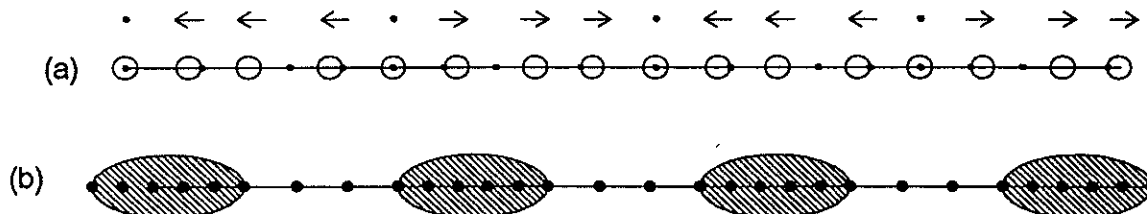


Figure 4.34. [a] Periodic lattice distortions of KCP shows a 0.5 percent displacement of atoms. [b] Charge distribution is also effected by this periodic distortion.

The electronic lattice distortion in KCP is intimately connected with its electronic properties. The KCP electrons interact strongly with atomic potential. The consequence of periodic distortion is shown in Figure 4.34[b]. The bonding between atoms is stronger where they are more closely spaced and the electrons have lower energy in these regions. They therefore tend to concentrate at intervals along the chain. The periodic build-up of electron density is known as a charge density wave. The energy gap produced in the band structure of KCP is essentially the energy required to move an electron from a more strongly bound region to one where the atoms are farther apart.

4.5.2. Two- and Three-Dimensional Systems

Properties similar to those of KCP have been observed in many other compounds containing chains of metal atoms with a square-planar ligand coordination. This geometry is found with elements such as iridium, nickel, and palladium. Metal chain compounds show some of the best examples of one-dimensional electronic structure. In general, however, the one-dimensional system theories do not apply to two or three dimensions. The interaction of electrons with a weak periodic potential does not give rise to an energy gap. There is some distortion of the density of states curves, but any energy lowering of the electrons is not usually sufficient to overcome the elastic interactions between atoms, which generally favor a regular lattice. Periodic lattice distortions and charge density waves are known in a number of layer compounds, but this only seems to happen when their band structure has rather special features. The best-known example is tantalum disulfide (TaS_2), in which the effect is much more pronounced than in KCP. At low temperatures the periodic distortion in TaS_2 involves an atomic displacement of 0.25 \AA and a charge displacement equivalent to nearly one electron per tantalum. As in KCP, the period of displacement is related to the band filling and is altered by changing the number of metallic electrons. Unlike KCP, TaS_2 is still metallic below the temperature at which the distortion occurs. This is because an energy gap is only produced for electrons moving in the direction corresponding to the distortion. In two dimensions, electrons have the freedom to move in other directions, and so the gap is avoided.

Periodic lattice distortions are often incommensurate and, as in KCP, they do not correspond to an integral number of normal lattice spacings. The distortion in TaS_2 is incommensurate between 350° K , when it first appears, and 200° K . Below 200° K , however, it becomes commensurate and locked onto the lattice. Figure 4.35 shows an STM image of TaS_2 layered compound undergoing a charge density wave transition. The cross-sectional view of this image clearly indicates the incommensurate nature of the CDW with the lattice. This image was acquired at room temperature. Sample bias was about 10 mV and tunneling current 5 nA . It shows seven-atom clusters with the center atom more highlighted compared to the outer six atoms.

CDW phenomena can be observed for 2H and 1T phases of a variety of layered compounds, such as TaS_2 , TaSe_2 , TiSe_2 , TiS_2 , VSe_2 and NbSe_2 .²⁷

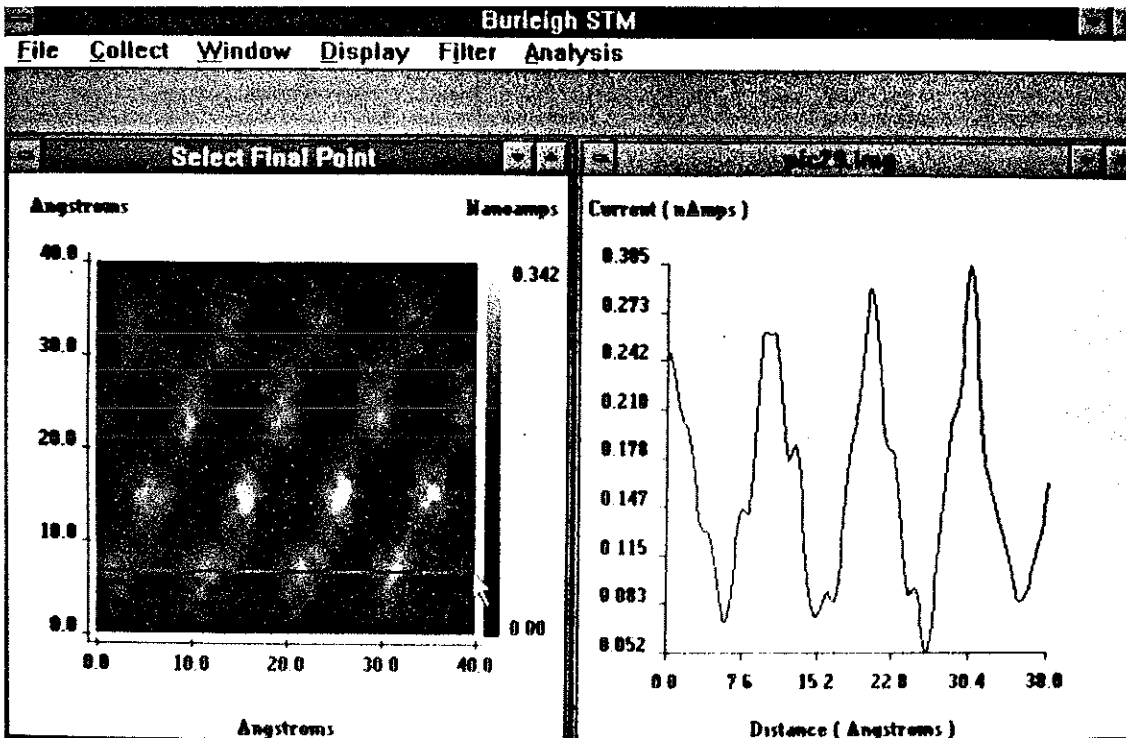


Figure 4.35. An STM image of the CDW of TaS₂ at room temperature. The cross section clearly show that the TaS₂ atoms are incommensurate (not in registry) with the CDW. (Samples provided by B.A. Parkinson.)

APPENDIX 1: REFERENCES

CHAPTER 1

1. Savile Bradbury, *The Evolution of the Microscope* (New York: Pergamon Press, 1967).
2. Clifford Dobell, *Anthony van Leeuwenhoek and His "Little Animals"* (New York: Harcourt, Brace and Co., 1932).
3. Steven Chu, "Laser manipulation of atoms and particles," *Science* 253: 5022 (23 August 1991): 861-866.
4. Peter G. Berman, *Introduction to the Theory of Relativity* (Edgewood Cliffs, NJ: Prentice-Hall, 1942), 143.
5. C.J. Davisson and L.H. Germer, "Diffraction of electrons by crystal of nickel," *Physical Review* 30: 6 (December 1927): 705-740.
6. The angstrom unit of measure will be adopted in this text because it is the one relevant to the interatomic length scale. In S.I. units, $1 \text{ \AA} = 10^{-10} \text{ m}$ or 0.1 nm (one hundred-millionth of a centimeter).
7. E. Ruska, "Development of the electron microscope and of electron microscopy," *Reviews of Modern Physics*, Vol. 59, Number 3, Part I, (1987): 627-638.
8. L.E. Brus, A.R. Kortan, R. Hull, R.L. Opila, M.G. Bawendi, M.L. Steigerwald, P.J. Carroll, "Nucleation and growth CdSe on ZnS quantum crystallite seeds, and in inverse micelle media," *Journal of the American Chemical Society* 112 (1990): 1327-1332.
9. Theodore G. Rochow and Eugene G. Rochow, *An Introduction to Microscopy by Means of Light, Electrons, X-Rays, or Ultrasound* (New York: Plenum Press, 1978).
10. Ibid
11. C.F. Quate, "Vacuum tunneling: A new technique for microscopy," *Physics Today* 39: 2 (26 August 1986): 26-33.

12. D.T.M. Williamson, "James Clayton Lecture: The pattern of batch manufacture and its influence on machine tool design," *Proceedings of the Institute of Mechanical Engineering* 182 (1967): 21ff.
13. R. Young, J. Word, and F. Scire, "Topografiner: An instrument for measuring surface microtopography," *Review of Scientific Instruments* 43 (1972): 999-1011.
14. G. Binnig and H. Rohrer, "Scanning tunneling microscopy," *Helvetica Physica Acta* 55 (1982): 741-762.
15. G. Binnig, H. Rohrer, Ch. Gerbert, E. Weibel, "7x7 reconstruction on Si(111) resolved in real space," *Physical Review Letters* 50 (1983): 120-123.
16. G. Binnig, C. F. Quate, and C. Gerber, "Atomic force microscope," *Physical Review Letters* 56 (3 March 1986): 930-933.
17. D. Rugar and P. Hansma, "Atomic force microscopy," *Physics Today* 43 (1990): 23-30.

CHAPTER 2

1. David A. Park, *Introduction to the Quantum Theory*, 2nd ed. (New York: McGraw-Hill Co., 1974).
Stephen Gasiorowicz, *Quantum Physics* (New York: John Wiley and Sons, Inc. 1974).

These attractive books are written on the same level as the present treatment.

Albert M.L. Messiah, *Quantum Mechanics* (New York: John Wiley and Sons, Inc., 1968). This book gives a complete coverage of quantum theory from the treatment of one-dimensional potentials through the quantization of electromagnetic field and the relativistic wave equation of Dirac. It is an advanced book and assumes the mathematical sophistication of a first-year graduate students. It is a worthwhile book.

Eugen Merzbacher *Quantum Mechanics*, 2nd ed. (New York: John Wiley and Sons Inc., 1970).

Leonard I. Schiff, *Quantum Mechanics*, 3rd ed. (New York: McGraw-Hill Book Co., 1968).

These two books are used as standard first-year graduate school textbooks, and deservedly so. Merzbacher and Schiff both treat the complete range of concepts and phenomena of quantum mechanics with economy.

2. Bernard Jaffe, William R. Cook Jr., and Hans Jaffe, *Piezoelectric Ceramics* (New York: Academic Press, 1971).

J. van Randerat and R.E. Settingington, *Piezoelectric Ceramics* (Mullard Limited, 1974).

J.M. Herbert, *Ferroelectric Transducers and Sensors* (New York: Gordon and Breach Science Publishers, 1982).

CHAPTER 3

1. D.W. Pohl, "Some design criteria in scanning tunneling microscopy," *IBM Journal of Research and Development* 30: 4 (July 1986): 417-427.
2. Mircea Fotino, "Nanotips by reverse electrochemical etching," *Applied Physics Letters* 60: 23 (8 June 1992): 2935-2937.
3. Allan J. Melmed, "The art and science and other aspects of making sharp tips," *Journal of Vacuum Science & Technology B* 9: 2, II (March/April 1991): 601-608.
4. Richard C. Dorf, *Modern Control Systems*, 4th ed. (Reading, MA: Addison-Wesley, 1983); and Andrew P. Sage and Chelsea C. White, *Optimum Systems Control*, 2nd ed. (Edgewood Cliffs, NJ: Prentice-Hall, 1977).
5. Edward R. Dougherty, Andrew D. Weisman, Howard A. Mizes, and R. J. Dwayne Miller, "Application of Morphological Pseudoconvolutions to Scanning Tunneling and Atomic Force Microscopy," *SPIE Proceedings* Volume 1567, (July 1991): 88-99.

CHAPTER 4

1. Figure 4.6 adapted from Walter J. Moore, *Physical Chemistry*, 4th ed. (Edgewood Cliffs, NJ: Prentice Hall, 1972).
2. G. Binnig and H. Rohrer, "Scanning tunneling microscopy," *IBM Journal of Research and Development* 30: 4 (July 1986): 355-367.
3. V.M. Hallmark, S. Chiang, J.F. Rabott, J.D. Swalen, and R.J. Wilson, "Observation of atomic corrugation on Au(111) by scanning tunneling microscopy," *Physical Review Letters* 59 (1987): 2879-2882.
4. Hidetoshi Honbo, Shizuo Sugawara, and Kingo Itaya, "Detailed in situ scanning tunneling microscopy of single crystal planes of gold(111) in aqueous solutions," *Analytical Chemistry* 62 (1990): 2424-2429.
5. Sang-Il Park and C.F. Quate, "Tunneling microscopy of graphite in air," *Applied Physics Letters* 48: 2 (January 13, 1986): 112-114.
6. G. Binnig, H. Fuchs, Ch. Gerber, H. Rohrer, E. Stoll and E. Tosatti, "Energy-dependent state-density corrugation of a graphite surface as seen by scanning tunneling microscopy," *Europhysics Letters* 1: 1 (1 January 1986): 31-36.
7. M. Kuwabara, D.R. Clarke, and D.A. Smith, "An anomalous super-periodicity in scanning tunneling microscope images of graphite," *IBM Research Report* RC15344 and J. E. Buckley, J.L. Wragg, H.W. White, A. Bruckdorfer, and D.L. Worcester, "Large-scale periodic features associated with surface boundaries in scanning tunneling microscope images of graphite," *Journal of Vacuum Science & Technology B* 9: 2, II (March/April 1991): 1079-1082.
8. H.P. Chang and A.J. Bard, "Scanning tunneling microscopy studies of carbon oxygen reactions on Highly-Oriented-Pyrolytic-Graphite," *Journal of the American Chemical Society* 113: 15 (1991): 5588-5596; and L. Porte, D. Richard, and P. Gallezot, "Scanning Tunneling Microscopy of Oxidized Graphite," *Journal of Microscopy* 152, II (November 1988): 515-520.
9. S. M. Sze, *Physics of Semiconductor Devices*, 2nd ed. (New York: John Wiley and Sons, 1981).

10. G. Binnig, H. Rohrer, Ch. Gerbert, E. Weibel, "7x7 reconstruction on Si(111) resolved in real space," *Physical Review Letters* 50 (1983): 120-123.
11. D.M. Eigler, P.S. Weiss, E.K. Schweizer, and N.D. Lang, "Imaging Xe with a low-temperature scanning tunneling microscope," *Physical Review Letters* 66: 9 (1991): 1189-1192.
12. J.A. Dagata, J. Schneir, H.H. Harary, J. Bennet, and W. Tseng, "Pattern generation on semiconductor surfaces by a scanning tunneling microscope operating in air," *Journal of Vacuum Science & Technology B* 9: 2, II (March/April 1991): 1384-1388.
13. M.G. Youngquist and J.D. Baldeschwieler, "Observation of negative differential resistance in tunneling microscopy of MoS₂ with a scanning tunneling microscope," *Journal of Vacuum Science & Technology B* 9: 2, II (March/April 1991): 1083-1087.
14. Wolfgang M. Heckl, Frank Ohnesorge, Gerd Binnig, Martin Specht, and M. Hashmi, "Ring structures on natural molybdenum disulfide investigated by scanning tunneling and scanning force microscopy," *Journal of Vacuum Science & Technology B* 9: 2, II (March/April 1991): 1072-1078.
15. M. Weimer, J. Kramar, C. Bai, and J. D. Baldeschwieler, "Tunneling Microscopy of 2H-MoS₂: A Compound Semiconductor Surface," *Physical Review B* 37: 8 (15 March 1988): 4292ff.
16. D. Sarid, T. D. Henderson, N. R. Armstrong, and L. S. Bell, "Probing of basal planes of MoS₂ by scanning tunneling microscopy," *Applied Physics Letters* 52 (27 June 1988): 2252-2254.
17. Roscoe G. Dickinson and Linus Pauling, "The crystal structure of molybdenite," *Journal of the American Chemical Society* 45: 6 (June 1923): 1466-1471.
18. P.G. deGennes, "Liquid Crystals," in *The Concise Encyclopedia of Solid State Physics*, ed. R.G. Lerner, G.L. Trigg (Addison-Wesley, Reading Mass, 1983); 143.
19. J.S. Foster and J.E. Frommer, "Imaging of liquid crystals using a tunneling microscope," *Nature* 333 (1988): 542-545.

20. D.P.E. Smith, J.K.H. Horber, G. Binning, and H. Nejh, "Structure, registry and imaging mechanism of alkylcyanobiphenyl molecules by tunneling microscopy," *Nature* 334 (1990):641-644.
 21. J.P. Rabe and S. Buchholz, "Commensurability and mobility in two-dimensional molecular patterns on graphite," *Science* 253 (1991): 424-427.
 22. A.J. Groscek, "Selective absorption at graphite-hydrocarbon interfaces," *Proc. Royal Society of London* A314 (1970): 473.
 23. G.C. McGonial, R.H. Bernhardt and D.J. Thomson, "Imaging alkane layers at the liquid/graphite interface with scanning tunneling microscope," *Journal of Applied Physics Letters* 57 (1990): 28-30.
 24. Private communication with J.P. Rabe.
 25. D.P.E. Smith, "Defects in alkylcyanobiphenyl molecular crystals studied by scanning tunneling microscopy," *Journal of Vacuum Science & Technology B* 9: 2, II (March/April 1991): 1119-1125.
 26. M. Hara, Y. Iwakabe, K. Tochigi, H. Sasabe, A.F. Garito, and A. Yamada, "Anchoring structure of smectic liquid crystal layers on MoS₂ observed by scanning tunneling microscopy," *Nature* 344 (1990): 228-230. See also D.P.E. Smith and W.H. Heckl, "Surface Phases," *Nature* 346 (1990): 616-617.
 27. H.Enomoto, H. Ozaki, M. Suzuki, T. Fuji, and M. Yamaguchi, "Angle-resolved tunneling spectroscopy of the charge density wave density of states in 1T-TaS₂," *Journal of Vacuum Science and Technology* Vol.9, Number 2, Part II (March, April 1991):1022-1026.
- J. Garnaes, S.A.C. Gould, P.K. Hansma, and R.V. Coleman, "Atomic force microscopy of charge density waves and atoms on 1T-TaSe₂, 1T-TaS₂, 1T-TiSe₂, and 2H-NbSe₂," *Journal of Vacuum Science and Technology* Vol.9, Number 2, Part II (March, April 1991): 1032-1035.
- C.G. Slough, W.W. McNairy, Chen Wang, and R.V. Coleman, "Long range modulation of the charge density wave structure in 1T-TaS₂ studied by scanning tunneling microscopy," *Journal of Vacuum Science and Technology* Vol.9, Number 2, Part II (March, April 1991): 1036-1038.

G.Raina, K. Sattler, U. Muller, N. Venkateswaran, and J. Xhie, "Scanning tunneling microscopy of 1T-TaSe₂ at room temperature," *Journal of Vacuum Science and Technology* Vol.9, Number 2, Part II (March, April 1991): 1039-1043.

Xian Liang Wu and Charles M. Lieber, "Variable temperature scanning tunneling microscopy studies of the charge density wave phases in tantalum disulfide," *Journal of Vacuum Science and Technology* Vol.9, Number 2, Part II (March, April 1991): 1044-1047.

Chen Wang, C.G. Slough, and R.V. Coleman, "Spectroscopy of dichalcogenides and trichalcogenides using scanning tunneling microscopy," *Journal of Vacuum Science and Technology* Vol.9, Number 2, Part II (March, April 1991):1048-1051.

RECEIVED

APPENDIX 2: IMAGE FILE FORMAT (Version 2.10)

Each image file contains a software version number that identifies the revision of the software under which it was created.

256 samples x 256 scan lines (square image) maximum. Sample/scan line values will be restricted to a power of two.

Raw image data is stored in the image file (*.img) as the (two-byte integer) number of A/D counts acquired during the sampling stage of the scanning process.

The image file format is as follows:

[version number] [# samples] [# scanlines]

[data[0] ... data[samples * scan lines]]

[image scan data]

where:

[version number] is a four-byte floating point value that identifies what software revision the image was created under.

[# samples] is a two-byte integer value from 2 to 256 in powers of two.

[# scanlines] is a two-byte integer value from 2 to 256 in powers of two.

[data [0] ... data[samples * scanlines]] is an array of two byte integer values that correspond to the A/D values sampled during the scanning process or some modified values corresponding to a filtering operation on the raw data. (The system A/D converter is a 12-bit converter; therefore the valid data values can range from 0 to 4095.)

[image scan data] is a stream of values defining the scanning parameters for the image described. This stream of values is defined as:

[max scan range X] is a four-byte integer value that holds the maximum number of angstroms that the system is capable of scanning in the X direction.

[max scan range Y] is a four-byte integer value that holds the maximum number of angstroms that the system is capable of scanning in the Y direction.

[max scan range Z] is a four-byte integer value that holds the maximum number of angstroms that the system is capable of scanning in the Z direction.

[X scan range] is a four byte integer value that holds the actual scanned range in the X direction in angstroms.

[Y scan range] is a four byte integer value that holds the actual scanned range in the Y direction in angstroms.

[Z scan range] is a four byte integer value that holds the actual scanned range in the Z direction in angstroms or thousands of nanoamps. This value is dependent on the scan data type parameter below.

[scan speed] is a two byte integer value that is used to calculate the delay time between sampled values. Each count of scan speed corresponds to 0.05 ms of delay between samples.

[zoom level] is a two byte integer value that holds the level of the microscope magnification factor in a range of 1 through 5. These levels correspond to zoom multipliers of 1, 2, 10, 50, and 250.

[scan data type] is a two byte integer value that represents the type of data that was sampled. A value of 0 represents "current" data and a value of 1 represents "height" data.

[system Z gain] is a two byte integer value that holds a number representing the Z axis gain that was used when the image was sampled. The actual data values should then be divided by this factor to get the actual data values. Note that this is a user-entered value and will only be valid if the correct entry was made at the time of sampling.

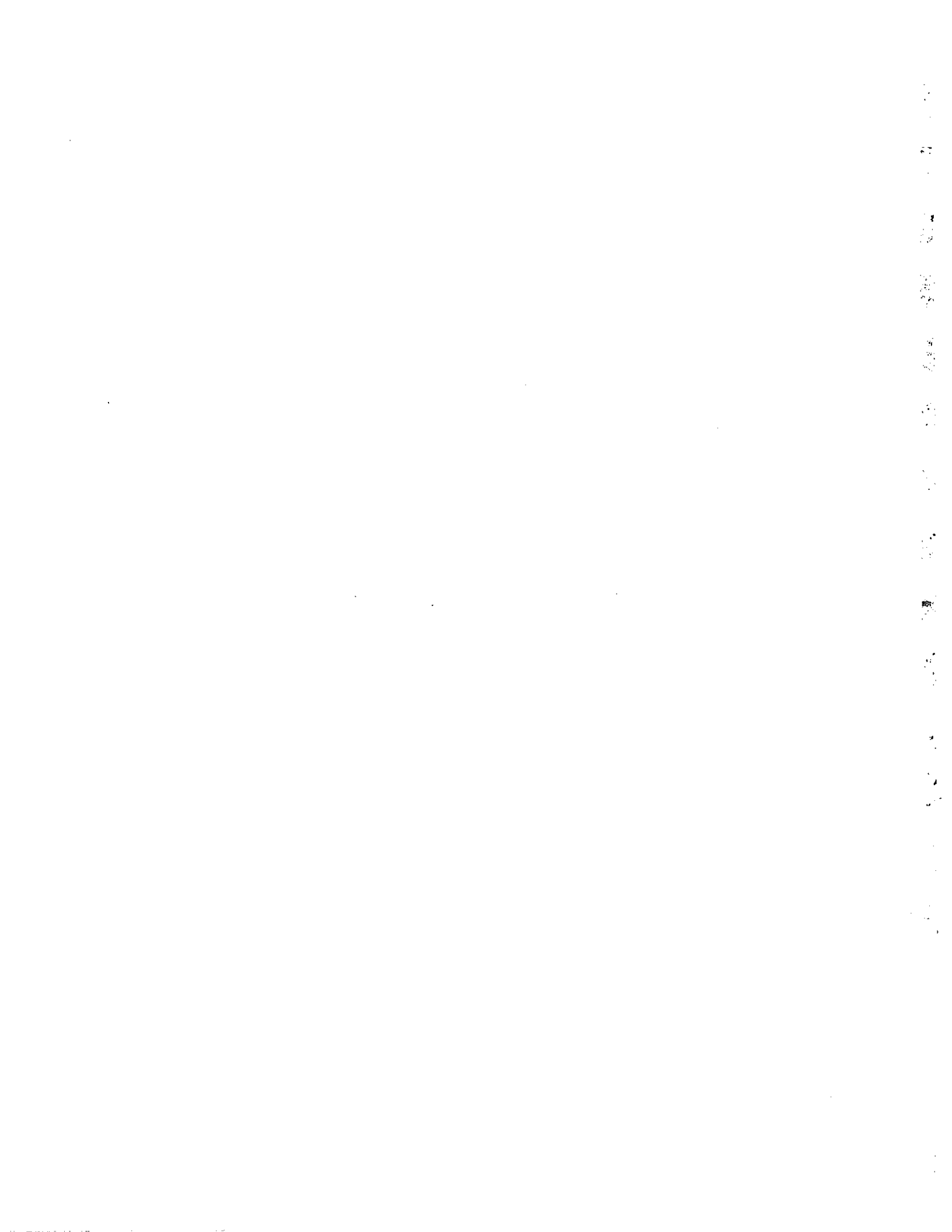
[bias volts] is a four-byte floating point value that holds the bias voltage applied to the tip when the image was sampled (in mV). Note that this is a user-entered value and will only be valid if the correct entry was made at the time of sampling.

[tunneling current] is a four-byte floating point value that holds the tunneling current used when the image was sampled. Note that this is a user-entered value and will only be valid if the correct entry was made at the time of sampling.

APPENDIX 3: FUTURE EXPERIMENTS

We recommend in addition, the following set of experiments. The student can find a list of references on each of these experiments.

- ◆ Layered compounds MoTe_2
- ◆ Molecular ordering: Acetone on graphite and MoS_2
- ◆ Ordering of metals on surfaces: Au oriented along (100) deposited on NaCl
Au oriented along (111) deposited on Mica
- ◆ Hydrogenation of silicon surface along (111) orientation. Hydrogen atoms remove (saturate) silicon dangling bonds.
- ◆ Charge density waves on NbSe.



INDEX

4

4'-n-octyl-4-cyanobiphenyl,..... 4-40

8

8CB,..... 3-8, 4-1, 4-40, 4-49

A

Acoustical Microscopy, 1-8

Alkanes, 4-1, 4-43

Angstrom, 1-4

Antibonding, 4-3

Atomic Tweezers,..... 4-39

Auto Approach, 3-17

B

Band, 4-4

Bias Voltage, 2-21, 3-15

Binnig and Rohrer, 1-10

Biphenyl Groups, 4-40

Bloch Wavefunctions, 4-4

Bonding, 4-3

Bonds, 4-16

C

C32H66, 3-8, 4-1, 4-43

Charge Density Waves, 4-1, 4-54

Cleaving, 4-18

Coarse Approach,	3-17
Coarse Retract,	3-17
Commensurate,	4-43
Controls, Scan/Offset,	3-14
Controls, Tip Approach,	3-14
Controls, Tunneling,	3-14
Covalent Bonding,	4-16
Current/Voltage Monitor,	3-15

D

Dangling Bonds,	4-30
Davidson and Germer,	1-4
de Broglie,	1-4
de Broglie Relation,	4-5
Diamond,	4-6
Diffraction Of Light,	1-1
Dopants,	4-29
Dotriacontane,	3-8, 4-43
Drude model,	2-7

E

Elastomer Spacers,	2-19
Electret,	2-14
Electrochemical,	3-10
Electrochemical Etching,	3-10
Electron Microscopy,	1-4
Electron Wavefunction,	2-8

Electronic Data Collection,	2-20
Energy, Electron,	2-4
Kinetic,.....	2-4
Potential,	2-4
Etching,	3-10

F

Fermi Dirac DISTRIBUTION,	4-6
Fermi-Dirac Statistics,	4-5
Fermions,	4-2
Field Emission Microscopy (FEM),	1-7
Field Ion Microscopy (FIM),	1-7
Filter (High Frequency),	3-16
Fine Retract,	3-17
Fullerene Structure,	4-28

G

Gain (Proportional),	3-16
Gold,	4-2
Gold Holographic Grating,	3-8
Graphite,	4-1, 4-15

H

Hamiltonian,	2-7
Highly-Oriented-Pyrolytic-Graphite (HOPG),	3-8, 4-15
Holographic Gold Grating,	4-9
Hypothesis,	1-4

I

Impurities,	4-29
Incommensurate,.....	4-55
Insulators,	4-2
Isotropic Solid,	4-5
ISTM Control Electronics,	3-14
ISTM Head,	3-2

K

KCP,	4-54
KOH,	3-10
KOH etching process,	3-11

L

Lattice Distortions,	4-54
Liquid Crystal,	3-8, 4-1, 4-38, 4-40, 4-49
Long Chain Alkanes,	4-38

M

Magnification (Scan Range),	3-16
Material Safety Data Sheets,	3-8
Metals,	4-2
Microscope,	1-1
Miller Indices,	4-8
Moire-Like Effect,	4-23
Molybdenite,	3-8, 4-30
Molybdenum Disulfide,	4-29
Molybdenum Tellurite,	4-31

Monitor,	3-14, 3-18
MoS ₂ ,	4-1
Mounting Sample,	3-9
Multiple Atomic Tips,	4-22

N

N-Alkane,	3-8
Negative Feedback,	2-17
Noble Metals,	4-2

O

Optical Microscopy,	1-1
Optical Tweezers,	1-2
Oxidation Of Graphite,	4-26

P

Particle Nature,	2-5
Piezoelectrics,	2-14
Plank's Constant,	2-7
Platinum Iridium,	3-9
Platinum-Iridium Wire,	3-8
PZT,	2-14

Q

Quantum Mechanical Tunneling,	2-1
-------------------------------------	-----

R

Reference Current,	3-15
Resistance,	4-2
Ring-Like Structures,	4-33

S

Sample Carriage,	3-3, 3-4
Sample Holder,	3-3, 3-4
Sample Position Dial,	3-3, 3-5
Scan/Offset Controls,	3-14, 3-16
Scanning Electron Microscope (SEM),	1-6
Scanning Probe Microscopy,	1-10
Schrödinger's Equation,	2-7
SEM Plug,	3-4
Semi-Liquid State,	4-40
Semi-Solid State,	4-40
Semiconductors,	4-2, 4-29
Semimetals,	4-15, 4-19
Servo Loop Response,	3-15
Silver Print,	3-8
Springs,	2-19
Superconducting Levitation,	2-18
Surface Reconstruction,	4-31
Surface States,	4-30
Surface Topographiner,	1-10

T

Tantalum Disulfide,	4-55
Time Constant (Integral),	3-16
Tip Approach Controls,	3-14, 3-17
Tip Carriage,	3-3

Tip Holder,	3-4
Tip Mount,	3-3
Tip Preparation,	3-9
Transistor,	4-29
Transmission Coefficient,	2-12
Transmission Electron Microscope (Tem), .	1-4
True-Image Software,	3-19
Tungsten,	3-9
Tungsten Wire,	3-8
Tunneling,	2-5, 3-15
Tunneling Controls,	3-14

V

Van Leeuwenhoek, Anthony,	1-1
Vibration Isolation,	2-18

W

Wave Nature,	2-5, 2-7
Workfunction,	2-7

X

X and Y Controls,	3-16
X-Y Rastering,	2-21

Z

Zoom,	3-16
-------------	------

